Chapter 4
Electrical and Electromagnetic Methods

4-1. Introduction

Electrical geophysical prospecting methods detect the surface effects produced by electric current flow in the ground. Using electrical methods, one may measure potentials, currents, and electromagnetic fields which occur naturally or are introduced artificially in the ground. In addition, the measurements can be made in a variety of ways to determine a variety of results. There is a much greater variety of electrical and electromagnetic techniques available than in the other prospecting methods, where only a single field of force or anomalous property is used. Basically, however, it is the enormous variation in electrical resistivity found in different rocks and minerals which makes these techniques possible (Telford et al. 1976).

a. Electrical properties of rocks. All materials, including soil and rock, have an intrinsic property, resistivity, that governs the relation between the current density and the gradient of the electrical potential. Variations in the resistivity of earth materials, either vertically or laterally, produce variations in the relations between the applied current and the potential distribution as measured on the surface, and thereby reveal something about the composition, extent, and physical properties of the subsurface materials. The various electrical geophysical techniques distinguish materials through whatever contrast exists in their electrical properties. Materials that differ geologically, such as described in a lithologic log from a drill hole, may or may not differ electrically, and therefore may or may not be distinguished by an electrical resistivity survey. Properties that affect the resistivity of a soil or rock include porosity, water content, composition (clay mineral and metal content), salinity of the pore water, and grain size distribution.

(1) In an electrically conductive body that lends itself to description as a one-dimensional body, such as an ordinary wire, the relationship between the current and potential distribution is described by Ohm's law:

$$V = IR \tag{4-1}$$

where

V = difference of potential between two points on the wire

I = current through the wire

R = resistance measured between the same two points as the difference of potential

The resistance (R) of a length of wire is given by

$$R = \rho\frac{L}{A} \tag{4-2}$$

where

ρ = resistivity of the medium composing the wire

L = length

A = area of the conducting cross section

Note that if R is expressed in ohms (Ω) the resistivity has the dimensions of ohms multiplied by a unit of length. It is commonly expressed in Ωm but may be given in Ω-cm or Ω-ft. The conductivity (σ) of a material is defined as the reciprocal of its resistivity (ρ). Resistivity is thus seen to be an intrinsic property of a material, in the same sense that density and elastic moduli are intrinsic properties.

(2) In most earth materials, the conduction of electric current takes place virtually entirely in the water occupying the pore spaces or joint openings, since most soil- and rock-forming minerals are essentially nonconductive. Clays and a few other minerals, notably magnetite, specular hematite, carbon, pyrite, and other metallic sulfides, may be found in sufficient concentration to contribute measurably to the conductivity of the soil or rock.

(3) Water, in a pure state, is virtually nonconductive but forms a conductive electrolyte with the presence of chemical salts in solution, and the conductivity is proportional to the salinity. The effect of increasing temperature is to increase the conductivity of the electrolyte. When the pore water freezes, there is an increase in resistivity, perhaps by a factor of 10^4 or 10^5, depending on the salinity. However, in soil or rock this effect is diminished by the fact that the pore water does not all freeze at the same time, and there is usually some unfrozen water present even at temperatures considerably below freezing. The presence of dissolved salts and the adsorption of water on grain surfaces act to reduce the freezing temperature. Even so, electrical resistivity surveys made on frozen ground are likely to encounter difficulties because of the

high resistivity of the frozen surface layer and high contact resistance at the electrodes. On the other hand, the effect of freezing on resistivity makes the resistivity method very useful in determining the depth of the frozen layer. It is very helpful in the interpretation of such surveys to have comparison data obtained when the ground is unfrozen.

(4) Since the conduction of current in soil and rock is through the electrolyte contained in the pores, resistivity is governed largely by the porosity, or void ratio, of the material and the geometry of the pores. Pore space may be in the form of intergranular voids, joint or fracture openings, and blind pores, such as bubbles or vugs. Only the interconnected pores effectively contribute to conductivity, and the geometry of the interconnections, or the tortuosity of current pathways, further affects it. The resistivity ρ of a saturated porous material can be expressed as

$$\rho = F\rho_w \tag{4-3}$$

where

F = "formation factor"

ρ_w = resistivity of pore water

The formation factor is a function only of the properties of the porous medium, primarily the porosity and pore geometry. An empirical relation, "Archie's Law," is sometimes used to describe this relationship:

$$F = a\phi^{-m} \tag{4-4}$$

where

a and m = empirical constants that depend on the geometry of the pores

ϕ = porosity of the material

Values of a in the range of 0.47 to 2.3 can be found in the literature. The value of m is generally considered to be a function of the kind of cementation present and is reported to vary from 1.3 for completely uncemented soils or sediments to 2.6 for highly cemented rocks, such as dense limestones. Equations 4-3 and 4-4 are not usually useful for quantitative interpretation of data from surface electrical surveys but are offered here to help clarify the role of the pore spaces in controlling resistivity.

(5) Bodies of clay or shale generally have lower resistivity than soils or rocks composed of bulky mineral grains. Although the clay particles themselves are nonconductive when dry, the conductivity of pore water in clays is increased by the desorption of exchangeable cations from the clay particle surfaces.

(6) Table 4-1 shows some typical ranges of resistivity values for manmade materials and natural minerals and rocks, similar to numerous tables found in the literature (van Blaricon 1980; Telford et al. 1976; Keller and Frischknecht 1966). The ranges of values shown are those commonly encountered but do not represent extreme values. It may be inferred from the values listed that the user would expect to find in a typical resistivity survey low resistivities for the soil layers, with underlying bedrock producing higher resistivities. Usually, this will be the case, but the particular conditions of a site may change the resistivity relationships. For example, coarse sand or gravel, if it is dry, may have a resistivity like that of igneous rocks, while a layer of weathered rock may be more conductive than the soil overlying it. In any attempt to interpret resistivities in terms of soil types or lithology, consideration should be given to the various factors that affect resistivity.

Table 4-1
Typical Electrical Resistivities of Earth Materials

Material	Resistivity (Ωm)
Clay	1-20
Sand, wet to moist	20-200
Shale	1-500
Porous limestone	100-1,000
Dense limestone	1,000-1,000,000
Metamorphic rocks	50-1,000,000
Igneous rocks	100-1,000,000

b. Classification.

(1) The number of electrical methods used since the first application around 1830 (Parasnis 1962) is truly large; they include self-potential (SP), telluric currents and magnetotellurics, resistivity, equipotential and mise-à-la-masse, electromagnetic (EM), and induced polarization (IP). Because of the large number of methods, there are many ways of classifying them for discussion. One common method is by the type of energy source involved, that is, natural or artificial. Of the methods listed above, the first two are grouped under natural sources and the rest as artificial. Another classification, which will be used here, is to group by whether the data are measured in the time domain or the frequency domain. Only techniques in

common use today for solving engineering, geotechnical, and environmental problems will be treated in this discussion, thus omitting telluric current techniques, magnetotellurics, and many of the EM methods.

(2) Time domain methods (often abbreviated as TDEM or TEM) are those in which the magnitude only or magnitude and shape of the received signal is measured. The techniques in this class are discussed under the headings DC resistivity, induced polarization, time-domain electromagnetics, and self-potential. Frequency domain methods (often abbreviated as FDEM or FEM) are those in which the frequency content of the received signal is measured. Generally FDEM methods are continuous source methods, and measurements are made while the source is on. The measurement is of magnitude at a given frequency. Techniques in this class are discussed under the headings of VLF, terrain conductivity, and metal detectors.

c. Resistivity methods versus electromagnetic methods. Before discussing the individual methods it is useful to outline the main differences between the resistivity (including induced polarization) methods and the electromagnetic methods. With resistivity methods, the source consists of electrical current injected into the ground through two electrodes. The transmitted current wave form may be DC, low frequency sinusoidal (up to about 20 Hz), or rectangular, as in induced polarization surveys with a frequency of about 0.1 Hz. The energizer, therefore, is the electrical current injected into the ground through current electrodes.

(1) With electromagnetic methods, the source most commonly consists of a closed loop of wire in which AC current flows. It can be a small, portable transmitter coil up to 1 m in diameter, in which case there are many turns of wire. Alternately, the source can be a large transmitter loop on the ground, as large as 1 km in diameter. The frequency of the transmitter current can range from about 0.1 to about 10,000 Hz. Instruments commonly used for engineering applications (such as the EM-31, EM-34, and EM-38) use the small, multiturn type of coil and frequencies above 2,500 Hz. Electric current in the transmitter loop generates a magnetic field. The magnetic field is the energizer in electromagnetic methods as compared with electric current in resistivity methods.

(2) In terms of response, with resistivity methods, anomalies result from resistivity contrasts. For example, if a target with a resistivity of 10 Ωm is in a host rock with a resistivity of 100 Ωm, the same anomaly results as if the target had a resistivity of 100 Ωm in a host rock with a resistivity of 1,000 Ωm. In both cases, there is a resistivity contrast of 10. This example holds as long as the transmitter frequency is low enough that there is no appreciable electromagnetic induction in the rocks. With electromagnetic methods, anomalies are due more to absolute resistivity rather than resistivity contrasts. The two examples mentioned previously for resistivity methods would not produce the same anomalies with electromagnetic methods (Klein and Lajoie 1980).

4-2. Self-Potential Method

a. General. Various potentials are produced in native ground or within the subsurface altered by our actions. Natural potentials occur about dissimilar materials, near varying concentrations of electrolytic solutions, and due to the flow of fluids. Sulfide ore bodies have been sought by the self potential generated by ore bodies acting as batteries. Other occurrences produce spontaneous potentials, which may be mapped to determine the information about the subsurface. Spontaneous potentials can be produced by mineralization differences, electrochemical action, geothermal activity, and bioelectric generation of vegetation.

(1) Four different electrical potentials are recognized. Electrokinetic, or streaming, potential is due to the flow of a fluid with certain electrical properties passing through a pipe or porous medium with different electrical properties (Figure 4-1). Liquid-junction, or diffusion, potential is caused by the displacement of ionic solutions of dissimilar concentrations. Mineralization, or electrolytic contact, potential is produced at the surface of a conductor with another medium. Nernst, or shale, potential occurs when similar conductors have a solution of differing concentrations about them. Telford, Geldart and Sheriff (1990) provide equations for differing potentials. Generally, the SP method is qualitative and does not attempt to quantify the anomalous volume size, owing to the unknown volumetric shapes, concentration/density of various masses, and electrical properties of the sought causative media.

(2) Recognition of different spontaneous-potential sources is important to eliminate noise, the low background voltages. Some engineering and environmental occurrences may be mapped by contouring surficial voltages between base/reference electrode(s) and the mobile electrodes. Flow of gasses and fluids in pipes, leakage of a reservoir within the foundation or abutment of a dam,

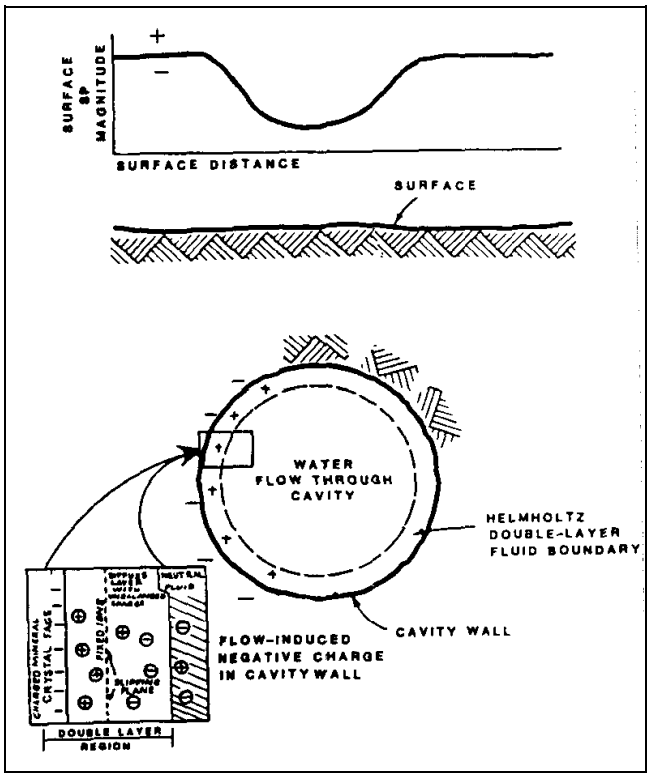

Figure 4-1. Schematic of flow-induced negative streaming potentials (Erchul and Slifer 1989)

movement of ionic fluids to or within the groundwater, flow of geothermal fluids, and movement of water into or through a karst system can be the origin of streaming potentials. These potentials may exceed the background voltage variation of a site.

b. Equipment and procedures. A simple SP survey consists of a base electrode position and a roving electrode to determine potential differences on a gridded survey or along profile lines. The required equipment merely includes electrodes, wire and a precise millivolt meter.

(1) Nonpolarizing electrodes. The electrodes in contact with the ground surface should be the nonpolarizing type, also called porous pots. Porous pots are metal electrodes suspended in a supersaturated solution of their own salts (such as a copper electrode suspended in copper sulfate) within a porous container. These pots produce very low electrolytic contact potential, such that the background voltage is as small as possible. Tinker and Rasor manufacture models of porcelain nonpolarizing electrodes that are reliable and sealed to avoid evaporation of the salt solution.

(a) Sealed pots can keep their supersaturated solutions for more than a week, even in arid locales. Refilling of the pots' solution must occur before a day's work due to the possible contact potential change while performing a measurement set. A useful procedure is to mix remaining fluids from pots in a single container, add new solution to the pots' mixture, and use the mixed solution to fill the pots. Then all pots contain the same solution mix.

(b) Multiple pots are purchased such that breakage and cleaning may be accomplished readily in the field. Only one set of a base and mobile electrode are used at any one measurement loop/grid. Base station pots are usually larger in size to assure constant electrical contact through the time of use of that station. Mobile or traveling pots are often smaller in volume of salt solution and size.

(c) Copper-clad steel electrodes are used in a variety of electrical surveys. Steel electrodes should be avoided in SP investigations. Contact potential of these electrodes is quite high and variable in the soil at various stations of the survey.

(2) Survey wire.

(a) The wire used in SP surveys must be strong, hardy, and of low resistance. Wire needs to have sufficient tensile strength to be able to withstand long-term pulls of survey work for multiple sites. For some field use, heavy twine or light rope may need to be twisted and knotted to long lengths of wire to add strength. Survey wire must have abrasion-resistant insulator wrapping. Pulling the wire over roadway surfaces can expose bare wire. Usually random bare wire positions will not fully ground to the soil, and the effects will be variable as differing lengths of wire are unreeled and occupy differing positions for the survey. This error will only modify the signal by a few to tens of millivolts (mV). Twisted two-conductor, 18-gauge, multistrand (not solid conductor) copper wire has been found to be strong and abrasion resistant.

(b) Resistance will be constant for survey wire between stations, if the wire for a reading set is not permanently stretched in length, does not develop insulator leaks and is not repaired. Repairs to wire should be made when needed because of bare wire or severe plastic stretching of the wire. Repairs and addition of wire to lengthen the survey use should only be made between measurement loops/grids. No changes to the wire may be

made during a loop or grid of readings without reoccupation of those positions. Wire accidentally severed requires a remeasurement of that complete set of circuit stations.

(3) Millivolt meter.

(a) An inexpensive, high-input-impedance voltmeter is used to read the potential in the millivolt range. Actual field voltage will be in error when the source potential is within an order of magnitude of the meter's input impedance. The meter uses a bias current to measure the desired potential. The input impedance should exceed 50 MΩ. Higher input impedances are desirable due to the impedance reduction of air's moisture. The resolution of the meter should be 0.1 or 1.0 m*V*.

(b) Several useful options on meters are available. Digital voltmeters are more easily read. Water-resistant or sealed meters are extremely beneficial in field use. Notch filters about 60 Hz will reduce stray alternating current (AC) potentials in industrial areas or near power lines.

b. Field deployment. Background potentials for these surveys may be at a level of a few tens of millivolts. Source self-potentials must exceed the background to be apparent. Potentials exceeding 1.0 *V* have occurred for shallow or downhole measurements of large sources. When large potentials are expected or have been found at the site with nonpolarizing electrodes, the easier to use copper-clad steel electrodes have been substituted for porous pots, but steel electrodes are not recommended. Contact potentials of the steel electrodes and reversing electrode positions are required systematically for steel electrodes. Large errors may develop from the use of steel electrodes (Corwin 1989).

(1) Measurements with the electrodes may require a system of reversing the electrode position to resolve contact potentials at the electrodes. Previously measured locations may need to be remeasured on a systematic or periodic basis. Reoccupation of stations is necessary when very accurate surveys are being conducted and for sites with temporal potential changes or spatial variations of electrode potential.

(2) Changes temporally in the electrodes or due to the field's self potential require the survey to be conducted in a gridded or loop array. Loops should have closure voltages of zero or only a few milli-volts. High closure potential requires remeasuring several to all of the loop stations. Station reoccupation should be in the same exact position of the earlier reading(s). Unclosed lines should be avoided. Reoccupation of particular station intervals should be made when closed loops are not possible.

(a) The traveling electrode should periodically remeasure the base location to observe contact potential, dirty electrodes, or other system changes. Reversing the survey electrodes or changing the wire polarity should only change the voltage polarity.

(b) Electrodes may have contact differences due to varying soil types, chemical variations, or soil moisture. Temporal and temperature variations are also possible, which may require the reoccupation of some of the survey positions on some arranged loop configuration. Electrode potentials have minor shifts with temperature changes (Ewing 1939).

(c) Variation in the flow of fluid due to rainfall, reservoir elevation changes, channelization of flow, or change of surface elevation where measurements are obtained are sources of variation of streaming potential. Self potentials may have temporal or spatial changes due to thunderstorm cloud passage, dissemination of mineralization or electrolytic concentration, and in the groundwater flow conduits and location. High telluric potential variations may require the SP survey to be delayed for a day.

(3) Some simple procedures are required to perform accurate and precise SP surveys. Good maintenance of porous pots, wires, and voltmeters must be observed through the survey.

(a) The traveling pot needs to be kept clean of soil with each position. Contact with moist soil, or more elaborate measures for good electrical contact with roadways or rock, must be assured. A water vessel or "skin" may be carried to moisten the soil hole and clean the porcelain surface.

(b) Wire reels speed the pulling of cable and wire recovery for changing loops, and lessen wear on the cable. Reversing the wire polarity for some measurements and reoccupation of adjacent stations assures the cable has not been grounded or stripped. Repair and checking of the wire must be made between loops and is easily done when rewinding the cable reel.

(c) Quality assurance in the field is conducted by reoccupation of loop closure points with the same base position. Repeated and reversed readings of particular

loop-end stations and checking base locations provide statistics for the assessment of measurement quality.

(4) Grid surveys offer some advantages in planning SP surveys. Changes in elevation (changing the distance to the potential source) and cognizance of cultural effects can be minimized with planning survey grids or loops. AC power lines, metal fences, and underground utilities are cultural features that affect the potential field extraneous to the normal sources of interest.

c. Interpretation. Most SP investigations use a qualitative evaluation of the profile amplitudes or grid contours to evaluate self- and streaming-potential anomalies. Flow sources produce potentials in the direction of flow: fluid inflow produces negative relative potentials, as would greater distance from the flow tube; outflow of the fluid results in positive potentials.

(1) Quantitative interpretations for a dam embankment with possible underseepage would be determined from the profiles across the crest. Negative anomalies may be indicative of flow from the reservoir at some depth. The width of the half-amplitude provides a depth estimate. Outflow at the toe of an embankment or at shallow depths beneath the toe would produce positive, narrow anomalies. Mineral or cultural utilities produce varying surface potentials depending on the source.

(2) Semiquantitative, forward solutions may be estimated by equations or programs (Corwin 1989, Wilt and Butler 1990) for sphere, line, and plate potential configurations. These solutions of potential configurations aid in evaluation of the corrected field readings, but are solutions of the data set taken.

d. Sample field surveys.

(1) Geothermal use of the SP method is documented in Corwin and Hoover (1979). Erchul and Slifer (1989) provide the included example for karst surveys. The leakage of water from a reservoir (Butler et al. 1989, Llopis and Butler 1988) through an abutment and the movement of rainfall into and through a karst system produce streaming potentials. High reservoir leakage through rock or soil forms the greatest streaming potential when confined flow conduits develop instead of diffuse flow through pore space. SP surveys have been recommended for grouting location, split spacing and effectiveness.[1] The self-potential due to water flow is a direct parameter for the grouting remediation of reservoir leakage.

(2) SP methods can be very useful for karst groundwater regimes in quick surveys of a site or in long-term surveys during a rainy season. Sinkholes can be pathways of surface water flow. The subsurface flow in karst can be erratic. Figure 4-2 shows the ability of an SP survey to resolve groundwater flow. Note the grid approach used in the survey for this site. There can be a qualitative evaluation of the flow volume in different subsurface routes if the ground surface may be assumed parallel to the surface through the irregular flow paths.

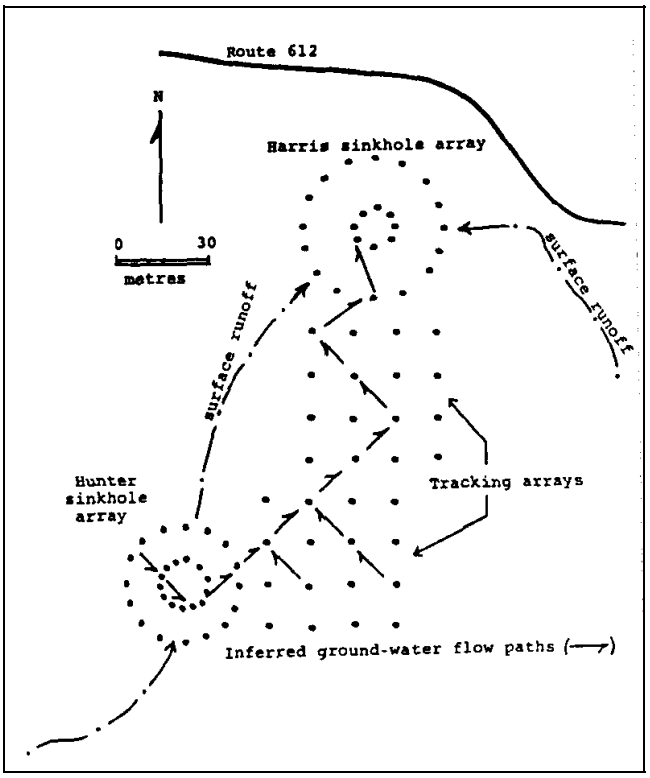

Figure 4-2. Electrode configurations at the Harris-Hunter sinkhole site, showing groundwater flowpaths inferred by SP anomalies (Erchul and Slifer 1989)

4-3. Equipotential and Mise-a-la-masse Methods

a. Introduction.

(1) According to Parasnis (1973), the equipotential method was one of the first electrical methods and was used as far back as 1912 by Schlumberger. As explained elsewhere in this volume, when electric energy is applied to two points at the ground surface, an electric current will flow between them because of their difference in

[1] Personal Communication, September 1992, David G. Taylor, Strata Services, St. Charles, MO.

potential. If the medium between the two electrodes is homogeneous, the current and potential distribution is regular and may be calculated. When good or poor conductors are imbedded in this homogeneous medium, a distortion of the electrical field occurs. Good conductors have a tendency to attract the current lines toward them while poor conductors force current flow away. Theoretically, it should be possible to detect bodies of different conductivity by measuring the geometric pattern of these current lines. In practice this cannot be done with sufficient accuracy; it is necessary to determine the direction in which no current flows by locating points which have no potential difference (Heiland 1940). The lines of identical potential, called "equipotential lines," are at right angles to the current lines. The equipotentials are circles in the immediate vicinity of the electrodes.

(2) In the past, equipotentials were traced individually in the field by using a null galvanometer, but such a procedure was tedious and time-consuming. The modern practice is to measure the electric voltage at each observation point with respect to a fixed point, plot the results, and draw contours. The equipotential method was used extensively in the early days of geophysics, but has been almost completely replaced by modern resistivity and electromagnetic methods. When the method is used, it is usually in a reconnaissance mode and quantitative interpretation of equipotential surveys is rarely attempted.

b. Mise-a-la-masse. One variant of the method, called mise-a-la-masse, is still used in mining exploration and occasionally in geotechnical applications. The name, which may be translated as "excitation of the mass," describes an electrode array which uses the conductive mass under investigation as one of the current electrodes. In mining, the conductive mass is a mineral body exposed in a pit or drill hole. In geotechnical applications the object under investigation might be one end of an abandoned metal waste pipe. The second current electrode is placed a large distance away. "Large" usually means five or ten times the size of the mass being investigated. The potential distribution from these two current electrodes will, to some extent, reflect the geometry of the conductive mass and would be expected to yield some information concerning the shape and extent of the body. The left-hand part of Figure 4-3 (Parasnis 1973) shows the equipotentials around a subsurface point electrode in a homogeneous isotropic earth. The right-hand part shows

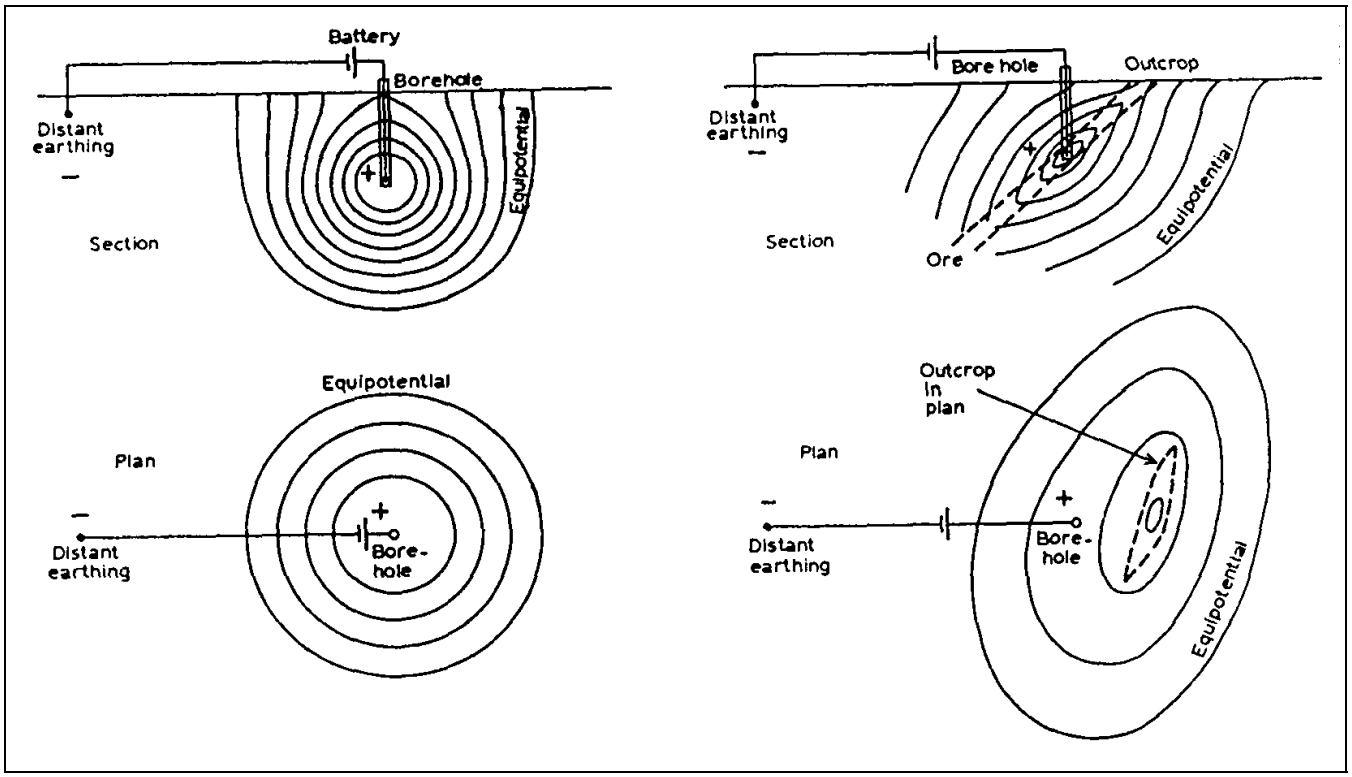

Figure 4-3. Principle of the mise-a-la-masse method. Right side of figure shows the distortion of the equipotential lines due to a conductive ore body (Parasnis 1973; copyright permission granted by Elsevier Science)

(schematically) the distribution of potentials such as might be expected when the point current electrode is placed in a conducting body situated in an otherwise homogeneous earth of lesser conductivity. In this case, the equipotentials tend to follow the ore body and on the ground surface the centroid of the equipotential map does not coincide with the point on the ground vertically above the electrode in the borehole.

(1) Example 1 - buried ammunition magazine. While classic equipotential surveys have all but been replaced by the mise-a-la-masse variant, there are occasions when passing an electric current directly through the mass under investigation might be ill-advised. Such a case is shown in Figure 4-4, in which Heiland (1940) shows the results of a classic equipotential survey over an abandoned ammunition magazine. Distortion of the equipotential lines clearly outlines the magazine, and shows that expensive and/or sophisticated techniques are not always necessary.

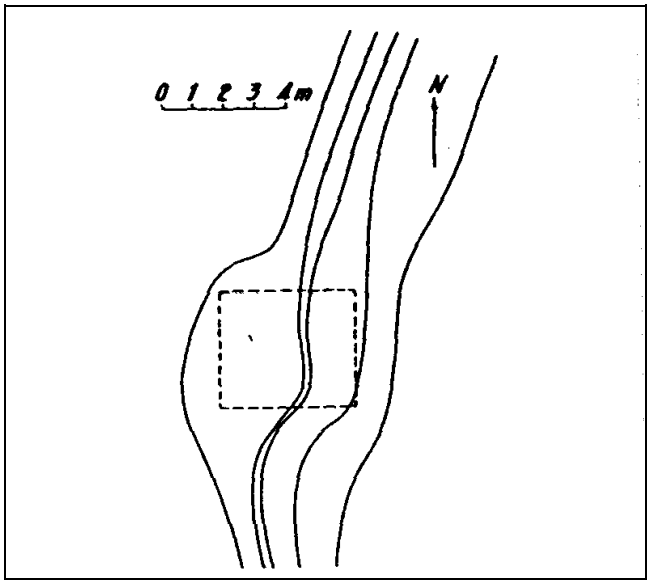

Figure 4-4. Location of a buried ammunition magazine by equipotential methods (Heiland 1940)

(2) Example 2 - advance of groundwater from an infiltration pit. Only one example of mise-a-la-masse used for groundwater investigations was found in the literature. Cahyna, Mazac, and Vendhodova (1990) claim mise-a-la-masse survey was successfully used to determine the prevailing direction of groundwater leaving an infiltration pit, but unfortunately no figures are included.

(3) Example 3 - partially exposed buried conductors. The need sometimes arises in hazardous-waste site restoration to trace the extent of buried metal objects such as pipes, cables, and tanks. Often electromagnetic and/or magnetic methods are used to trace these objects, but a special opportunity arises for surveying by mise-a-la-masse when part of the object under investigation has been partially exposed at the surface or in a drill hole. Although no geotechnical examples were found in the literature, one of the numerous mining examples will be used, as the results should be similar. Hallof (1980) shows the results of a mise-a-la-masse survey at York Harbour, Newfoundland, where sulfides were exposed in underground workings. The objective was to find where the ore most closely approached the surface and if the H-1 zone and the H-2 zone were the lower portions of a single zone near the surface. Figure 4-5 shows the equipotential pattern for the near current electrode located at depth but NOT in one of the ore zones. The patten pattern is nearly circular and its center is immediately above the current electrode at depth. This was not the case when the current electrode was placed first in the H-1 zone (Figure 4-6) and then in the H-2 zone (not shown). In both cases the center of the surface potential distribution is considerably to the east of the underground position of the mineralization. Further, since almost exactly the same potential distribution was measured for both locations for the current electrode at depth, both zone H-1 and zone H-2 are probably part of a single mineralization that has its most shallow position beneath the center of the surface potential pattern.

4-4. Resistivity Methods

a. Introduction. Surface electrical resistivity surveying is based on the principle that the distribution of electrical potential in the ground around a current-carrying electrode depends on the electrical resistivities and distribution of the surrounding soils and rocks. The usual practice in the field is to apply an electrical direct current (DC) between two electrodes implanted in the ground and to measure the difference of potential between two additional electrodes that do not carry current. Usually, the potential electrodes are in line between the current electrodes, but in principle, they can be located anywhere. The current used is either direct current, commutated direct current (i.e., a square-wave alternating current), AC of low frequency (typically about 20 Hz). All analysis and interpretation are done on the basis of direct currents. The distribution of potential can be related theoretically to ground resistivities and their distribution for some simple cases; notably, the case of a horizontally stratified ground and the case of homogeneous masses separated by vertical planes (e.g., a vertical fault with a large throw or a

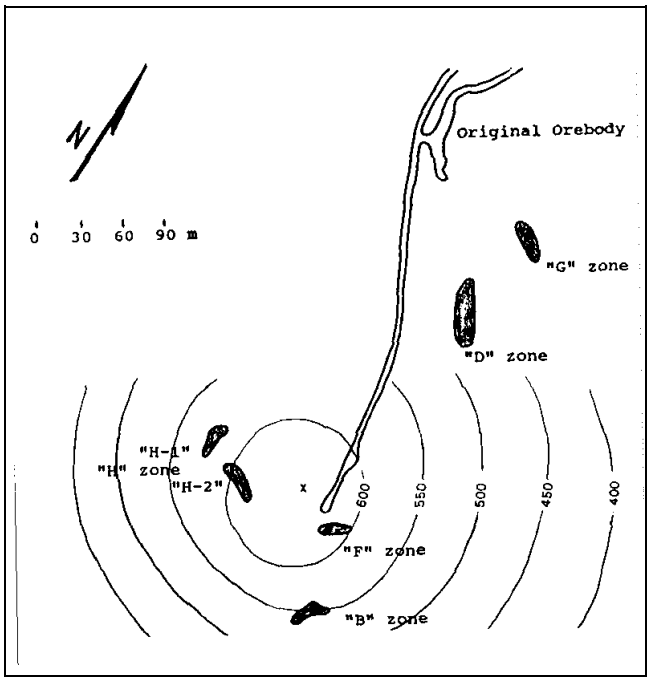

Figure 4-5. Potential pattern from current source in test position (modified from Hallof (1980))

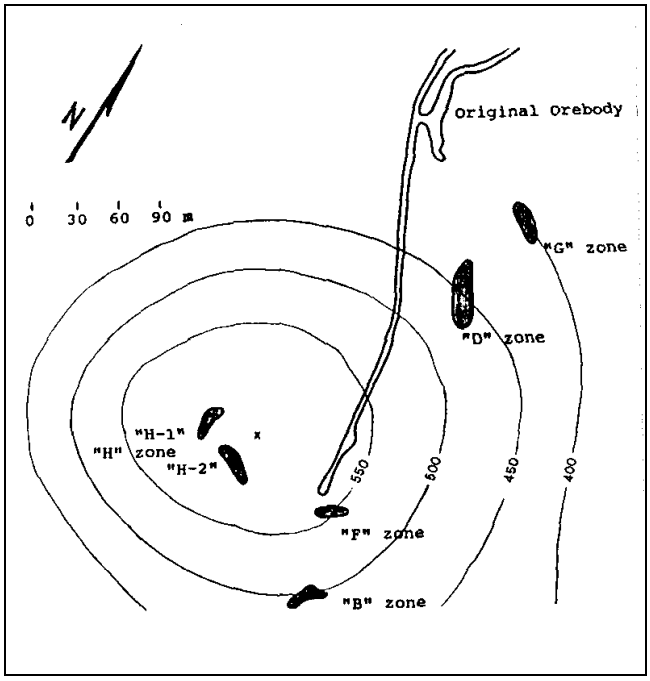

Figure 4-6. Potential pattern from current source in H-1 zone (modified from Hallof (1980))

vertical dike). For other kinds of resistivity distributions, interpretation is usually done by qualitative comparison of observed response with that of idealized hypothetical models or on the basis of empirical methods.

(1) Mineral grains composing soils and rocks are essentially nonconductive, except in some exotic materials such as metallic ores, so the resistivity of soils and rocks is governed primarily by the amount of pore water, its resistivity, and the arrangement of the pores. To the extent that differences of lithology are accompanied by differences of resistivity, resistivity surveys can be useful in detecting bodies of anomalous materials or in estimating the depths of bedrock surfaces. In coarse granular soils, the groundwater surface is generally marked by an abrupt change in water saturation and thus by a change of resistivity. In fine-grained soils, however, there may be no such resistivity change coinciding with a piezometric surface. Generally, since the resistivity of a soil or rock is controlled primarily by the pore water conditions, there are wide ranges in resistivity for any particular soil or rock type, and resistivity values cannot be directly interpreted in terms of soil type or lithology. Commonly, however, zones of distinctive resistivity can be associated with specific soil or rock units on the basis of local field or drill hole information, and resistivity surveys can be used profitably to extend field investigations into areas with very limited or nonexistent data. Also, resistivity surveys may be used as a reconnaissance method, to detect anomalies that can be further investigated by complementary geophysical methods and/or drill holes.

(2) The electrical resistivity method has some inherent limitations that affect the resolution and accuracy that may be expected from it. Like all methods using measurements of a potential field, the value of a measurement obtained at any location represents a weighted average of the effects produced over a large volume of material, with the nearby portions contributing most heavily. This tends to produce smooth curves, which do not lend themselves to high resolution for interpretations. There is another feature common to all potential field geophysical methods; a particular distribution of potential at the ground surface does not generally have a unique interpretation. While these limitations should be recognized, the non-uniqueness or ambiguity of the resistivity method is scarcely less than with the other geophysical methods. For these reasons, it is always advisable to use several complementary geophysical methods in an integrated exploration program rather than relying on a single exploration method.

b. Theory.

(1) Data from resistivity surveys are customarily presented and interpreted in the form of values of apparent resistivity ρ_a. Apparent resistivity is defined as the resistivity of an electrically homogeneous and isotropic half-space that would yield the measured relationship between the applied current and the potential difference for a particular arrangement and spacing of electrodes. An equation giving the apparent resistivity in terms of applied current, distribution of potential, and arrangement of electrodes can be arrived at through an examination of the potential distribution due to a single current electrode. The effect of an electrode pair (or any other combination) can be found by superposition. Consider a single point electrode, located on the boundary of a semi-infinite, electrically homogeneous medium, which represents a fictitious homogeneous earth. If the electrode carries a current I, measured in amperes (a), the potential at any point in the medium or on the boundary is given by

$$U = \rho \frac{I}{2\pi r} \tag{4-5}$$

where

U = potential, in V

ρ = resistivity of the medium

r = distance from the electrode

The mathematical demonstration for the derivation of the equation may be found in textbooks on geophysics, such as Keller and Frischknecht (1966).

(a) For an electrode pair with current I at electrode A, and -I at electrode B (Figure 4-7), the potential at a point is given by the algebraic sum of the individual contributions:

$$U = \frac{\rho I}{2\pi r_A} - \frac{\rho I}{2\pi r_B} = \frac{\rho I}{2\pi}\left[\frac{1}{r_A} - \frac{1}{r_B}\right] \tag{4-6}$$

where

r_A and r_B = distances from the point to electrodes A and B

Figure 4-7 illustrates the electric field around the two electrodes in terms of equipotentials and current lines.

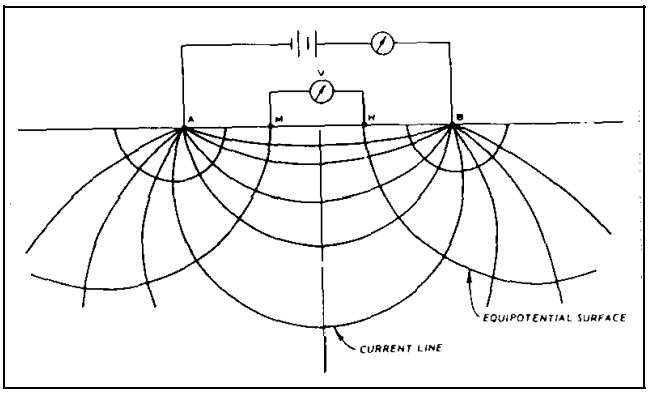

Figure 4-7. Equipotentials and current lines for a pair of current electrodes A and B on a homogeneous half-space

The equipotentials represent imagery shells, or bowls, surrounding the current electrodes, and on any one of which the electrical potential is everywhere equal. The current lines represent a sampling of the infinitely many paths followed by the current, paths that are defined by the condition that they must be everywhere normal to the equipotential surfaces.

(b) In addition to current electrodes A and B, Figure 4-7 shows a pair of electrodes M and N, which carry no current, but between which the potential difference V may be measured. Following the previous equation, the potential difference V may be written

$$V = U_M - U_N = \frac{\rho I}{2\pi}\left[\frac{1}{\overline{AM}} - \frac{1}{\overline{BM}} + \frac{1}{\overline{BN}} - \frac{1}{\overline{AN}}\right] \tag{4-7}$$

where

U_M and U_N = potentials at M and N

AM = distance between electrodes A and M, etc.

These distances are always the actual distances between the respective electrodes, whether or not they lie on a line. The quantity inside the brackets is a function only of the various electrode spacings. The quantity is denoted $1/K$, which allows rewriting the equation as

$$V = \frac{\rho I}{2\pi}\frac{1}{K} \quad (4\text{-}8)$$

where

K = array geometric factor

Equation 4-8 can be solved for ρ to obtain

$$\rho = 2\pi K \frac{V}{I} \quad (4\text{-}9)$$

The resistivity of the medium can be found from measured values of V, I, and K, the geometric factor. K is a function only of the geometry of the electrode arrangement.

(2) Apparent resistivity.

(a) Wherever these measurements are made over a real heterogeneous earth, as distinguished from the fictitious homogeneous half-space, the symbol ρ is replaced by ρ_a for apparent resistivity. The resistivity surveying problem is, reduced to its essence, the use of apparent resistivity values from field observations at various locations and with various electrode configurations to estimate the true resistivities of the several earth materials present at a site and to locate their boundaries spatially below the surface of the site.

(b) An electrode array with constant spacing is used to investigate lateral changes in apparent resistivity reflecting lateral geologic variability or localized anomalous features. To investigate changes in resistivity with depth, the size of the electrode array is varied. The apparent resistivity is affected by material at increasingly greater depths (hence larger volume) as the electrode spacing is increased. Because of this effect, a plot of apparent resistivity against electrode spacing can be used to indicate vertical variations in resistivity.

(3) The types of electrode arrays that are most commonly used (Schlumberger, Wenner, and dipole-dipole) are illustrated in Figure 4-8. There are other electrode configurations which are used experimentally or for non-geotechnical problems or are not in wide popularity today. Some of these include the Lee, half-Schlumberger, polar dipole, bipole dipole, and gradient arrays. In any case, the geometric factor for any four-electrode system can be found from Equation 4-7 and can be developed for more

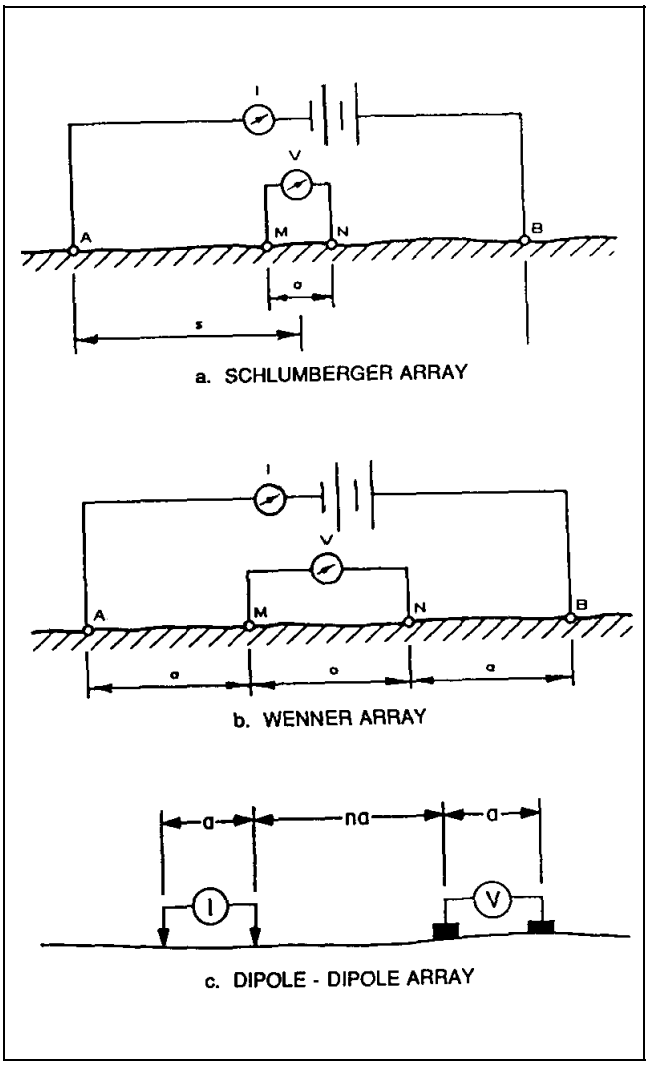

Figure 4-8. Electrode (array) configurations for resistivity measurements

complicated systems by using the rule illustrated by Equation 4-6. It can also be seen from Equation 4-7 that the current and potential electrodes can be interchanged without affecting the results; this property is called reciprocity.

(a) Schlumberger array (Figure 4-8a). For this array, in the limit as a approaches zero, the quantity V/a approaches the value of the potential gradient at the midpoint of the array. In practice, the sensitivity of the instruments limits the ratio of s to a and usually keeps it within the limits of about 3 to 30. Therefore, it is typical practice to use a finite electrode spacing and Equation 4-7 to compute the geometric factor (Keller and Frischknecht 1966). The apparent resistivity is:

$$\rho_a = \pi \left[\frac{s^2}{a} - \frac{a}{4} \right] \frac{V}{I} = \pi a \left[\left(\frac{s}{a} \right)^2 - \frac{1}{4} \right] \frac{V}{I} \qquad (4\text{-}10)$$

In usual field operations, the inner (potential) electrodes remain fixed, while the outer (current) electrodes are adjusted to vary the distance *s*. The spacing *a* is adjusted when it is needed because of decreasing sensitivity of measurement. The spacing *a* must never be larger than 0.4*s* or the potential gradient assumption is no longer valid. Also, the *a* spacing may sometimes be adjusted with *s* held constant in order to detect the presence of local inhomogeneities or lateral changes in the neighborhood of the potential electrodes.

(b) Wenner array. This array (Figure 4-8b) consists of four electrodes in line, separated by equal intervals, denoted *a*. Applying Equation 4-7, the user will find that the geometric factor K is equal to *a* , so the apparent resistivity is given by

$$\rho_a = 2\pi a \frac{V}{I} \qquad (4\text{-}11)$$

While the Schlumberger array has always been the favored array in Europe, until recently, the Wenner array was used more extensively than the Schlumberger array in the United States. In a survey with varying electrode spacing, field operations with the Schlumberger array are faster, because all four electrodes of the Wenner array are moved between successive observations, but with the Schlumberger array, only the outer ones need to be moved. The Schlumberger array also is said to be superior in distinguishing lateral from vertical variations in resistivity. On the other hand, the Wenner array demands less instrument sensitivity, and reduction of data is marginally easier.

(4) Dipole-dipole array. The dipole-dipole array (Figure 4-8c) is one member of a family of arrays using dipoles (closely spaced electrode pairs) to measure the curvature of the potential field. If the separation between both pairs of electrodes is the same *a* and the separation between the centers of the dipoles is restricted to *a(n+1)*, the apparent resistivity is given by

$$\rho_a = \pi \, a \, n(n+1)(n+2) \frac{V}{I} \qquad (4\text{-}12)$$

This array is especially useful for measuring lateral resistivity changes and has been increasingly used in geotechnical applications.

c. Depth of investigation. To illustrate the major features of the relationship between apparent resistivity and electrode spacing, Figure 4-9 shows a hypothetical earth model and some hypothetical apparent resistivity curves. The earth model has a surface layer of resistivity ρ_1 and a "basement" layer of resistivity ρ_n that extends downward to infinity. There may be intermediate layers of arbitrary thicknesses and resistivities. The electrode spacing may be either the Wenner spacing *a* or the Schlumberger spacing *a*; curves of apparent resistivity versus spacing will have the same general shape for both arrays, although they will not generally coincide.

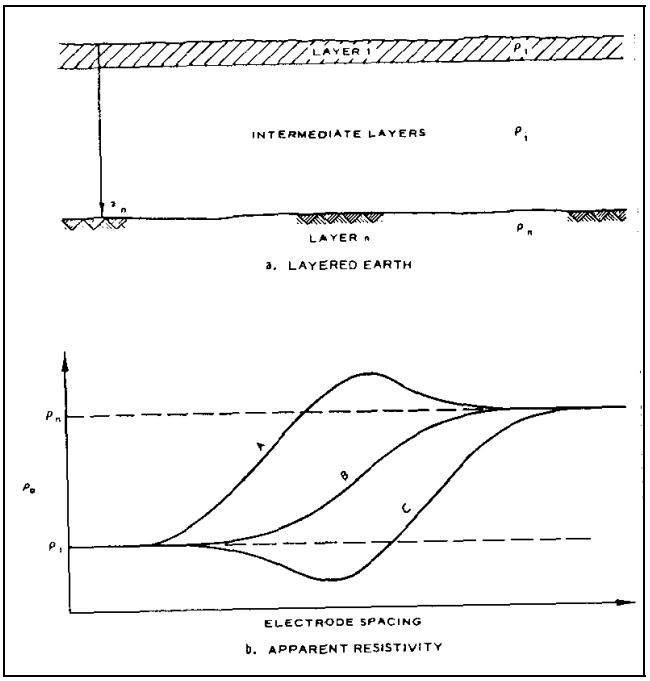

Figure 4-9. Asymptotic behavior of the apparent resistivity curves at very small and very large electrode spacings

(1) For small electrode spacings, the apparent resistivity is close to the surface layer resistivity, while at large electrode spacings, it approaches the resistivity of the basement layer. Every apparent resistivity curve thus has two asymptotes, the horizontal lines $\rho_a = \rho_1$ and $\rho_a = \rho_n$, that it approaches at extreme values of electrode

spacing. This is true whether ρ_n is greater than ρ_1, as shown in Figure 4-9b, or the reverse. The behavior of the curve between the regions where it approaches the asymptotes depends on the distribution of resistivities in the intermediate layers. Curve A represents a case in which there is an intermediate layer with a resistivity greater than ρ_n. The behavior of curve B resembles that for the two-layer case or a case where resistivities increase from the surface down to the basement. The curve might look like curve C if there were an intermediate layer with resistivity lower than ρ_1 . Unfortunately for the interpreter, neither the maximum of curve A nor the minimum of curve C reach the true resistivity values for the intermediate layers, though they may be close if the layers are very thick.

(2) There is no simple relationship between the electrode spacing at which features of the apparent resistivity curve are located and the depths to the interfaces between layers. The depth of investigation will ALWAYS be less than the electrode spacing. Typically, a maximum electrode spacing of three or more times the depth of interest is necessary to assure that sufficient data have been obtained. The best general guide to use in the field is to plot the apparent resistivity curve (Figure 4-9b) as the survey progresses, so that it can be judged whether the asymptotic phase of the curve has been reached.

d. Instruments and measurements. The theory and field methods used for resistivity surveys are based on the use of direct current, because it allows greater depth of investigation than alternating current and because it avoids the complexities caused by effects of ground inductance and capacitance and resulting frequency dependence of resistivity. However, in practice, actual direct current is infrequently used for two reasons: (1) direct current electrodes produce polarized ionization fields in the electrolytes around them, and these fields produce additional electromotive forces that cause the current and potentials in the ground to be different from those in the electrodes; and (2) natural earth currents (telluric currents) and spontaneous potentials, which are essentially unidirectional or slowly time-varying, induce potentials in addition to those caused by the applied current. The effects of these phenomena, as well as any others that produce unidirectional components of current or potential gradients, are reduced by the use of alternating current, because the polarized ionization fields do not have sufficient time to develop in a half-cycle, and the alternating component of the response can be measured independently of any superimposed direct currents. The frequencies used are very low, typically below 20 Hz, so that the measured resistivity is essentially the same as the direct current resistivity.

(1) In concept, a direct current (I), or an alternating current of low frequency, is applied to the current electrodes, and the current is measured with an ammeter. Independently, a potential difference *V* is measured across the potential electrodes, and ideally there should be no current flowing between the potential electrodes. This is accomplished either with a null-balancing galvanometer (old technology) or very high input impedance operational amplifiers. A few resistivity instruments have separate "sending" and "receiving" units for current and potential; but in usual practice, the potential measuring circuit is derived from the same source as the potential across the current electrodes, so that variations in the supply voltage affect both equally and do not affect the balance point.

(2) Power is usually supplied by dry cell batteries in the smaller instruments and motor generators in the larger instruments. From 90 V up to several hundred volts may be used across the current electrodes in surveys for engineering purposes. In the battery-powered units, the current usually is small and is applied only for very short times while the potential is being measured, so battery consumption is low. Care should be taken to NEVER energize the electrodes while they are being handled, because with applied potentials of hundreds of volts, DANGEROUS AND POTENTIALLY LETHAL shocks could be caused.

(3) Current electrodes used with alternating current (or commutated direct current) instruments commonly are stakes of bronze, copper, steel with bronze jackets, or, less desirably, steel, about 50 cm in length. They must be driven into the ground far enough to make good electrical contact. If there is difficulty because of high contact resistance between electrodes and soil, it can sometimes be alleviated by pouring salt water around the electrodes. Many resistivity instruments include an ammeter to verify that the current between the current electrodes is at an acceptable level, a desirable feature. Other instruments simply output the required potential difference to drive a selected current into the current electrodes. Typical currents in instruments used for engineering applications range from 2 mA to 500 mA. If the current is too small, the sensitivity of measurement is degraded. The problem may be corrected by improving the electrical contacts at the electrodes. However, if the problem is due to a combination of high earth resistivity and large electrode spacing, the remedy is to increase the voltage across the current electrodes. Where the ground is too hard or rocky

to drive stakes, a common alternative is sheets of aluminum foil buried in shallow depressions or within small mounds of earth and wetted.

(4) One advantage of the four-electrode method is that measurements are not sensitive to contact resistance at the potential electrodes so long as it is low enough that a measurement can be made, because observations are made with the system adjusted so that there is no current in the potential electrodes. With zero current, the actual value of contact resistance is immaterial, since it does not affect the potential. On the current electrodes, also, the actual value of contact resistance does not affect the measurement, so long as it is small enough that a satisfactory current is obtained, and so long as there is no gross difference between the two electrodes. Contact resistance affects the relationship between the current and the potentials on the electrodes, but because only the measured value of current is used, the potentials on these electrodes do not figure in the theory or interpretation.

(5) When direct current is used, special provisions must be made to eliminate the effects of electrode polarization and telluric currents. A nonpolarizing electrode is available in the form of a porous, unglazed ceramic pot, which contains a central metallic electrode, usually copper, and is filled with a liquid electrolyte that is a saturated solution of a salt of the same metal (copper sulphate is used with copper). The central electrode is connected to the instrument, and electrical contact with the ground is made through the electrolyte in the pores of the ceramic pot. This type of electrode may be advantageous for use on rock surfaces where driving rod-type electrodes is difficult. Good contact of the pot with the ground can be aided by clearing away grass and leaves beneath it, embedding it slightly in the soil, and if the ground is dry, pouring a small amount of water on the surface before placing the pot. The pots must be filled with electrolyte several hours before they are used to allow the electrolyte to penetrate the fine pores of the ceramic. The porous pot electrodes should be checked every several hours during the field day to verify the electrolyte level and the presence of the solid salt to maintain the saturated solution.

(6) Telluric currents are naturally occurring electric fields that are widespread, some being of global scale. They are usually of small magnitude, but may be very large during solar flares or if supplemented by currents of artificial origin. Spontaneous potentials in the earth may be generated by galvanic phenomena around electrochemically active materials, such as pipes, conduits, buried scrap materials, cinders, and ore deposits. They may also occur as streaming potentials generated by groundwater movement. (Electric fields associated with groundwater movement will have the greatest amplitude where groundwater flow rates are high, such as through subsurface open-channel flow. Groundwater movement in karst areas can exhibit rapid flow through dissolved channels within the rock. Springs and subsurface flow may be the cause of telluric sources, which may obscure resistivity measurements.) Telluric currents and spontaneous potential effects can be compensated by applying a bias potential to balance the potential electrodes before energizing the current electrodes. Because telluric currents generally vary with time, frequent adjustments to the bias potential may be necessary in the course of making an observation. If the instrument lacks a provision for applying a bias potential, a less satisfactory alternative is to use a polarity reversing switch to make readings with alternately reversed current directions in the current electrodes. The average values of V and I for the forward and reverse current directions are then used to compute the apparent resistivity.

(7) Layout of electrodes should be done with nonconducting measuring tapes, since tapes of conducting materials, if left on the ground during measurement, can influence apparent resistivity values. Resistivity measurements can also be affected by metallic fences, rails, pipes, or other conductors, which may induce spontaneous potentials and in addition provide short-circuit paths for the current. The effects of such linear conductors as these can be minimized, but not eliminated, by laying out the electrode array on a line perpendicular to the conductor; but in some locations, such as some urban areas, there may be so many conductive bodies in the vicinity that this cannot be done. Also, electrical noise from power lines, cables, or other sources may interfere with measurements. Because of the nearly ubiquitous noise from 60-Hz power sources in the United States, the use of 60 Hz or its harmonics in resistivity instruments is not advisable. In some cases, the quality of data affected by electrical noise can be improved by averaging values obtained from a number of observations; sometimes electrical noise comes from temporary sources, so better measurements can be obtained by waiting until conditions improve. Occasionally, ambient electrical noise and other disturbing factors at a site may make resistivity surveying infeasible. Modern resistivity instruments have capability for data averaging or stacking; this allows resistivity surveys to proceed in spite of most noisy site conditions and to improve signal-to-noise ratio for weak signals.

e. Field procedures. Resistivity surveys are made to satisfy the needs of two distinctly different kinds of

interpretation problems: (1) the variation of resistivity with depth, reflecting more or less horizontal stratification of earth materials; and (2) lateral variations in resistivity that may indicate soil lenses, isolated ore bodies, faults, or cavities. For the first kind of problem, measurements of apparent resistivity are made at a single location (or around a single center point) with systematically varying electrode spacings. This procedure is sometimes called vertical electrical sounding (VES), or vertical profiling. Surveys of lateral variations may be made at spot or grid locations or along definite lines of traverse, a procedure sometimes called horizontal profiling.

(1) Vertical electrical sounding (VES). Either the Schlumberger or, less effectively, the Wenner array is used for sounding, since all commonly available interpretation methods and interpretation aids for sounding are based on these two arrays. In the use of either method, the center point of the array is kept at a fixed location, while the electrode locations are varied around it. The apparent resistivity values, and layer depths interpreted from them, are referred to the center point.

(a) In the Wenner array, the electrodes are located at distances of a/2 and 3a/2 from the center point. The most convenient way to locate the electrode stations is to use two measuring tapes, pinned with their zero ends at the center point and extending away from the center in opposite directions. After each reading, each potential electrode is moved out by half the increment in electrode spacing, and each current electrode is moved out by 1.5 times the increment. The increment to be used depends on the interpretation methods that will be applied. In most interpretation methods, the curves are sampled at logarithmically spaced points. The ratio between successive spacings can be obtained from the relation

$$\frac{a_i}{a_{i-1}} = 10^{\frac{1}{n}} \qquad (4\text{-}13)$$

where

n = number of points to be plotted in each logarithmic cycle

For example, if six points are wanted for each cycle of the logarithmic plot, then each spacing a will be equal to 1.47 times the previous spacing. The sequence starting at 10 m would then be 10, 14.7, 21.5, 31.6, 46.4, 68.2, which for convenience in layout and plotting could be rounded to 10, 15, 20, 30, 45, 70. In the next cycle, the spacings would be 100, 150, 200, and so on. Six points per cycle is the minimum recommended; 10, 12, or even more per cycle may be necessary in noisy areas.

(b) VES surveys with the Schlumberger array are also made with a fixed center point. An initial spacing s (the distance from the center of the array to either of the current electrodes) is chosen, and the current electrodes are moved outward with the potential electrodes fixed. According to Van Nostrand and Cook (1966) errors in apparent resistivity are within 2 to 3 percent if the distance between the potential electrodes does not exceed $2s/5$. Potential electrode spacing is therefore determined by the minimum value of s. As s is increased, the sensitivity of the potential measurement decreases; therefore, at some point, if s becomes large enough, it will be necessary to increase the potential electrode spacing. The increments in s should normally be logarithmic and can be chosen in the same way as described for the Wenner array.

(c) For either type of electrode array, minimum and maximum spacings are governed by the need to define the asymptotic phases of the apparent resistivity curve and the needed depth of investigation. Frequently, the maximum useful electrode spacing is limited by available time, site topography, or lateral variations in resistivity. For the purpose of planning the survey, a maximum electrode spacing of a least three times the depth of interest may be used, but the apparent resistivity curve should be plotted as the survey progresses in order to judge whether sufficient data have been obtained. Also, the progressive plot can be used to detect errors in readings or spurious resistivity values due to local effects. Sample field data sheets are shown in Figures 4-10 through 4-12.

(2) In a normal series of observations, the total resistance, $R = V/I$, decreases with increasing electrode spacing. Occasionally, the normal relationship may be reversed for one or a few readings. If these reversals are not a result of errors in reading, they are caused by some type of lateral or local changes in resistivity of the soil or rock. Such an effect can be caused by one current electrode being placed in a material of much higher resistivity than that around the other; for instance, in a pocket of dry gravel, in contact with a boulder of highly resistive rock, or close to an empty cavity. Systematic reversals might be caused by thinning of a surface conductive stratum where an underlying resistant stratum approaches the surface because it dips steeply or because of surface topography. In hilly terrains, the line of electrodes should be laid out along a contour if possible. Where beds are known to dip steeply (more than about 10 deg), the line

SCHLUMBERGER ELECTRICAL RESISTIVITY DATA SHEET

STATION NO. _____ DIRECTION _____ DATE_____

PROJECT _____ LOCATION _____

OPERATOR _____ EQUIP _____

REMARKS _____

$$\rho_a = \pi b \left[\left(\frac{a}{b}\right) - \frac{1}{4}\right]\frac{V}{I}$$

a (AB)/2 (m)	b MN (m)	V (mv)	I (ma)	R=V/I (ohms)	ρ_a (ohm-m)	remarks

Figure 4-10. Data sheet for Schlumberger vertical sounding

WENNER ELECTRICAL RESISTIVITY DATA SHEET

STATION NO. _____ DIRECTION _____ DATE_____

PROJECT _____ LOCATION _____

OPERATOR _____ EQUIP _____

REMARKS _____

$$\rho_a = 2 \pi a \frac{V}{I}$$

a (m)	V (mv)	I (ma)	R=V/I (ohms)	ρ_a (ohm-m)	remarks

Figure 4-11. Data sheet for Wenner array

DIPOLE-DIPOLE ELECTRICAL RESISTIVITY DATA SHEET

STATION NO. _____ DIRECTION _____ DATE_____

PROJECT _____ LOCATION _____

OPERATOR _____ EQUIP _____

REMARKS _____ DIPOLE LENGTH ____ m

$$\rho_a = \pi\, a\, n(n+1)(n+2)\, \frac{V}{I}$$

TX	RX	n	V (mv)	I (ma)	R=V/I (ohms)	ρ_a (ohm-m)	remarks

Figure 4-12. Data sheet for dipole-dipole array

should be laid out along the strike. Electrodes should not be placed in close proximity to boulders, so it may sometimes be necessary to displace individual electrodes away from the line. The theoretically correct method of displacing one electrode, e.g., the current electrode A, would be to place it at a new position A' such that the geometric factor *K* is unchanged. This condition would be satisfied (see Equation 4-7) if

$$\frac{1}{AM} - \frac{1}{AN} = \frac{1}{A'M} - \frac{1}{A'N} \qquad (4\text{-}14)$$

If the electrode spacing is large as compared with the amount of shift, it is satisfactory to shift the electrode on a line perpendicular to the array. For large shifts, a reasonable approximation is to move the electrode along an arc centered on the nearest potential electrode, so long as it is not moved more than about 45 deg off the line.

(3) The plot of apparent resistivity versus spacing is always a smooth curve where it is governed only by vertical variation in resistivity. Reversals in resistance and irregularities in the apparent resistivity curve, if not due to errors, both indicate lateral changes and should be further investigated. With the Wenner array, the Lee modification may be used to detect differences from one side of the array to the other, and a further check can be made by taking a second set of readings at the same location but on a perpendicular line. Where the Schlumberger array is used, changing the spacing of the potential electrodes may produce an offset in the apparent resistivity curve as a result of lateral inhomogeneity. Such an offset may occur as an overall shift of the curve without much change in its shape (Zohdy 1968). Under such conditions, the cause of the offset can often be determined by repeating portions of the sounding with different potential electrode spacing.

(4) Horizontal profiling. Surveys of lateral variations in resistivity can be useful for the investigation of any geological features that can be expected to offer resistivity contrasts with their surroundings. Deposits of gravel, particularly if unsaturated, have high resistivity and have been successfully prospected for by resistivity methods. Steeply dipping faults may be located by resistivity traverses crossing the suspected fault line, if there is sufficient resistivity contrast between the rocks on the two sides of the fault. Solution cavities or joint openings may be detected as a high resistivity anomaly, if they are open, or low resistivity anomaly if they are filled with soil or water.

(a) Resistivity surveys for the investigation of areal geology are made with a fixed electrode spacing, by moving the array between successive measurements. Horizontal profiling, per se, means moving the array along a line of traverse, although horizontal variations may also be investigated by individual measurements made at the points of a grid. If a symmetrical array, such as the Schlumberger or Wenner array, is used, the resistivity value obtained is associated with the location of the center of the array. Normally, a vertical survey would be made first to determine the best electrode spacing. Any available geological information, such as the depth of the features of interest, should also be considered in making this decision, which governs the effective depth of investigation. The spacing of adjacent resistivity stations, or the fineness of the grid, governs the resolution of detail that may be obtained. This is very much influenced by the depths of the features, and the achievable resolution diminishes with depth. As a general rule, the spacing between resistivity stations should be smaller than the width of the smallest feature to be detected, or smaller than the required resolution in the location of lateral boundaries.

(b) Field data may be plotted in the form of profiles or as contours on a map of the surveyed area. For a contour map, resistivity data obtained at grid points are preferable to those obtained from profile lines, unless the lines are closely spaced, because the alignment of data along profiles tends to distort the contour map and gives it an artificial "grain" that is distracting and interferes with interpretation of the map. The best method of data collection for a contour map is to use a square grid, or at least a set of stations with uniform coverage of the area, and without directional bias.

(c) Occasionally, a combination of vertical and horizontal methods may be used. Where mapping of the depth to bedrock is desired, a vertical sounding may be done at each of a set of grid points. However, before a commitment is made to a comprehensive survey of this type, the results of resistivity surveys at a few stations should be compared with the drill hole logs. If the comparison indicates that reliable quantitative interpretation of the resistivity can be made, the survey can be extended over the area of interest.

(d) When profiling is done with the Wenner array, it is convenient to use a spacing between stations equal to the electrode spacing, if this is compatible with the spacing requirements of the problem and the site conditions.

In moving the array, the rearmost electrode need only be moved a step ahead of the forward electrode, by a distance equal to the electrode spacing. The cables are then reconnected to the proper electrodes and the next reading is made. With the Schlumberger array, however, the whole set of electrodes must be moved between stations.

(5) Detection of cavities. Subsurface cavities most commonly occur as solution cavities in carbonate rocks. They may be empty or filled with soil or water. In favorable circumstances, either type may offer a good resistivity contrast with the surrounding rock since carbonate rocks, unless porous and saturated, usually have high resistivities, while soil or water fillings are usually conductive, and the air in an empty cavity is essentially nonconductive. Wenner or Schlumberger arrays may be used with horizontal profiling to detect the resistivity anomalies produced by cavities, although reports in the literature indicate mixed success. The probability of success by this method depends on the site conditions and on the use of the optimum combination of electrode spacing and interval between successive stations. Many of the unsuccessful surveys are done with an interval too large to resolve the anomalies sought.

f. Interpretation of vertical electrical sounding data. The interpretation problem for VES data is to use the curve of apparent resistivity versus electrode spacing, plotted from field measurements, to obtain the parameters of the geoelectrical section: the layer resistivities and thicknesses. From a given set of layer parameters, it is always possible to compute the apparent resistivity as a function of electrode spacing (the VES curve); but unfortunately, for the converse of that problem, it is not generally possible to obtain a unique solution. There is an interplay between thickness and resistivity; there may be anisotropy of resistivity in some strata; large differences in geoelectrical section, particularly at depth, produce small differences in apparent resistivity; and accuracy of field measurements is limited by the natural variability of surface soil and rock and by instrument capabilities. As a result, different sections may be electrically equivalent within the practical accuracy limits of the field measurements.

(1) To deal with the problem of ambiguity, the interpreter should check all interpretations by computing the theoretical VES curve for the interpreted section and comparing it with the field curve. The test of geological reasonableness should be applied. In particular, interpreted thin beds with unreasonably high resistivity contrasts are likely to be artifacts of interpretation rather than real features. Adjustments to the interpreted values may be made on the basis of the computed VES curves and checked by computing the new curves. Because of the accuracy limitations caused by instrumental and geological factors, effort should not be wasted on excessive refinement of the interpretation. As an example, suppose a set of field data and a three-layer theoretical curve agree within 10 percent. Adding several thin layers to achieve a fit of 2 percent is rarely a “better” geologic fit.

(2) All of the direct interpretation methods, except some empirical and semi-empirical methods such as the Moore cumulative method and the Barnes layer method which should be avoided, rely on curve-matching, in some form, to obtain the layer parameters. Because the theoretical curves are always smooth, the field curves should be smoothed before their interpretation is begun, to remove obvious observational errors and effects of lateral variability. Isolated one-point “spikes” in resistivity are removed rather than interpolated. The curves should be inspected for apparent distortion due to effects of lateral variations. Comparison with theoretical multilayer curves is helpful in detecting such distortion. The site conditions should be considered; excessive dip of subsurface strata along the survey line (more than about 10 percent), unfavorable topography, or known high lateral variability in soil or rock properties may be reasons to reject field data as unsuitable for interpretation in terms of simple vertical variation of resistivity.

(a) The simplest multilayer case is that of a single layer of finite thickness overlying a homogeneous half-space of different resistivity. The VES curves for this case vary in a relatively simple way, and a complete set of reference curves can be plotted on a single sheet of paper. Standard two-layer curves for the Schlumberger array are included in Figure 4-13. The curves are plotted on a logarithmic scale, both horizontally and vertically, and are normalized by plotting the ratio of apparent resistivity to the first layer resistivity (ρ_a/ρ_1) against the ratio of electrode spacing to the first layer thickness (a/d_1). Each curve of the family represents one value of the parameter *k*, which is defined by

$$k = \frac{\rho_2 - \rho_1}{\rho_2 + \rho_1} \tag{4-15}$$

Because the apparent resistivity for small electrode spacings approaches ρ_1 and for large spacings approaches ρ_2, these curves begin at $\rho_a/\rho_1 = 1$, and asymptotically approach $\rho_a/\rho_1 = \rho_2/\rho_1$.

(b) Any two-layer curve for a particular value of k, or for a particular ratio of layer resistivities, must have the same shape on the logarithmic plot as the corresponding standard curve. It differs only by horizontal and vertical shifts, which are equal to the logarithms of the thickness and resistivity of the first layer. The early (i.e., corresponding to the smaller electrode spacings) portion of more complex multiple-layer curves can also be fitted to two-layer curves to obtain the first layer parameters ρ_1 and d_1 and the resistivity ρ_2 of layer 2. The extreme curves in Figure 4-13 correspond to values of k equal to 1.0 and -1.0; these values represent infinitely great resistivity contrasts between the upper and lower layers. The first case represents a layer 2 that is a perfect insulator; the second, a layer 2 that is a perfect conductor. The next nearest curves in both cases represent a ratio of 19 in the layer resistivities. Evidently, where the resistivity contrast is more than about 20 to 1, fine resolution of the layer 2 resistivity cannot be expected. Loss of resolution is not merely an effect of the way the curves are plotted, but is representative of the basic physics of the problem and leads to ambiguity in the interpretation of VES curves.

(c) Where three or more strata of contrasting resistivity are present, the VES curves are more complex than the two-layer curves. For three layers, there are four possible types of VES curves, as shown in Figure 4-14, depending on the nature of the successive resistivity contrasts. The classification of these curves is found in the literature with the notations H, K, A, and Q. These symbols correspond respectively to bowl-type curves, which occur with an intermediate layer of lower resistivity than layers 1 or 3; bell-type curves, where the intermediate layer is of higher resistivity; ascending curves, where resistivities successively increase; and descending curves, where resistivities successively decrease. With four layers, another curve segment is present, so that 16 curve types can be identified: HK for a bowl-bell curve, AA for a monotonically ascending curve, and so on.

(d) Before the availability of personal computers, the curve matching process was done graphically by plotting the field data plotted on transparent log-log graph paper at the same scale of catalogs of two- and three-layer standard curves. The use of standard curves requires an identification of the curve type followed by a comparison with standard curves of that type to obtain the best match. Two-layer and three-layer curves can be used for complete interpretation of VES curves of more layers by the Auxiliary Point Method, which requires the use of a small set of auxiliary curves and some constructions. Discussions and step-by-step examples of this method are given by Zohdy (1965), Orellana and Mooney (1966), and Keller and Frischknecht (1966). Sets of standard curves have been developed by several workers. Orellana and Mooney (1966) published a set of 1,417 two-, three-, and four-layer Schlumberger curves, accompanied by a set of auxiliary curves, and tabulated values for both Schlumberger and Wenner curves. Apparent resistivity values for 102 three-layer Wenner curves were published by Wetzel and McMurray (1937). A collection of 2,400 two-, three-, and four-layer curves was published by Mooney and Wetzel (1956). Most, if not all, of these publications are out of print, but copies may be available in libraries.

(3) Ghosh (1971a, 1971b) and Johansen (1975) used linear filter theory to develop a fast numerical method for computing apparent resistivity values from the resistivity transforms, and vice versa. With these methods, new standard curves or trial VES curves can be computed as needed, with a digital computer or a calculator, either to match the curves or to check the validity of an interpretation of the field data. Thus, trial-and-error interpretation of VES data is feasible. Trial values of the layer parameters can be guessed, checked with a computed apparent resistivity curve, and adjusted to make the field and computed curves agree. The process will be much faster, of course, if the initial guess is guided by a semiquantitative comparison with two- and three-layer curves. Computer programs have been written by Zohdy (1973, 1974a, 1975), Zohdy and Bisdorf (1975), and several commercial software companies for the use of this method to obtain the layer parameters automatically by iteration, starting with an initial estimate obtained by an approximate method. Most computer programs require a user-supplied initial estimate (model), while some programs can optionally generate the initial mode. After a suite of sounding curves have been individually interpreted in this manner, a second pass can be made where certain layer thicknesses and/or resistivities can be fixed to give a more consistent project-wide interpretation.

g. Interpretation of horizontal profiling data. Data obtained from horizontal profiling, for engineering applications, are normally interpreted qualitatively. Apparent resistivity values are plotted and contoured on maps, or plotted as profiles, and areas displaying anomalously high or low values, or anomalous patterns, are identified. Interpretation of the data, as well as the planning of the survey, must be guided by the available knowledge of the local geology. The interpreter normally knows what he is looking for in terms of geological features and their expected influence on apparent resistivity, because the resistivity survey is motivated by geological evidence of a particular kind of exploration problem (e.g., karst terrain).

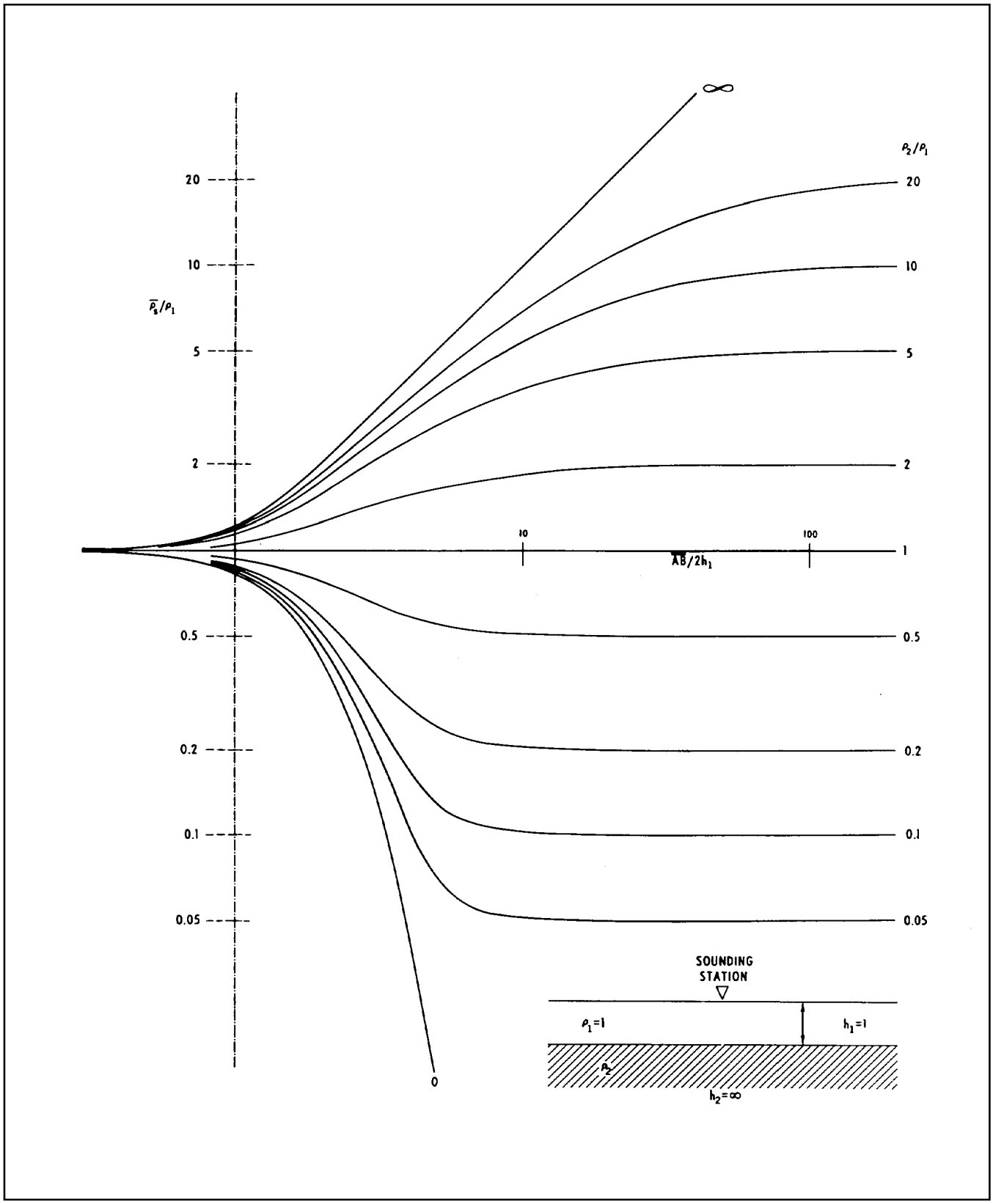

Figure 4-13. Two-layer master set of sounding curves for the Schlumberger array (Zohdy 1974a, 1974b)

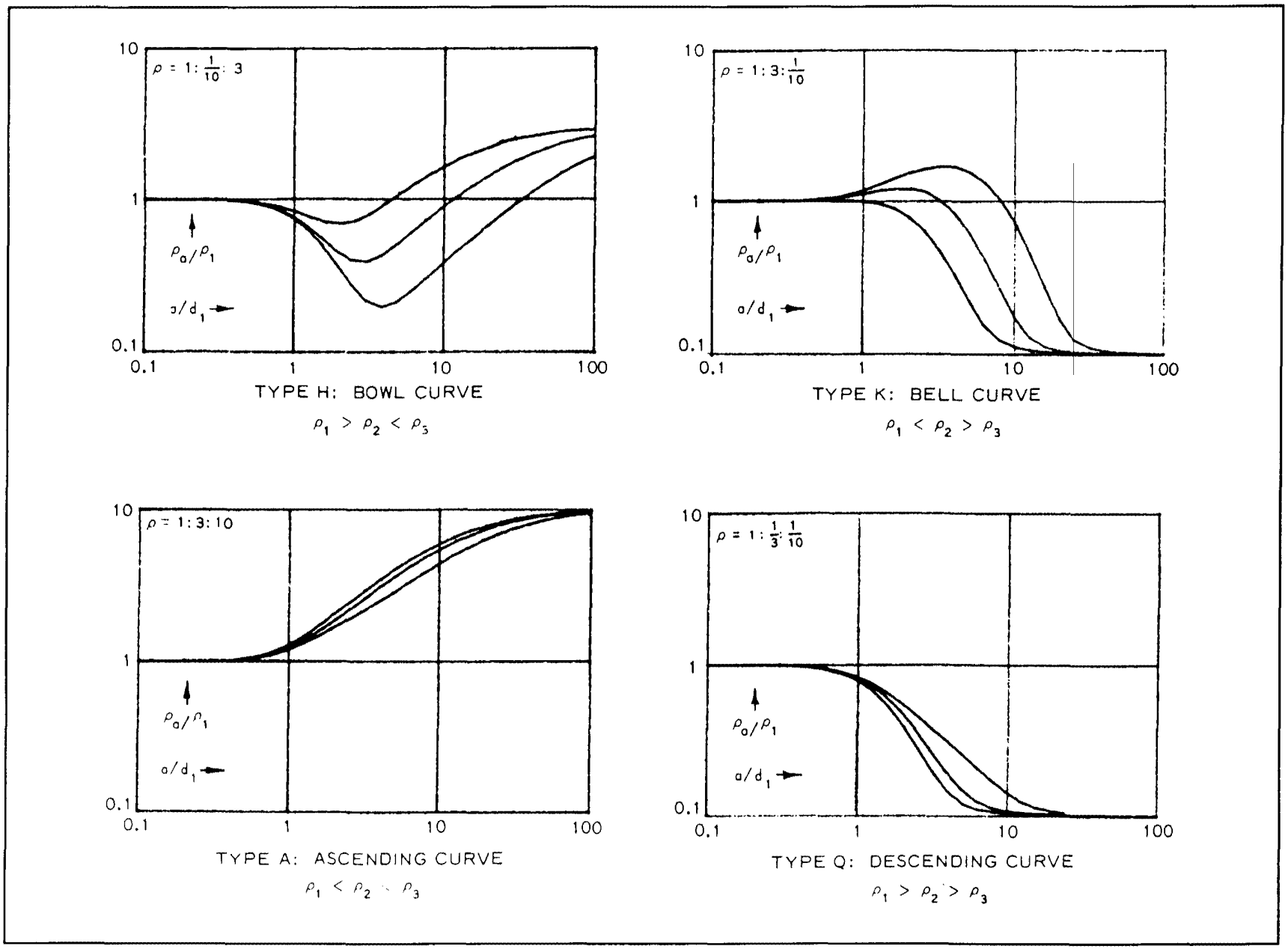

Figure 4-14. Four types of three-layer VES curves; the three sample curves for each of the four types represent values of d2/d1 = 1/3, 1, and 3

The survey is then executed in a way that is expected to be most responsive to the kinds of geological or hydrogeological features sought. A pitfall inherent in this approach is that the interpreter may be misled by his preconceptions if he is not sufficiently alert to the possibility of the unexpected occurring. Alternative interpretations should be considered, and evidence from as many independent sources as possible should be applied to the interpretation. One way to help plan the survey is to construct model VES sounding curves for the expected models, vary each model parameter separately by say 20 percent and then choose electrode separations that will best resolve the expected resistivity/depth variations. Most investigators then perform a number of VES soundings to verify and refine the model results before commencing horizontal profiling.

(1) The construction of theoretical profiles is feasible for certain kinds of idealized models, and the study of such profiles is very helpful in understanding the significance of field profiles. Van Nostrand and Cook (1966) give a comprehensive discussion of the theory of electrical resistivity interpretation and numerous examples of resistivity profiles over idealized models of faults, dikes, filled sinks, and cavities.

(2) Figure 4-15 illustrates a theoretical Wenner profile crossing a fault, a situation that can be thought of more generally as a survey line crossing any kind of abrupt transition between areas of different resistivity. The figure compares a theoretical curve, representing continuous variation of apparent resistivity with location of the center of the electrode array, and a theoretical field curve that would be obtained with an interval of $a/2$ between stations. More commonly, an interval equal to the electrode spacing would be used; various theoretical field curves for that case can be drawn by connecting points on the continuous curve at intervals of a. These curves would fail to reveal much of the detail of the continuous curve and could look quite different from one another. Figure 4-16 illustrates a profile across a shale-filled sink (i.e., a body of relatively low resistivity) and compares it with the theoretical continuous curve and a theoretical field curve. The theoretical curves are for a conductive body exposed at the surface, while the field case has a thin cover of alluvium, but the curves are very similar. Figure 4-17a shows a number of theoretical continuous profiles across buried perfectly insulating cylinders. This model would closely approximate a subsurface tunnel and less closely an elongated cavern. A spherical cavern would produce a similar response but with less pronounced maxima and minima. Figure 4-17b shows a set of similar curves for cylinders of various resistivity contrasts.

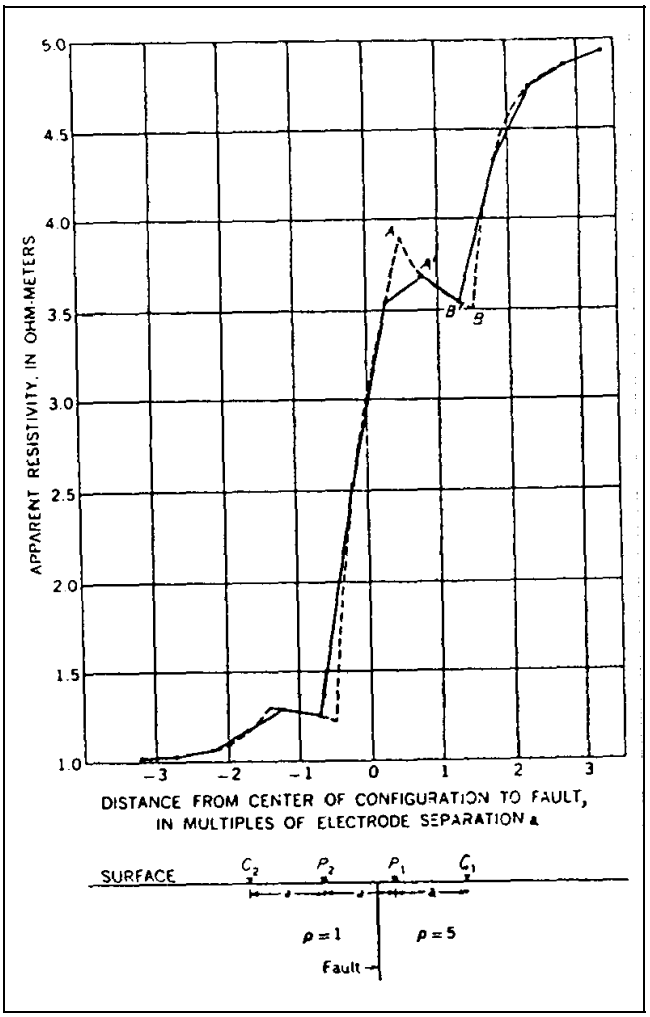

Figure 4-15. Wenner horizontal resistivity profile over a vertical fault; typical field curve (solid line), theoretical curve (dashed line) (Van Nostrand and Cook 1966)

4-5. Induced Polarization

a. Introduction. Conrad Schlumberger (Dobrin 1960) probably was first to report the induced polarization phenomenon, which he called "provoked polarization." While making conventional resistivity measurements, he noted that the potential difference, measured between the potential electrodes, often did not drop instantaneously to zero when the current was turned off. Instead, the potential difference dropped sharply at first, then gradually decayed to zero after a given interval of time. Certain layers in the ground can become electrically polarized,

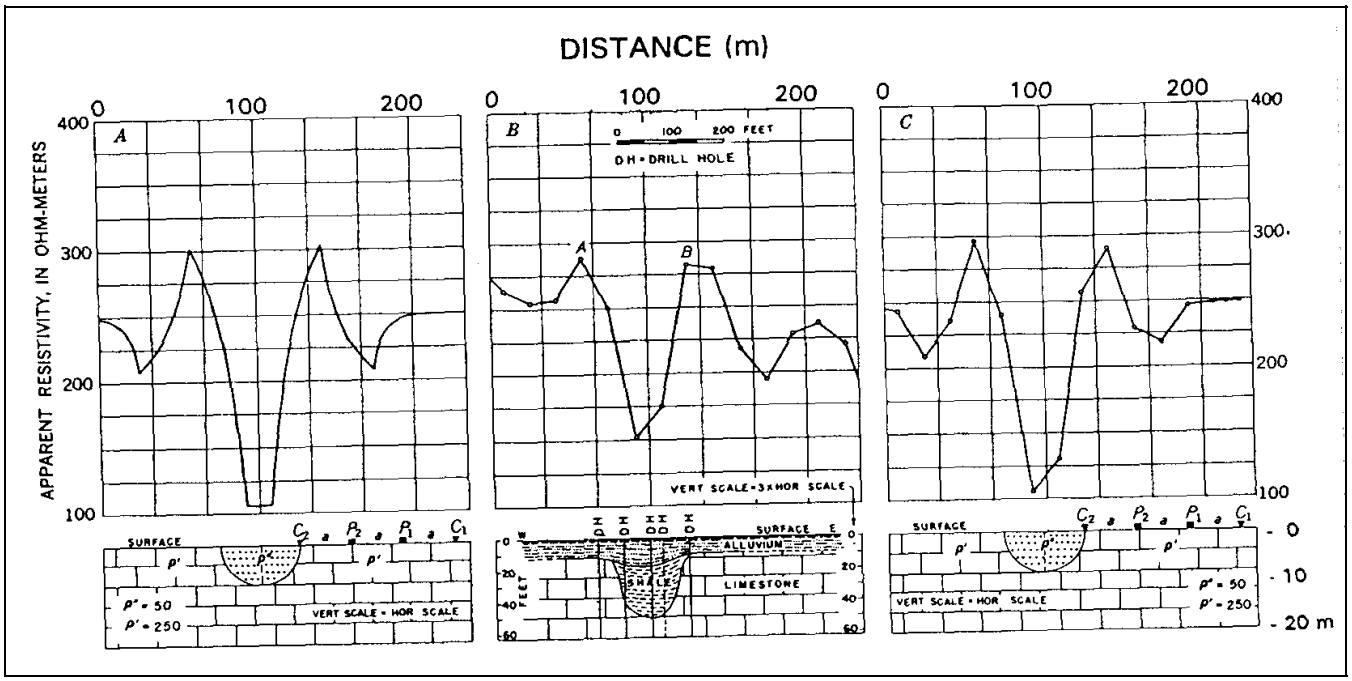

Figure 4-16. Wenner horizontal resistivity profiles over a filled sink: (a) continuous theoretical curve over hemispherical sink, (b) observed field curve with geologic cross section, (c) theoretical field plot over hemispherical sink (Van Nostrand and Cook 1966)

forming a battery when energized with an electric current. Upon turning off the polarizing current, the ground gradually discharges and returns to equilibrium.

(1) The study of the decaying potential difference as a function of time is now known as the study of induced polarization (IP) in the "time domain." In this method the geophysicist looks for portions of the earth where current flow is maintained for a short time after the applied current is terminated. Another technique is to study the effect of alternating currents on the measured value of resistivity, which is called IP in the "frequency domain." In this method the geophysicist tries to locate portions of the earth where resistivity decreases as the frequency of applied current is increased. The induced electrical polarization method is widely used in exploration for ore bodies, principally of disseminated sulfides. Use of IP in geotechnical and engineering applications has been limited, and has been mainly for groundwater exploration. Groundwater IP studies generally have been made with time-domain IP.

(2) General theory of the IP effect. The origin of induced electrical polarization is complex and is not well understood. This is primarily because several physiochemical phenomena and conditions are likely responsible for its occurrence. Only a fairly simple discussion will be given here. According to Seigel (1970), when a metal electrode is immersed in a solution of ions of a certain concentration and valence, a potential difference is established between the metal and the solution sides of the interface. This difference in potential is an explicit function of the ion concentration, valence, etc. When an external voltage is applied across the interface, a current is caused to flow and the potential drop across the interface changes from its initial value. The change in interface voltage is called the 'overvoltage' or 'polarization' potential of the electrode. Overvoltages are due to an accumulation of ions on the electrolyte side of the interface, waiting to be discharged. The time constant of buildup and decay is typically several tenths of a second.

(a) Overvoltage is therefore established whenever current is caused to flow across an interface between ionic and electronic conduction. In normal rocks the current which flows under the action of an applied emf does so by ionic conduction in the electrolyte in the pores of the rock. There are, however, certain minerals which have a measure of electronic conduction (almost all the metallic sulfides (except sphalerite) such as pyrite, graphite, some coals, magnetite, pyrolusite, native metals, some arsenides, and other minerals with a metallic lustre). Figure 4-18 is a simplified representation of how overvoltages are formed on an electronic conducting particle in an electrolyte under the influence of current flow.

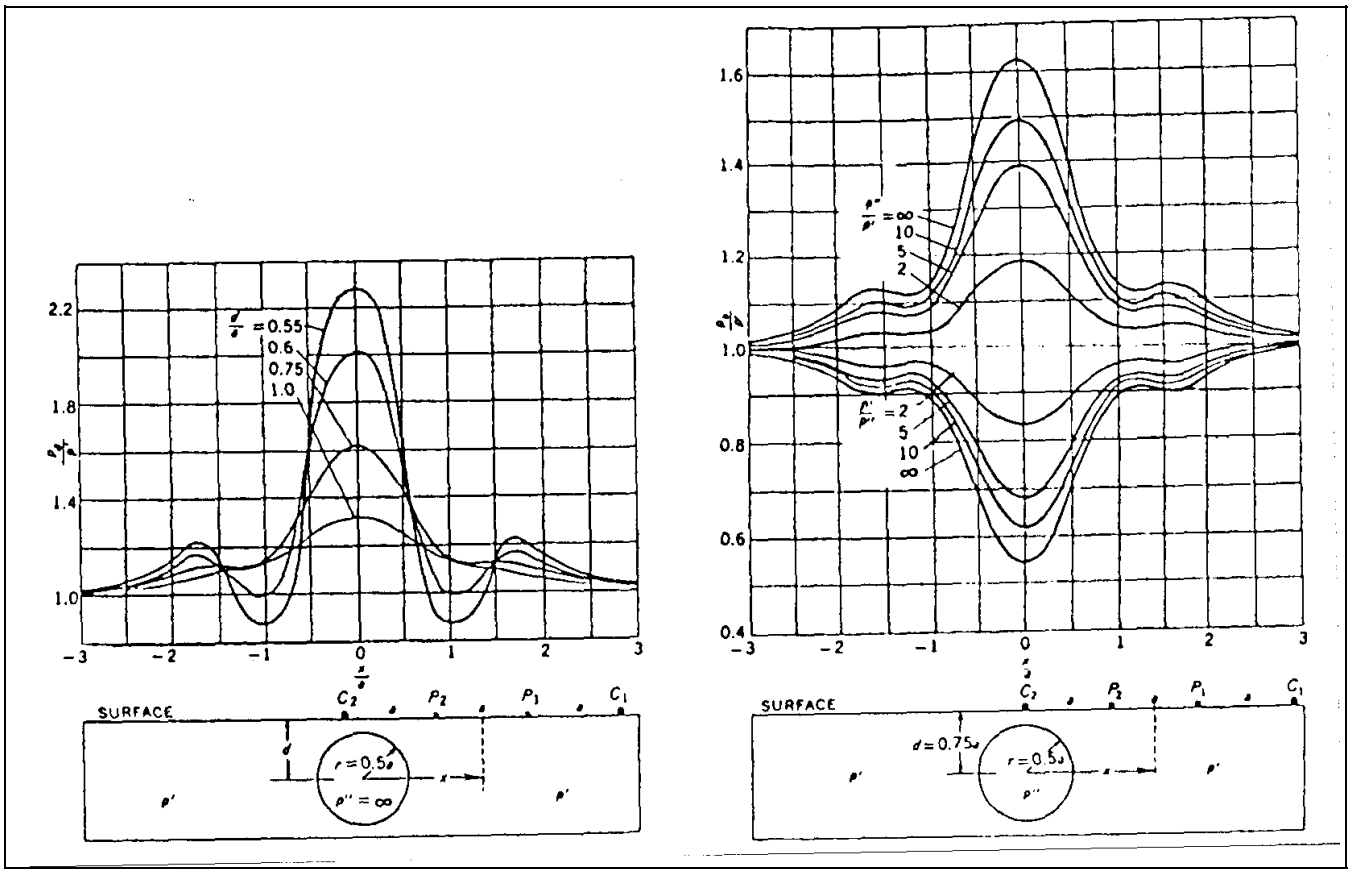

Figure 4-17. Theoretical Wenner profiles across a buried circular cylinder: (a) perfectly insulating cylinders at different depths, (b) cylinders of different resistivity contrasts (Van Nostrand and Cook 1966)

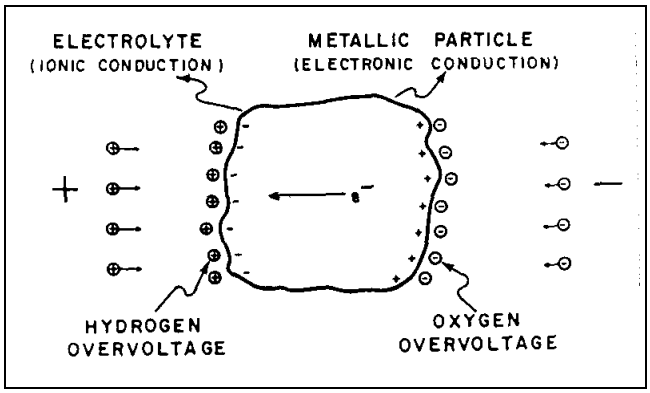

Figure 4-18. Overvoltage on a metallic particle in electrolyte (Seigel 1970; copyright permission granted by Geological Survey of Canada)

(b) The most important sources of nonmetallic IP in rocks are certain types of clay minerals (Vacquier 1957, Seigel 1970). These effects are believed to be related to electrodialysis of the clay particles. This is only one type of phenomenon which can cause 'ion-sorting' or 'membrane effects.' For example, Figure 4-19 shows a cation-selective membrane zone in which the mobility of the cation is increased relative to that of the anion, causing ionic concentration gradients and therefore polarization.

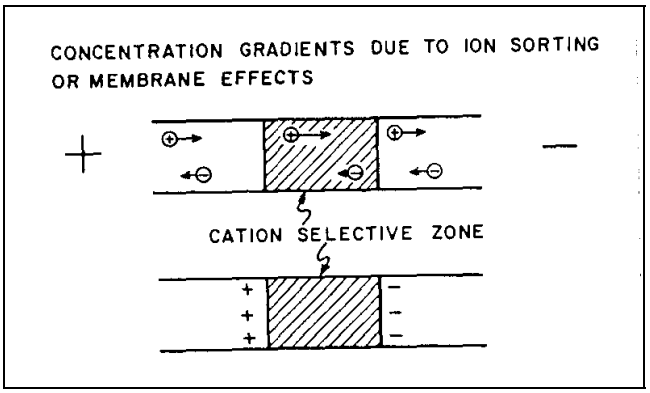

Figure 4-19. Nonmetallic induced polarization agent (Seigel 1970; copyright permission granted by Geological Survey of Canada)

A second group of phenomena includes electrokinetic effects which produce voltage gradients through the 'streaming potential' phenomenon. These voltage gradients will have the same external appearance as polarization effects due to separation of charge. Electrokinetic effects seem less important than membrane effects in the overall polarization picture.

(c) In time-domain IP, several indices have been used to define the polarizability of the medium. Seigel (1959) defined "chargeability" (in seconds) as the ratio of the area under the decay curve (in millivolt-seconds, mV-s) to the potential difference (in mV) measured before switching the current off. Komarov et al. (1966) define "polarizability" as the ratio of the potential difference after a given time from switching the current off to the potential difference before switching the current off. Polarizability is expressed as a percentage.

(d) Seigel (1959) showed that over a heterogeneous medium comprised of *n* different materials, apparent chargeability η_a is approximately related to apparent resistivity by

$$\eta_a = \sum_{i=1}^{n} \eta_i \frac{\partial \log \rho_a}{\partial \log \rho_i} \tag{4-16}$$

where

η_i = chargeability of the ith material

ρ_i = resistivity of the ith material

Seigel provided the validity of

$$\sum_{i=1}^{n} \frac{\partial \log \rho_a}{\partial \log \rho_i} = 1 \tag{4-17}$$

Equations 4-16 and 4-17 yield the useful formula:

$$\frac{\eta_a}{\eta_1} = 1 + \sum_{i=2}^{n} \frac{\partial \log \rho_a}{\partial \log \rho_i} \left[\frac{\eta_i}{\eta_1} - 1 \right] \tag{4-18}$$

If the theoretical expression for apparent resistivity ρ_a is known, then the corresponding expression for the reduced apparent chargeability η_a/η_i can be derived.

b. Sounding and profiling. The techniques of sounding and profiling, used in resistivity measurements, are also used in the IP method. IP soundings are most commonly made using the Schlumberger array, pole-dipole array, or Wenner array, and usually in the time domain. The apparent chargeability η_a versus the electrode spacing *a* is plotted on logarithmic coordinates. The IP sounding curve is an interpreted curve matching procedures, either graphically, using sets of IP sounding master curves, or by computer. At present, only a few two-layer master curves (for the Wenner array) have been published in the United States (Seigel 1959; Frische and von Buttlar 1957). Three- and four-layer curves have been published in the Soviet Union.

(1) An IP sounding curve can be of significant value in complementing a resistivity sounding curve. For example, the resistivity and IP sounding curves for the following four-layer geoelectric section are shown in Figure 4-20:

Layer No.	Thickness (m)	Resistivity (Ωm)	Chargeability (s)
1	10	10	1
2	10	160	1
3	5	40	10
4	∞	∞	1

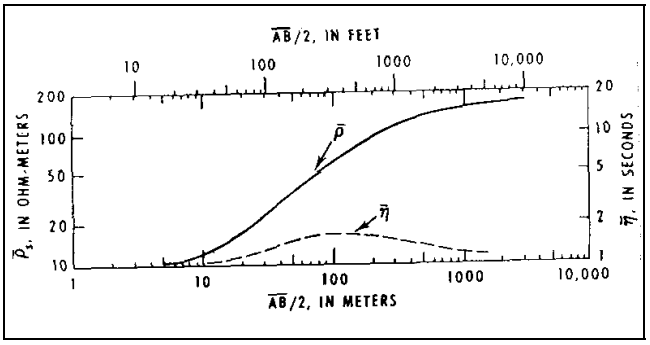

Figure 4-20. Apparent resistivity and apparent chargeability (IP) sounding curves for a four-layer model (Zohdy 1974a, 1974b)

It is obvious that layer 3 cannot be distinguished on the four-layer resistivity curve (which resembles a two- or three-layer curve). But layer 3 is characterized by a different chargeability from the surrounding layers and its presence is indicated clearly by the IP sounding curve.

(2) When profiling, the pole-dipole or dipole-dipole (see Figure 4-21) arrays are used almost exclusively. It can be easily employed in the field using short lengths of

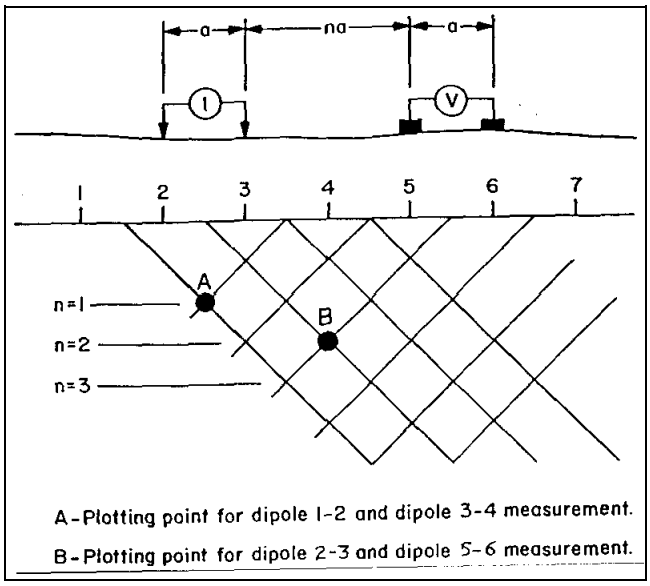

Figure 4-21. Dipole-dipole plotting method

wire or multi-conductor cables allowing several values of the spacing multiplier (n) to be measured from one current dipole location. For one or two values of n, the IP and resistivity results are plotted as profiles. For more than two values of n, the profile method of presentation becomes confusing. A two-dimensional (usually called pseudosection) format has been developed to present the data (Figure 4-21). This form of presentation helps the interpreter separate the effects of IP and resistivity variations along the line from vertical variations. The 45-deg angle used to plot the data is entirely arbitrary. The pseudosection plots are contoured, and the resulting anomalous patterns can be recognized as being caused by a particular source geometry and/or correlated from line to line. However, "the contoured data are MOST EMPHATICALLY NOT meant to represent sections of the electrical parameters of the subsurface" (Hallof 1980). The pseudosection data plots are merely a convenient method for showing all of the data along one given line in one presentation. It cannot be overemphasized that PSEUDOSECTION PLOTS ARE NOT CROSS SECTIONS. Although several commercial IP and resistivity modeling programs are available, trying to model every variation in a pseudosection is not recommended.

(3) Examples.

(a) Example 1 - Groundwater exploration. The majority of published case histories using IP surveys have been for mining exploration, but those treating groundwater exploration is growing: Vacquier et al. (1957), Kuzmina and Ogil'vi (1965), Bodmer et al. (1968), and Sternberg et al. (1990). Kuzmina and Ogil'vi reported on work done near the Sauk-Soo River in Crimea and in the Kalinino region of Armenia. In Crimea the IP work consisted essentially of IP sounding (time domain) using the Wenner array. The alluvial deposits in the studied area were poorly differentiated by their resistivities, but three horizons were clearly distinguished by their polarizabilities (Figure 4-22). The section consisted of a top layer of weak polarizability (h1 = 2-4 m; η1 = 0.8-1.5%), which represents a dry loamy layer; a second layer of strong polarizability (h2 = 18-20 m; η2 = 3-5%), which represented a clayey sand layer saturated with fresh water; and a third layer of weak polarizability (h3 very thick; η3 = 1%) which represents impervious siltstones. The survey in this area demonstrates that the IP work provided more complete information about the groundwater occurrence than did the resistivity soundings alone.

(b) Example 2 - detection of metal pipes and cables. Zhang and Luo (1990) show model experiments and analytical results which show that, in certain circumstances, a buried metal pipe or armored cable can introduce anomalies in IP (and apparent resistivity) with large amplitude and wide range. These results are important for two reasons. The first is that such man-made features have the potential to cause "noise" or errors in electrical surveys. The general rule of thumb when planning a survey is to orient soundings and profiles as nearly perpendicular to any known buried pipes or cables as the field conditions allow. The obvious second reason for the importance of this paper is that the IP may be used to locate a pipe or cable. Figure 4-23 (Zhang and Luo 1990) shows results of an IP survey using the gradient array in Baima, China. An η_a anomaly of ±10 to 3 percent with a width of more than 200 m was obtained near the road (the dot-and-dash lines on the figure). This anomaly can be traced for 4 km along the road. The trend of the anomalies is basically consistent with road and independent of the stratum strike or structural direction within the prospect area. Apparently, it results from a buried communication cable along the highway rather than geological features. The apparent resistivity profiles (the dot-and-double-dash lines on the figure) also appear to correlate with the cable, but with much less consistency or amplitude.

(c) Example 3 - mapping soil and groundwater contamination. Cahyna, Mazac, and Vendhodova (1990) show a valuable IP example used to determine the slag-type material containing cyanide complexes which have contaminated groundwater in Czechoslovakia. Figure 4-24 shows contours of η_a (percent) obtained from a

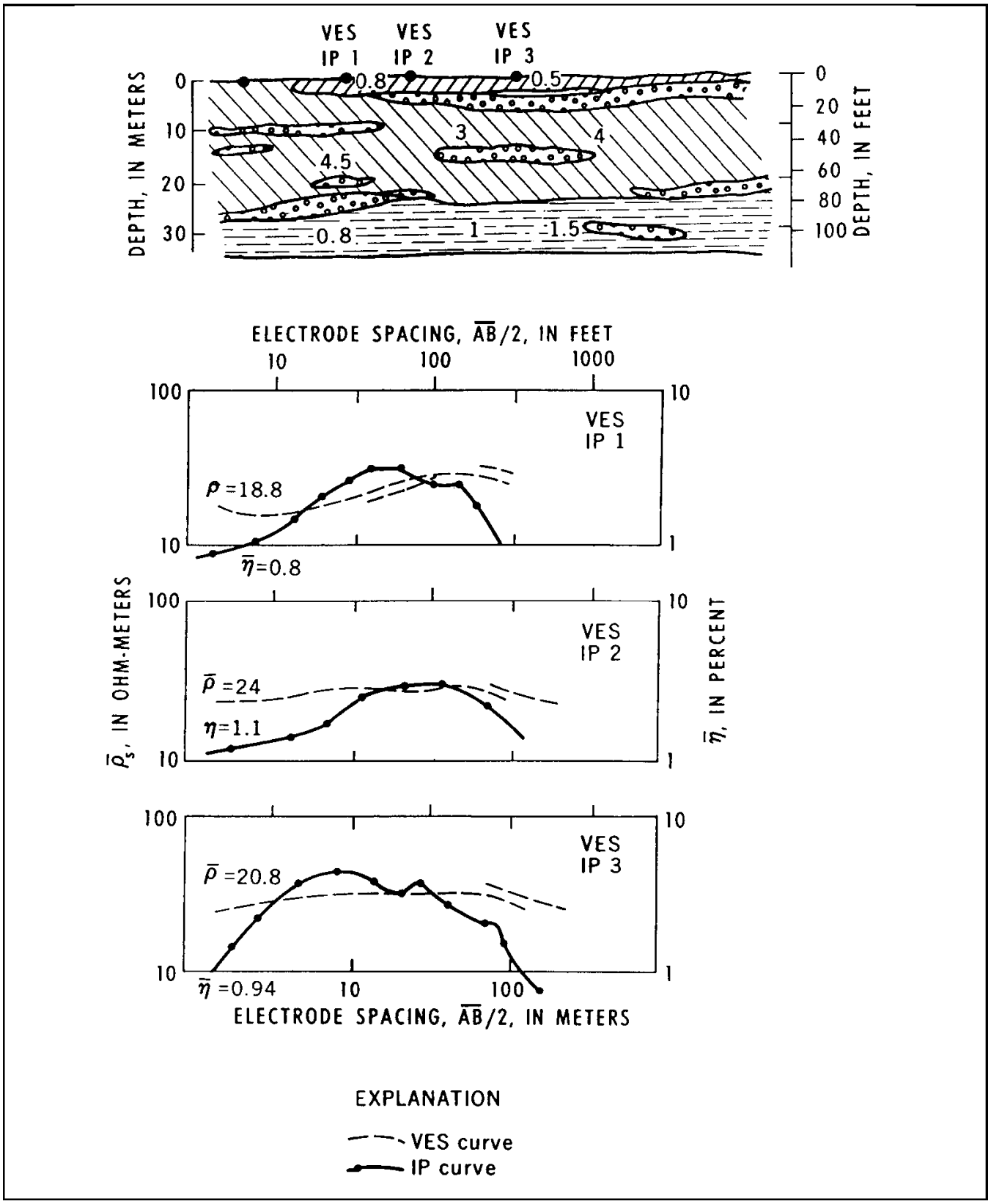

Figure 4-22. Geoelectric section, VES and IP sounding curves of alluvial deposits (Zohdy 1974b)

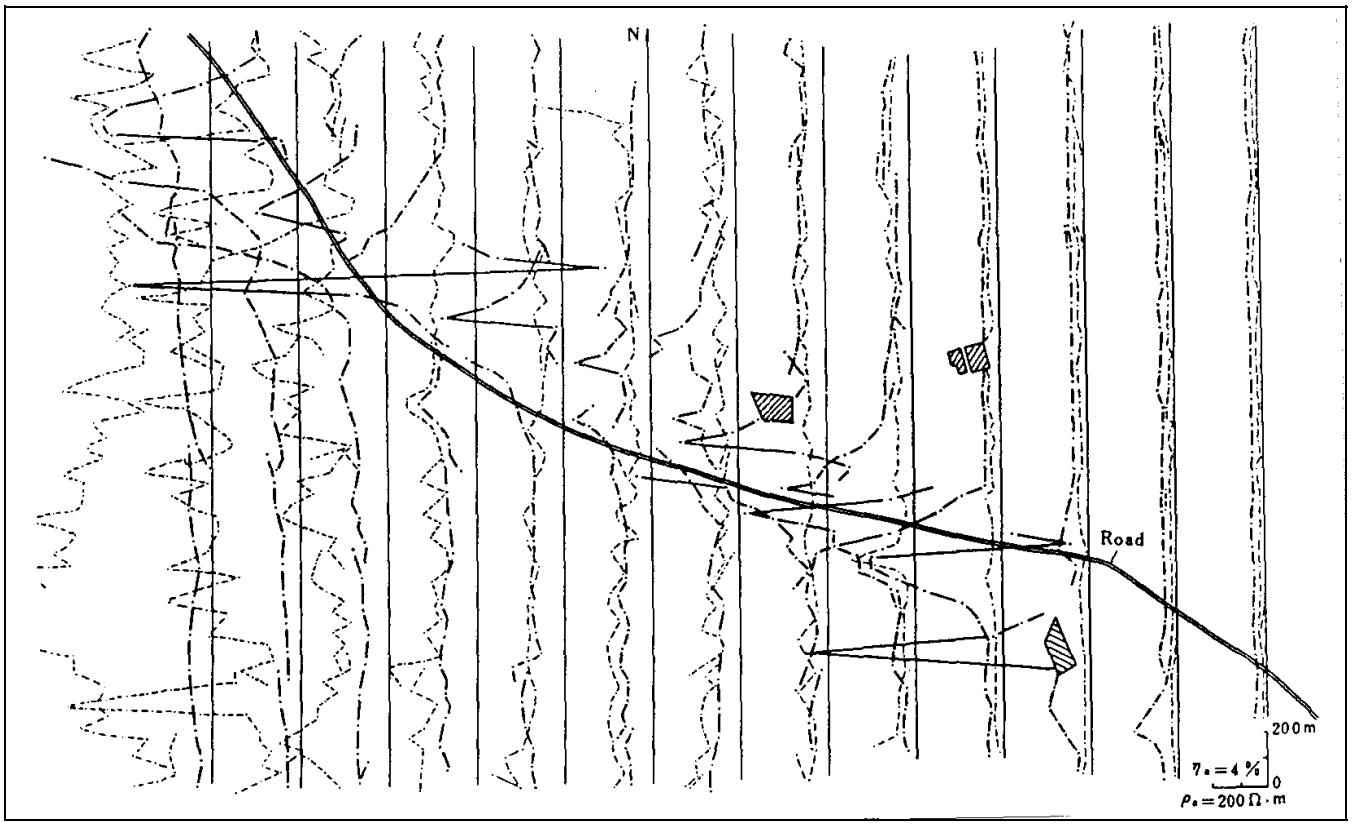

Figure 4-23. Plan profiles for ηa and ρa using the gradient array in Baima, China, over a buried cable (Zhang and Luo 1990; copyright permission granted by Society of Exploration Geophysicists)

10-m grid of profiles. The largest IP anomaly (ηa = 2.44 percent) directly adjoined the area of the outcrop of the contaminant (labeled A). The hatched region exhibits polarizability over 1.5 percent and probably represents the maximum concentration of the contaminant. The region exhibiting polarizability of less than 0.75 percent was interpreted as ground free of any slag-type contaminant.

4-6. Time-Domain Electromagnetic Techniques for Resistivity Sounding

a. General. Conventional DC resistivity techniques (Section 4-4) have been applied for many years to a variety of geotechnical applications. More recently, electromagnetic techniques, with different advantages (and disadvantages) compared with conventional DC, have been used effectively to measure the resistivity (or its reciprocal, the conductivity) of the earth.

(1) Electromagnetic techniques can be broadly divided into two groups. In frequency-domain instrumentation (FDEM), the transmitter current varies sinusoidally with time at a fixed frequency which is selected on the basis of the desired depth of exploration of the measurement (high frequencies result in shallower depths). FDEM instrumentation is described in Sections 4-7 through 4-11. In most time-domain (TDEM) instrumentation, on the other hand, the transmitter current, while still periodic, is a modified symmetrical square wave, as shown in Figure 4-25. It is seen that after every second quarter-period the transmitter current is abruptly reduced to zero for one quarter period, whereupon it flows in the opposite direction.

(2) A typical TDEM resistivity sounding survey configuration is shown in Figure 4-26, where it is seen that the transmitter is connected to a square (usually single turn) loop of wire laid on the ground. The side length of the loop is approximately equal to the desired depth of exploration except that, for shallow depths (less than 40 m) the length can be as small as 5 to 10 m in relatively resistive ground. A multi-turn receiver coil, located at the center of the transmitter loop, is connected to the receiver through a short length of cable.

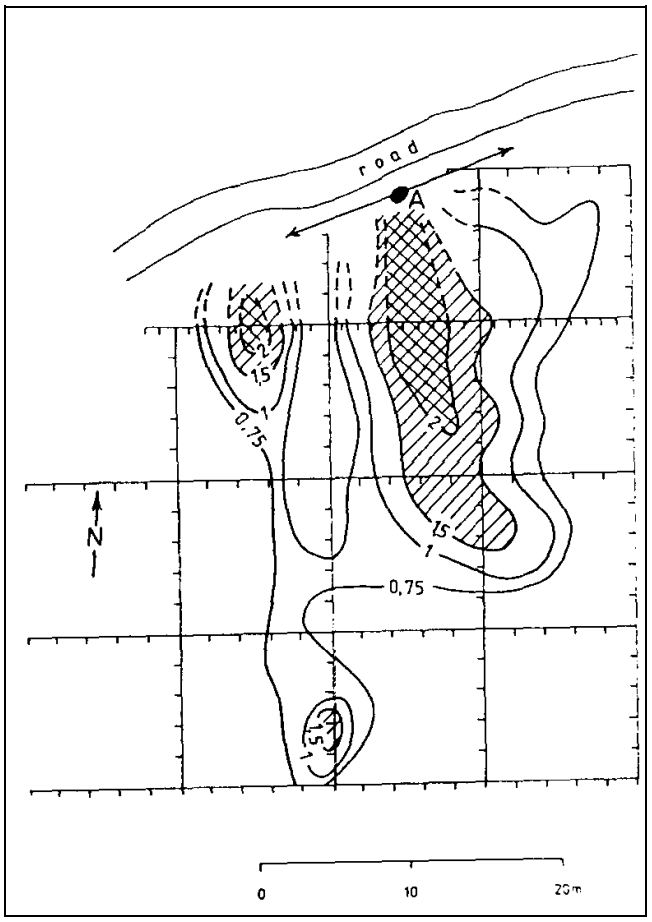

Figure 4-24. Network of SRP-IP profiles with the contours of IP values η_a(percent) and the extent of the contaminant interpreted on the basis of the geophysical survey; location A is the known outcrop of the slag-type contaminant and the position of the VES-IP measurement (Cahyna, Mazac, and Vendhodova 1990; copyright permission granted by Society of Exploration Geophysicists)

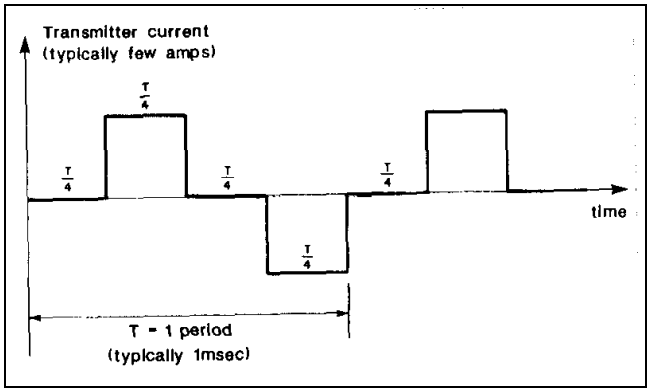

Figure 4-25. Transmitter current wave form

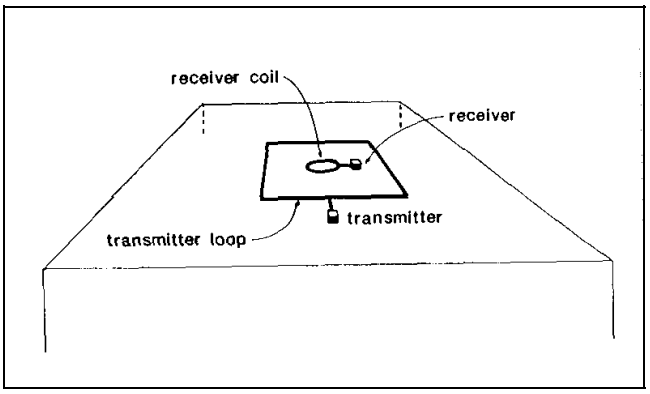

Figure 4-26. Central loop sounding configuration

(3) The principles of TDEM resistivity sounding are relatively easily understood. The process of abruptly reducing the transmitter current to zero induces, in accord with Faraday's law, a short-duration voltage pulse in the ground, which causes a loop of current to flow in the immediate vicinity of the transmitter wire, as shown in Figure 4-27. In fact, immediately after transmitter current is turned off, the current loop can be thought of as an image in the ground of the transmitter loop. However, because of finite ground resistivity, the amplitude of the current starts to decay immediately. This decaying current similarly induces a voltage pulse which causes more current to flow, but now at a larger distance from the transmitter loop, and also at greater depth, as shown in Figure 4-27. This deeper current flow also decays due to finite resistivity of the ground, inducing even deeper current flow and so on. The amplitude of the current flow as a function of time is measured by measuring its decaying magnetic field using a small multi-turn receiver coil usually located at the center of the transmitter loop. From the above it is evident that, by making measurement of the voltage out of the receiver coil at successively later

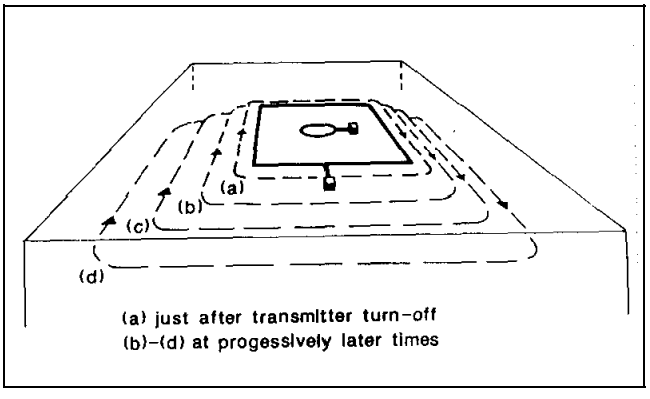

Figure 4-27. Transient current flow in the ground

times, measurement is made of the current flow and thus also of the electrical resistivity of the earth at successively greater depths. This process forms the basis of central loop resistivity sounding in the time domain.

(4) The output voltage of the receiver coil is shown schematically (along with the transmitter current) in Figure 4-28. To accurately measure the decay characteristics of this voltage the receiver contains 20 narrow time gates (indicated in Figure 4-29), each opening sequentially to measure (and record) the amplitude of the decaying voltage at 20 successive times. Note that, to minimize distortion in measurement of the transient voltage, the early time gates, which are located where the transient voltage is changing rapidly with time, are very narrow, whereas the later gates, situated where the transient is varying more slowly, are much broader. This technique is desirable since wider gates enhance the signal-to-noise ratio, which becomes smaller as the amplitude of the transient decays at later times. It will be noted from Figure 4-28 that there are four receiver voltage transients generated during each complete period (one positive pulse plus one negative pulse) of transmitter current flow. However, measurement is made only of those two transients that occur when the transmitter current has just been shut off, since in this case accuracy of the measurement is not affected by small errors in location of the receiver coil. This feature offers a very significant advantage over FDEM measurements, which are generally very sensitive to variations in the transmitter coil/receiver coil spacing since the FDEM receiver measures while the transmitter current is flowing. Finally, particularly for shallower sounding, where it is not necessary to measure the transient characteristics out to very late times, the period is typically of the order of 1 msec or less, which means

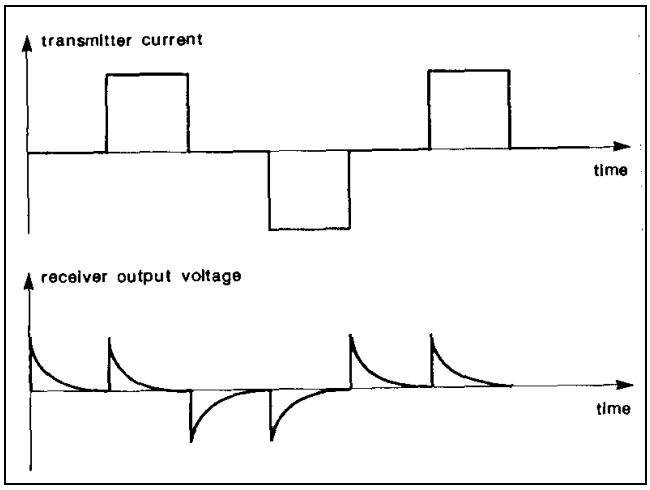

Figure 4-28. Receiver output wave form

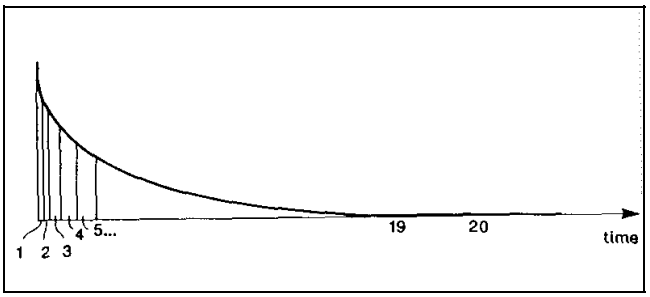

Figure 4-29. Receiver gate locations

that in a total measurement time of a few seconds,measurement can be made and stacked on several thousand transient responses. This is important since the transient response from one pulse is exceedingly small and it is necessary to improve the signal-to-noise ratio by adding the responses from a large number of pulses.

b. Apparent resistivity in TDEM soundings.

(1) Figure 4-29 shows, schematically, a linear plot of typical transient response from the earth. It is useful to examine this response when plotted logarithmically against the logarithm of time, particularly if the earth is homogeneous (i.e. the resistivity does not vary with either lateral distance or depth). Such a plot is shown in Figure 4-30, which suggests that the response can be divided into an early stage (where the response is constant with time), an intermediate stage (response shape continually varying with time), and a late stage (response is now a straight line on the log-log plot). The response is generally a mathematically complex function of conductivity and time; however, during the late stage, the mathematics simplifies considerably and it can be shown that during this time the response varies quite simply with time and conductivity as

$$e(t) = \frac{k_1 M \sigma^{3/2}}{t^{5/2}} \qquad (4\text{-}19)$$

where

$e(t)$ = output voltage from a single-turn receiver coil of area 1 m^2

k_1 = a constant

M = product of Tx current x area (a-m^2)

σ = terrain conductivity (siemens/m = S/m = 1/Ωm)

t = time (s)

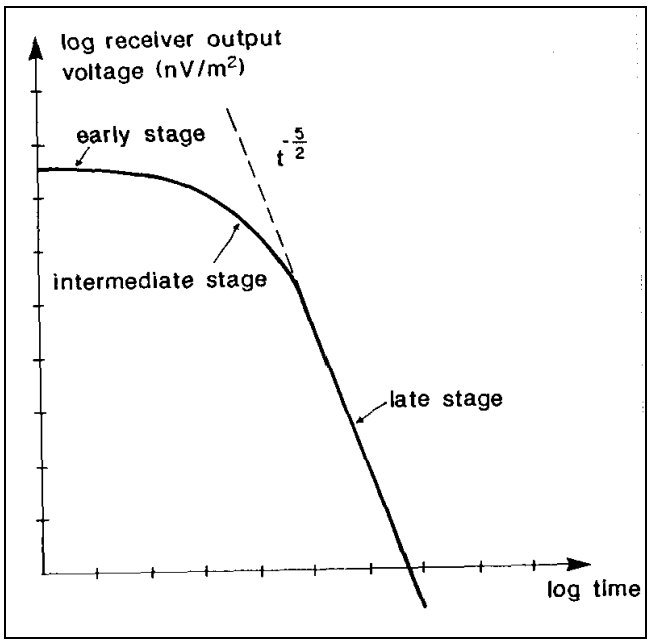

Figure 4-30. Log plot-receiver output voltage versus time (one transient)

(2) Unlike the case for conventional resistivity measurement, where the measured voltage varies linearly with terrain resistivity, for TDEM, the measured voltage $e(t)$ varies as $\sigma^{3/2}$, so it is intrinsically more sensitive to small variations in the conductivity than conventional resistivity. Note that during the late stage, the measured voltage is decaying at the rate $t^{-5/2}$, which is very rapidly with time. Eventually the signal disappears into the system noise and further measurement is impossible. This is the maximum depth of exploration for the particular system.

(3) With conventional DC resistivity methods, for example the commonly used Wenner array, the measured voltage over a uniform earth from Equation 4-8 can be shown to be

$$V(a) = \rho I/2\pi a \qquad (4\text{-}20)$$

where

a = interelectrode spacing (m)

ρ = terrain resistivity (Ωm)

I = current into the outer electrodes

$V(a)$ = voltage measured across the inner electrodes for the specific value of a

In order to obtain the resistivity of the ground, Equation 4-20 is rearranged (inverted) to give Equation 4-11:

$$\rho = 2\pi a\, V(a)/I$$

If ground resistivity is uniform as the interelectrode spacing (a) is increased, the measured voltage increases directly with a so that the right-hand side of Equation 4-11 stays constant, and the equation gives the true resistivity. Suppose now that the ground is horizontally layered (i.e. that the resistivity varies with depth); for example it might consist of an upper layer of thickness h and resistivity ρ_1, overlying a more resistive basement of resistivity $\rho_2 > \rho_1$, (this is called a two-layered earth). At very short interelectrode spacing ($a<<h$) virtually no current penetrates into the more resistive basement and resistivity calculation from Equation 4-11 will give the value ρ_1. As interelectrode spacing is increased, the current (I) is forced to flow to greater and greater depths. Suppose that, at large values of a ($a>>h$), the effect of the near surface material of resistivity ρ_1 will be negligible, and resistivity calculated from Equation 4-11 will give the value ρ_2, which is indeed what happens. At intermediate values of a ($a \simeq h$) the resistivity given by Equation 4-11 will lie somewhere between ρ_1 and ρ_2.

(4) Equation 4-11 is, in the general case, used to define an apparent resistivity $\rho_a(a)$ which is a function of a. The variation of $a\ \rho_a(a)$ with a

$$\rho_a(a) = 2\pi a\, V(a)/I \qquad (4\text{-}21)$$

is descriptive of the variation of resistivity with depth. The behavior of the apparent resistivity $\rho_a(a)$ for a Wenner array for the two-layered earth above is shown schematically in Figure 4-31. It is clear that in conventional resistivity sounding, to increase the depth of exploration, the interelectrode spacing must be increased.

(5) In the case of TDEM sounding, on the other hand, it was observed earlier that as time increased, the depth to the current loops increased, and this phenomenon is used to perform the sounding of resistivity with depth. Thus, in analogy with Equation 4-21, Equation 4-19 is inverted to read (since $\rho = 1/\sigma$)

$$\rho_a(t) = \frac{k_2\, M^{2/3}}{e(t)^{2/3} t^{5/3}} \qquad (4\text{-}22)$$

(a) Suppose once again that terrain resistivity does not vary with depth (i.e. a uniform half-space) and is of

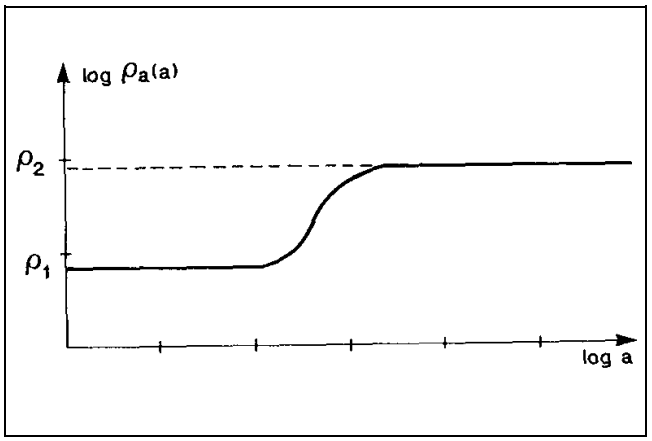

Figure 4-31. Wenner array: apparent resistivity, two-layer curve

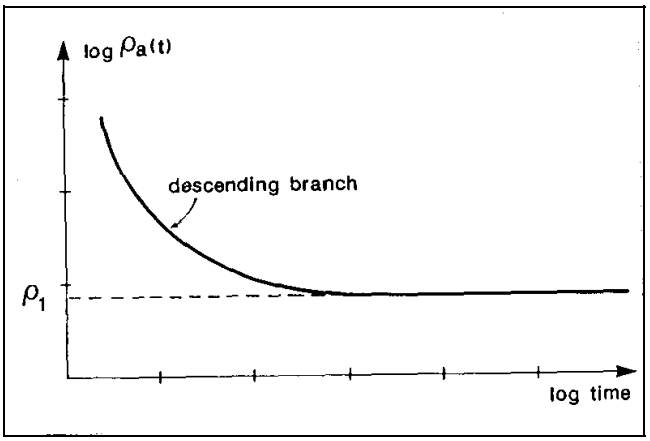

Figure 4-32. TDEM: apparent resistivity, homogenous half-space

resistivity ρ_1. For this case, a plot of $\rho_a(t)$ against time would be as shown in Figure 4-32. Note that at late time the apparent resistivity $\rho_a(t)$ is equal to ρ_1, but at early time $\rho_a(t)$ is much larger than ρ_1. The reason for this is that the definition of apparent resistivity is based (as seen from Figure 4-30) on the time behavior of the receiver coil output voltage at late time when it decays as $t^{-5/2}$. At earlier and intermediate time, Figure 4-30 shows that the receiver voltage is too low (the dashed line indicates the voltage given by the "late stage approximation") and thus, from Equation 4-22, the apparent resistivity will be too high. For this reason, there will always be, as shown on Figure 4-32, a "descending branch" at early time where the apparent resistivity is higher than the half-space resistivity (or, as will be seen later, is higher than the upper layer resistivity in a horizontally layered earth). This is not a problem, but it is an artifact of which we must be aware.

(b) Suppose that once again, we let the earth be two-layered, of upper layer resistivity ρ_1, and thickness *h*, and basement resistivity ρ_2 ($>\rho_1$). At early time when the currents are entirely in the upper layer of resistivity ρ_1 the decay curve will look like that of Figure 4-30, and the apparent resistivity curve will look like Figure 4-32. However, later on the currents will lie in both layers, and at much later time they will be located entirely in the basement, of resistivity ρ_2. Since $\rho_2>\rho_1$, Equation 4-22 shows that, as indicated in Figure 4-33a, the measured voltage will now be less than it should have been for the homogeneous half-space of resistivity ρ_1. The effect on the apparent resistivity curve is shown in Figure 4-34a; since at late times all the currents are in the basement, the apparent resistivity $\rho_a(t)$ becomes equal to ρ_2, completely in analogy for Figure 4-31 for conventional resistivity measurements. In the event that $\rho_2<\rho_1$, the inverse behavior is also as expected, i.e. at late times the measured voltage response, shown in Figure 4-33, is greater than that from a homogeneous half-space of resistivity ρ_1, and the apparent resistivity curve correspondingly becomes that of Figure 4-34b, becoming equal to the new value of ρ_2 at late time. Note that, for the case of a (relatively) conductive basement there is a region of intermediate time (shown as t^*), where the voltage response temporarily falls before continuing on to adopt the value appropriate to ρ_2. This behavior, which is a

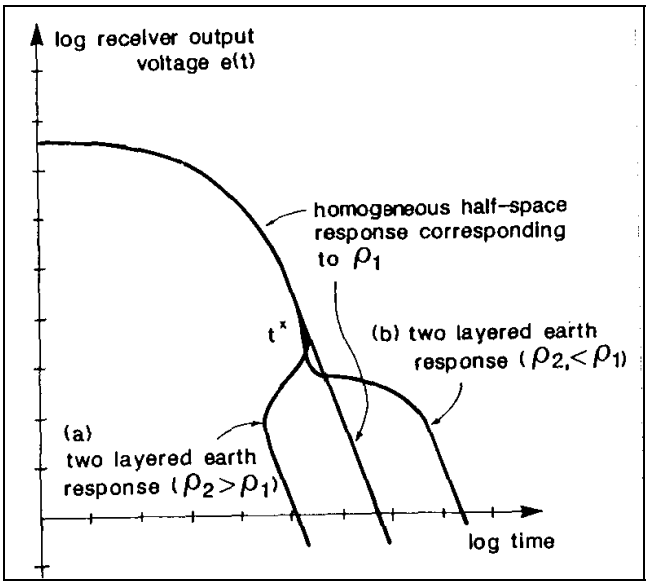

Figure 4-33. TDEM: receiver output voltage, two-layered earth

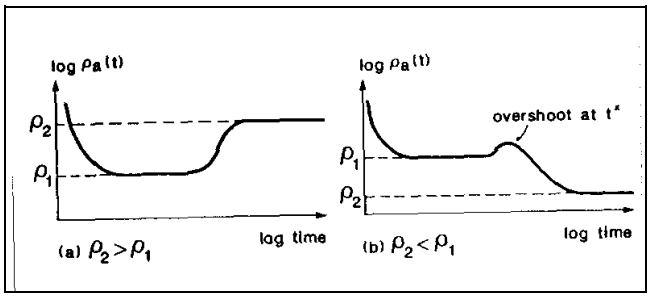

Figure 4-34. TDEM: apparent resistivity, two-layered earth

characteristic of TDEM, is again not a problem, as long as it is recognized. The resultant influence of the anomalous behavior on the apparent resistivity is also shown on Figure 4-34b at *t**.

(c) To summarize, except for the early-time descending branch and the intermediate-time anomalous region described above, the sounding behavior of TDEM is analogous to that of conventional DC resistivity if the passage of time is allowed to achieve the increasing depth of exploration rather than increasing interelectrode spacing.

(6) Curves of apparent resistivity such as Figure 4-34 tend to disguise the fact, that, at very late times, there is simply no signal, as is evident from Figure 4-33. In fact in the TDEM central loop sounding method it is unusual to see, in practical data, the curve of apparent resistivity actually asymptote to the basement resistivity, due to loss of measurable signal. Fortunately, both theoretically and in practice, the information about the behavior of the apparent resistivity curve at early time and in the transition region is generally sufficient to allow the interpretation to determine relatively accurately the resistivity of the basement without use of the full resistivity sounding curve.

c. Measurement procedures. As stated in Section 1 a common survey configuration consists of a square single turn loop with a horizontal receiver coil located at the center. Data from a resistivity sounding consist of a series of values of receiver output voltage at each of a succession of gate times. These gates are located in time typically from a few microseconds up to tens or even hundreds of milliseconds after the transmitter current has been turned off, depending on the desired depth of exploration. The receiver coil measures the time rate of change of the magnetic field $e(t)=dB/dt$, as a function of time during the transient. Properly calibrated, the units of $e(t)$ are V/m^2 of receiver coil area; however, since the measured signals are extremely small it is common to use nV/m^2, and measured decays typically range from many thousands of nV/m^2 at early times to less than 0.1 nV/m^2 at late times. Modern receivers are calibrated in nV/m^2 or V/m^2. To check the calibration, a "Q-coil," which is a small short-circuited multi-turn coil laid on the ground at an accurate distance from the receiver coil is often used, so as to provide a transient signal of known amplitude.

(1) The two main questions in carrying out a resistivity sounding are (a) how large should the side lengths of the (usually single-turn) transmitter be, and (b) how much current should the loop carry? Both questions are easily answered by using one of the commercially available forward layered-earth computer modelling programs. A reasonable guess as to the possible geoelectric section (i.e. the number of layers, and the resistivity and thickness of each) is made. These data are then fed into the program, along with the proposed loop size and current, and the transient voltage is calculated as a function of time. For example, assume that it is suspected that a clay aquitard may exist at a depth of 20 m in an otherwise clay-free sand. Resistivity of the sand might be 100 Ωm, and that of the clay layer 15 Ωm. Desired information includes the minimum thickness of the clay layer that is detectable, and the accuracy with which this thickness can be measured. The depth of exploration is of the order of the loop edge size, so 10 m × 10 m represents a reasonable guess for model calculation, along with a loop current of 3 A, which is characteristic of a low-power, shallow-depth transmitter. Before doing the calculations, one feature regarding the use of small (i.e. less than 60 m × 60 m) transmitter loops for shallow sounding should be noted. In these small loops the inducing primary magnetic field at the center of the loop is very high, and the presence of any metal, such as the receiver box, or indeed the shielding on the receiver coil itself, can cause sufficient transient response to seriously distort the measured signal from the ground. This effect is greatly reduced by placing the receiver coil (and receiver) a distance of about 10 m outside the nearest transmitter edge. As shown later, the consequence of this on the data is relatively small.

(a) The first task is to attempt to resolve the difference between, for example, a clay layer 0 m thick (no clay) and 1 m thick. Results of the forward layered-earth calculation, shown in Figure 4-35, indicate that the apparent resistivity curves from these two cases are well separated (difference in calculated apparent resistivity is about 10 percent) over the time range from about 8 μs to 100 μs, as would be expected from the relatively shallow

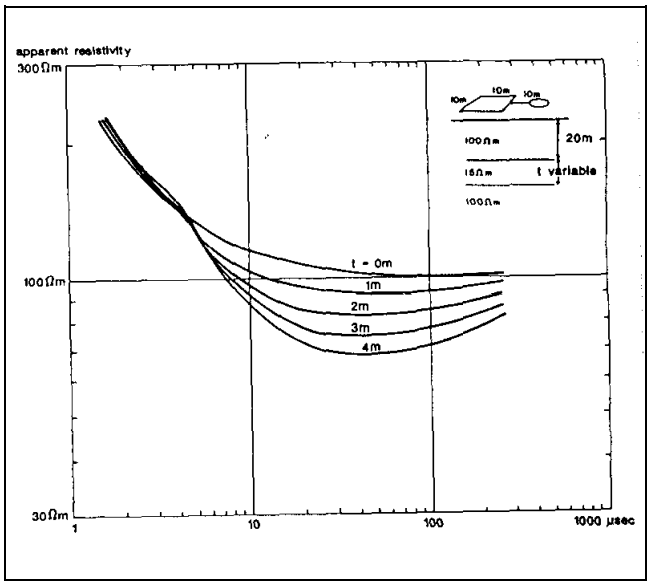

Figure 4-35. Forward layered-earth calculations

depths. Note that, to use this early time information, a receiver is required that has many narrow early time gates in order to resolve the curve, and also has a wide bandwidth so as not to distort the early portions of the transient decay. Note from the figure that resolving thicknesses from 1 to 4 m and greater will present no problem.

(b) Having ascertained that the physics of TDEM sounding will allow detection of this thin layer, the next test is to make sure that the 10- by 10-m transmitter running at 3 A will provide sufficient signal-to-noise over the time range of interest (8 to 100 µs). The same forward layered-earth calculation also outputs the actual measured voltages that would be measured from the receiver coil. These are listed (for the case of thickness of 0 m, which will produce the lowest voltage at late times) in Table 4-2. Focus attention on the first column (which gives the time, in seconds) and the third column (which gives the receiver output as a function of time, in V/m^2). Now the typical system noise level (almost invariably caused by external noise sources, see Section 4) for gates around 100 to 1,000 µs is about 0.5 nV/m^2 or 5 x $10^{-10}V/m^2$. From columns 1 and 3 see that, for the model chosen, the signal falls to 5 x $10^{-10}V/m^2$ at a time of about 630 µs and is much greater than this for the early times when the apparent resistivity curves are well-resolved, so it is learned that the 10-m by 10-m transmitter at 3 A is entirely adequate. In fact, if a 5-m by 5-m transmitter was used, the dipole moment (product of transmitter current and area) would fall by 4, as would the measured signals, and the signal-to-noise ratio would still be excellent over the time range of interest. Thus assured, assuming that the model realistically represents the actual conditions of resistivity, the procedure will be able to detect the thin clay layer. Before proceeding with the actual measurement it would be wise to vary some of the model parameters, such as the matrix and clay resistivities, to see under what other conditions the clay will be detectable. The importance of carrying out such calculations cannot be overstated. The theory of TDEM resistivity sounding is well understood, and the value of such modelling, which is inexpensive and fast, is very high.

(c) It was stated above that offsetting the receiver coil from the center of the transmitter loop would not greatly affect the shape of the apparent resistivity curves. The reason for this is that the vertical magnetic field arising from a large loop of current (such as that shown in the ground at late time in Figure 4-27) changes very slowly in moving around the loop center. Thus, at late time, when the current loop radius is significantly larger than the transmitter loop radius, it would be expected that moving the receiver from the center of the transmitter loop to outside the loop would not produce a large difference, whereas at earlier times when the current loop radius is approximately the same as the transmitter radius, such offset will have a larger effect. This behavior is illustrated in Figure 4-36, which shows the apparent resistivity curves for the receiver at the center and offset by 15 m from the center of the 10- by 10-m transmitter loop. At late time the curves are virtually identical.

(d) How closely spaced should the soundings be? One of the big advantages of TDEM geoelectric sounding over conventional DC sounding is that for TDEM the overall width of the measuring array is usually much less than the depth of exploration, whereas for conventional DC sounding the array dimension is typically (Wenner array) of the order of 3 times the exploration depth. Thus, in the usual event that the terrain resistivity is varying laterally, TDEM sounding will generally indicate those variations much more accurately. If the variations are very closely spaced one might even take measurements at a station spacing of every transmitter loop length. It should be noted that most of the time spent doing a sounding (especially deeper ones where the transmitter loop is large) is utilized in laying out the transmitter loop. In this case, it can be much more efficient to have one or even two groups laying out loops in advance of the survey party, who then follow along with the actual transmitter, receiver, and receiver coil to make the sounding in a matter of minutes, again very favorable compared with DC sounding. A further advantage of TDEM geoelectric sounding is that, if a geoelectric interface is not

Table 4-2
Forward Response Calculation

1. Title	:TEST
2. Number of layers	:1
3&4. Thickness & Resistivity	: Thickness [m] Resistivity [Ohmm] INFINITE .100000E+03
5. Source - RECTANGULAR LOOP	: 10.00 × 10.00
6. Point of receiver (XO,YO)	: .000E+00, .150E+02
7. Current in transmitter	: 3.00 [A]
8. Induction numbers	:DEFAULT SELECTION
9. Real time [sec]	:TO= .1000E-05 NT= 5 TM= .1000E-02
10. Field component	:BZ
11. On output file	:TIME DOMAIN
12. Output file name	:X.DAT record 1
13. Turn off time	: 1 [us]
14. Runon correction	:NO
15. Low pass filter correct.	:NO
16. Asymptotic approximation	:TAS= .00000E+00

TIME DOMAIN RESPONSE

Real Time	Tau	dBz/dt	App. Res.	Tau/H1	App./R01
.10000E-05	.79267E+02	.85461E-03	.31459E+03	.79267E+02	.31459E+01
.15849E-05	.99791E+02	.47244E-03	.21679E+03	.99791E+02	.21679E+01
.25119E-05	.12563E+03	.22169E-03	.16663E+03	.12563E+03	.16663E+01
.39811E-05	.15816E+03	.87414E-04	.14384E+03	.15816E+03	.14384E+01
.63096E-05	.19911E+03	.34155E-04	.12492E+03	.19911E+03	.12492E+01
.10000E-04	.25066E+03	.11955E-04	.11674E+03	.25066E+03	.11674E+01
.15849E-04	.31557E+03	.41257E-05	.11014E+03	.31557E+03	.11014E+01
.25119E-04	.39727E+03	.13721E-05	.10650E+03	.39727E+03	.10650E+01
.39811E-04	.50014E+03	.44950E-06	.10402E+03	.50014E+03	.10402E+01
.63096E-04	.62964E+03	.14541E-06	.10246E+03	.62964E+03	.10246E+01
.10000E-03	.79267E+03	.46628E-07	.10151E+03	.79267E+03	.10151E+01
.15849E-03	.99791E+03	.15002E-07	.10035E+03	.99791E+03	.10035E+01
.25119E-03	.12563E+04	.45975E-08	.10247E+03	.12563E+04	.10247E+01
.39811E-03	.15816E+04	.14868E-08	.10094E+03	.15816E+04	.10094E+01
.63096E-03	.19911E+04	.48920E-09	.98312E+02	.19911E+04	.98312E+00
.10000E-02	.25066E+04	.15192E-09	.99507E+02	.25066E+04	.99507E+00

horizontal, but is dipping, the TDEM still gives a reasonably accurate average depth to the interface. Similarly TDEM sounding is much less sensitive (especially at later times) to varying surface topography.

(e) It was explained above that, particularly at later times, the shape of the apparent resistivity curve is relatively insensitive to the location of the receiver coil. This feature is rather useful when the ground might be sufficiently inhomogeneous to invalidate a sounding (in the worst case, for example, due to a buried metallic pipe). In this case a useful and quick procedure is to take several measurements at different receiver locations, as shown in Figure 4-37. Curve 5 is obviously anomalous, and must be rejected. Curves 1-4 can all be used in the inversion process, which handles both central and offset receiver coils. Another useful way to ensure, especially for deep soundings, that the measurement is free from errors caused by lateral inhomogeneities (perhaps a nearby fault structure) is to use a three- component receiver coil, which measures, in addition to the usual vertical component of the decaying magnetic field, both horizontal components. When the ground is uniform or horizontally layered, the two horizontal components are both essentially equal to zero, as long as the measurement is made near the transmitter loop center (which is why the technique is particularly relative to deep sounding). Departures from zero are a sure indication of lateral inhomogeneities which might invalidate the sounding.

(f) Finally, most receivers, particularly those designed for shallower sounding, have an adjustable base frequency

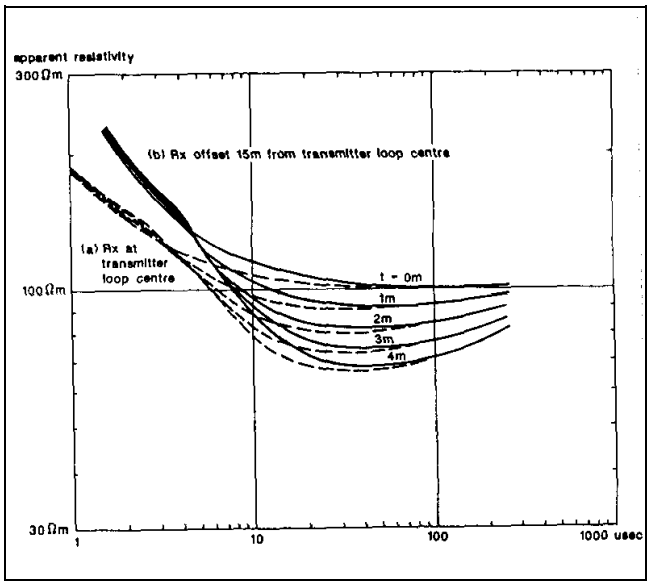

Figure 4-36. Forward layered earth calculations, (a) central loop sounding, (b) offset sounding

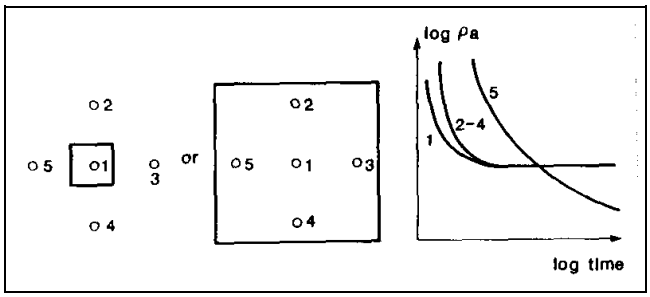

Figure 4-37. Offset Rx locations to check lateral homogeneity, position 5 is near lateral inhomogeneity

to permit changing the length of the measurement time. With reference to Figures 4-25 and 4-28, changing the base frequency f_b will change the period T ($T=1/f_b$), and thus the measurement duration T/4. For transients which decay quickly, such as shallow sounding, the measurement period, which should be of the order of duration of the transient, should be short, and thus the base frequency high. This has the advantage that, for a given total integration time of, say 5 s, more transient responses will be stacked, to improve the signal-to-noise ratio and allow the use of smaller, more mobile, transmitter loops, increasing survey speed. On the other hand, for deep sounding, where the response must be measured out to very long time, it is clear that the measurement period must be greatly extended so that the transient response does not run on to the next primary field cycle or indeed the next transient response, and thus the base frequency must be significantly reduced. The signal-to-noise ratio will deteriorate due to fewer transients being stacked, and must be increased by either using a larger transmitter loop and transmitter current (to increase the transmitter dipole) and/or integrating the data for a longer stacking time, perhaps for 30 s or even a minute. It should be noted that should such run-on occur because too high a base frequency was employed, it can still be corrected for in modern data inversion programs; however, in extreme cases, accuracy and resolution of the inversion will start to deteriorate.

(2) Finally, both in Figure 4-28 and in this discussion, it was assumed that the transmitter current is turned off instantaneously. To actually accomplish this with a large loop of transmitter wire is impossible, and modern transmitters shut the current down using a very fast linear ramp. The duration of this ramp is maintained as short as possible (it can be shown to have an effect similar to that of broadening the measurement gate widths) particularly for shallow sounding where the transient decays very rapidly at early times. The duration of the transmitter turn-off ramp (which can also be included in modern inversion programs) is usually controlled by transmitter loop size and/or loop current.

d. Sources of noise.

(1) Noise sources for TDEM soundings can be divided into four categories:

(a) Circuit noise (usually so low in modern receivers as to rarely cause a problem).

(b) Radiated and induced noise.

(c) Presence of nearby metallic structures.

(d) Soil electrochemical effects (induced polarization).

(2) Radiated noise consists of signals generated by radio and radar transmitters and also from thunderstorm lightning activity. The first two are not usually a problem; however, on summer days when there is extensive local thunderstorm activity the electrical noise from lightning strikes (similar to the noise heard on AM car radios) can cause problems and it may be necessary to increase the integration (stacking) time or, in severe cases, to discontinue the survey until the storms have passed by or abated.

(3) The most important source of induced noise consists of the intense magnetic fields from 50- to 60-Hz

power lines. The large signals induced in the receiver from these fields (which fall off more or less linearly with distance from the powerline) can overload the receiver if the receiver gain is set to be too high, and thus cause serious errors. The remedy is to reduce the receiver gain so that overload does not occur, although in some cases this may result in less accurate measurement of the transient since the available dynamic range of the receiver is not being fully utilized. Another alternative is to move the measurement array further from the power line.

(4) The response from metallic structures can be very large compared with the response from the ground. Interestingly, the power lines referred to above can often also be detected as metallic structures, as well as sources of induced noise. In this case they exhibit an oscillating response (the response from all other targets, including the earth, decays monotonically to zero). Since the frequency of oscillation is unrelated to the receiver base frequency, the effect of power line structural response is to render the transient "noisy" as shown in Figure 4-38. Since these oscillations arise from response to eddy currents actually induced in the power line by the TDEM transmitter, repeating the measurement will produce an identical response, which is one way that these oscillators are identified. Another way is to take a measurement with the transmitter turned off. If the "noise" disappears it is a good indication that power-line response is the problem. The only remedy is to move the transmitter further from the power line.

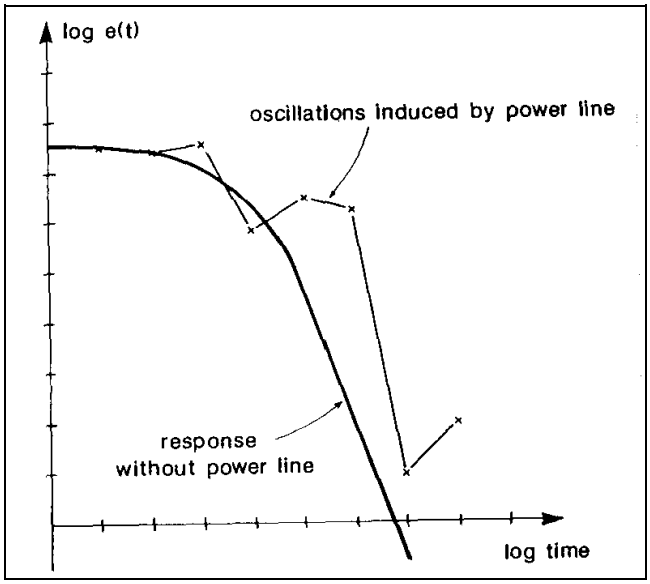

Figure 4-38. Oscillations induced in receiver response by power line

(5) Other metallic responses, such as those from buried metallic trash, or pipes, can also present a problem, a solution for which was discussed in the previous section (multiple receiver sites, as shown in Figure 4-37). If the response is very large, another sounding site must be selected. Application of another instrument such as a metal detector or ground conductivity meter to quickly survey the site for pipes can often prove useful.

(6) A rather rare effect, but one which can occur, particularly in clayey soils, is that of induced polarization. Rapid termination of the transmitter current can charge up the minute electrical capacitors in the soil interfaces (induced polarization). These capacitors subsequently discharge, producing current flow similar to that shown in Figure 4-27, but in the opposite direction. The net effect is to reduce the amplitude of the transient response (thus increasing the apparent resistivity) or even, where the effect is very severe, to cause the transient response to become negative over some range of the measurement time. Since these sources of reverse current are localized near the transmitter loop, using the offset configuration usually reduces the errors caused by them to small values.

(7) In summary, it should be noted that in TDEM soundings the signal-to-noise ratio is usually very good over most of the time range. However, in general the transient response is decaying extremely rapidly (of the order of $t^{-5/2}$, or by a factor of about 300 for a factor of 10 increase in time). The result is that towards the end of the transient the signal-to-noise ratio suddenly deteriorates completely and the data become exceedingly noisy. The transient is over!

e. Data reduction and interpretation.

(1) In the early days of TDEM sounding, particularly in Russia where the technique was developed (Kaufman and Keller 1983) extensive use was made of numerically calculated apparent resistivity curves for a variety of layered earth geometrics. Field data would be compared with a selection of curves, from which the actual geoelectric section would be determined.

(2) More recently the advent of relatively fast computer inversion programs allows field transient data to be automatically inverted to a layered earth geometry in a matter of minutes. An inversion program offers an additional significant advantage. All electrical sounding techniques (conventional DC, magneto-telluric, TDEM) suffer to a greater or less extent from equivalence, which

basically states that, to within a given signal-to-noise ratio in the measured data, more than one specific geoelectric model will fit the measured data. This problem, which is seldom addressed in conventional DC soundings, is one of which the interpreter must be aware, and the advantage of the inversion program is that, given an estimate of the signal-to-noise ratio in the measured data, the program could calculate a selection of equivalent geoelectric sections that will also fit the measured data, immediately allowing the interpreter to decide exactly how unique his solution really is. Equivalence is a fact of life, and must be included in any interpretation.

f. Summary. The advantages of TDEM geoelectric sounding over conventional DC resistivity sounding are significant. They include the following:

(1) Improved speed of operation.

(2) Improved lateral resolution.

(3) Improved resolution of conductive electrical equivalence.

(4) No problems injecting current into a resistive surface layer.

The disadvantages of TDEM techniques are as follows:

(5) Do not work well in very resistive material.

(6) Interpretational material for TDEM on, for example, 3D structures is still under development.

(7) TDEM equipment tends to be somewhat more costly due to its greater complexity.

As mentioned above, the advantages are significant, and TDEM is becoming a widely used tool for geoelectrical sounding.

4-7. Frequency-Domain Electromagnetic Methods

a. The electromagnetic induction process.

(1) The electromagnetic induction process is conceptually summarized in Figure 4-39 from Klein and Lajoie (1980). An EM transmitter outputs a time-varying electric current into a transmitter coil. The current in the transmitter coil generates a magnetic field of the same frequency and phase. Lines of force of this magnetic field penetrate the earth and may penetrate a conductive

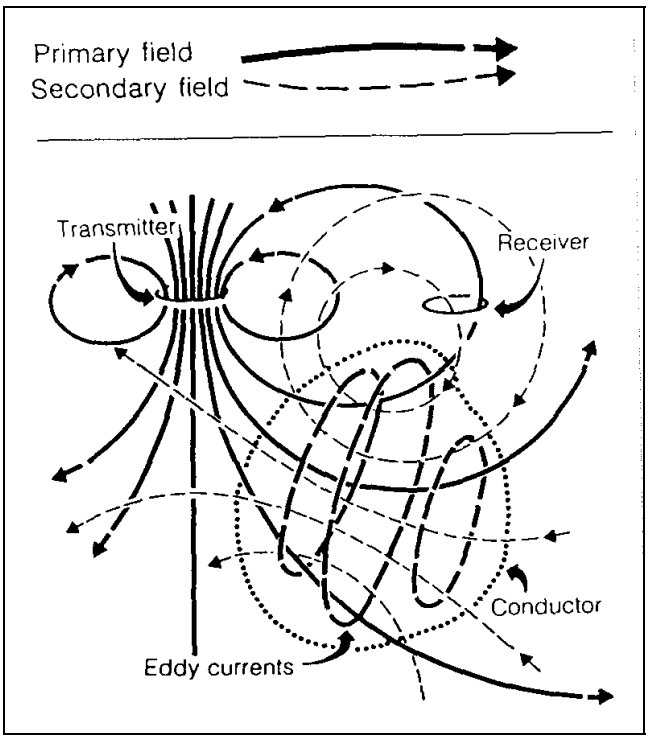

Figure 4-39. Generalized picture of electromagnetic induction prospecting (Klein and Lajoie 1980; copyright permission granted by Northwest Mining Association and Klein)

body. When this occurs, an electromotive force or voltage is set up within the conductor, according to Faraday's Law:

$$EMF_C = M_{TC} \frac{dI_T}{dt} \tag{4-23}$$

where

EMF_C = electromotive force or voltage in the conductor

M_{TC} = mutual inductance between the transmitter and the conductive body in the ground (a complex number)

dI_T/dt = time rate of change (derivative) of the current (I_T) in the transmitter loop

(2) Current will flow in the conductor in response to the induced electromotive force. These currents will usually flow through the conductor in planes

perpendicular to lines of magnetic field of force from the transmitter, unless restricted by the conductor's geometry. Current flow within the conductor generates a secondary magnetic field whose lines of force, at the conductor, are such that they oppose those of the primary magnetic field. The receiver coil, at some distance from the transmitter coil, is therefore energized by two fields: from the transmitter and from the induced currents in the ground.

(3) From Faraday's Law, the EMF induced in the receiver may be expressed as

$$EMF_R = M_{RT} \frac{dI_T}{dt} + M_{RC} \frac{dI_C}{dt} \qquad (4\text{-}24)$$

where

EMF_R = EMF induced in the receiver

M_{RT} = mutual inductance between the receiver (R) and transmitter (T)

M_{RC} = mutual inductance between the receiver (R) and conductor (C) in the ground, a complex number

dI_C/dt or dI_T/dt = time derivative of the current induced in the conductor (C) or transmitter (T)

I_T or I_C = current induced in the conductor (C) or transmitter (T)

(4) Note that the induced currents occur throughout the subsurface, and that the magnitude and distribution are functions of the transmitter frequency, power, and geometry and the distribution of all 'electrical properties' in the subsurface, i.e., everything (not just an isolated 'conductor'). The above discussion simplifies the problem by assuming the presence of only one conductor embedded in a much less conducting medium.

b. Frequency domain EM method. In the frequency domain method, the transmitter emits a sinusoidally varying current at a specific frequency. For example, at a frequency of 100 Hz the magnetic field amplitude at the receiver will be that shown in the top part of Figure 4-40. Because the mutual inductance between the transmitter and conductor is a complex quantity, the electromagnetic force induced in the conductor will be shifted in phase with respect to the primary field, similar to the illustration

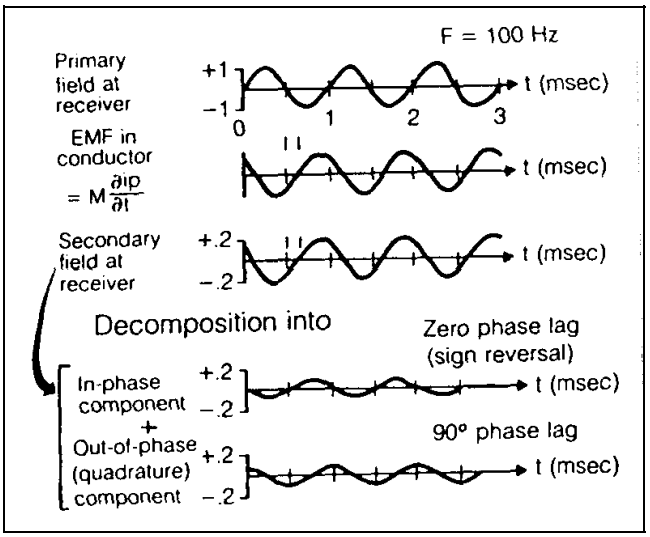

Figure 4-40. Generalized picture of the frequency domain EM method (Klein and Lajoie 1980; copyright permission granted by Northwest Mining Association and Klein)

in the lower part of Figure 4-40. At the receiver, the secondary field generated by the currents in the conductor will also be shifted in phase by the same amount. There are three methods of measuring and describing the secondary field.

(1) Amplitude and phase. The amplitude of the secondary field can be measured and is usually expressed as a percentage of the theoretical primary field at the receiver. Phase shift, the time delay in the received field by a fraction of the period, can also be measured and displayed.

(2) In phase and out-of-phase components. The second method of presentation is to electronically separate the received field into two components, as shown in the lower part of Figure 4-40.

(a) The first component is in phase with the transmitted field while the second component is exactly 90 deg out-of-phase with the transmitted field. The in-phase component is sometimes called the real component, and the out-of-phase component is sometimes called the "quadrature" or "imaginary" component.

(b) Both of the above measurements require some kind of phase link between transmitter and receiver to establish a time or phase reference. This is commonly done with a direct wire link, sometimes with a radio link,

or through the use of highly accurate, synchronized crystal clocks in both transmitter and receiver.

(3) Tilt angle systems. The simpler frequency domain EM systems are tilt angle systems which have no reference link between the transmitter and receiver coils. The receiver simply measures the total field irrespective of phase, and the receiver coil is tilted to find the direction of maximum or minimum magnetic field strength. As shown conceptually in Figure 4-39, at any point the secondary magnetic field may be in a direction different from the primary field. With tilt angle systems, therefore, the objective is to measure deviations from the normal in-field direction and to interpret these in terms of geological conductors.

(4) The response parameter of a conductor is defined as the product of conductivity-thickness (σt), permeability (μ), angular frequency ($\omega = 2\pi f$), and the square of some mean dimension of the target (a^2). The response parameter is a dimensionless quantity. In MKS units, a poor conductor will have a response parameter of less than about 1, whereas an excellent conductor will have a response value greater than 1,000. The relative amplitudes of in-phase and quadrature components as a function of response parameter are given in Figure 4-41 for the particular case of the sphere model in a uniform alternating magnetic field. For low values of the response parameter (< 1), the sphere will generally produce a low-amplitude out-of-phase anomaly; at moderate values of the response parameter (10-100), the response will be a moderate-amplitude in-phase and out-of-phase anomaly, whereas for high values of the response parameter (>1,000), the response will usually be in the in-phase component. Although Figure 4-41 shows the response only for the particular case of a sphere in a uniform field, the response functions for other models are similar.

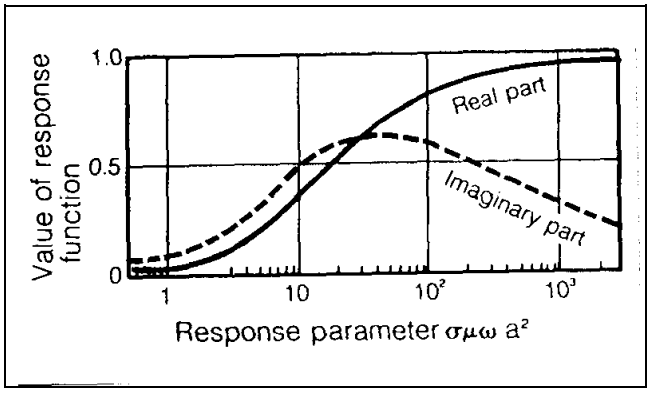

Figure 4-41. In-phase and out-of-phase response of a sphere in a uniform alternating magnetic field (Klein and Lajoie 1980; copyright permission granted by Northwest Mining Association and Klein)

(5) In frequency domain EM, depth and size of the conductor primarily affect the amplitude of the secondary field. The quality of the conductor (higher conductivity means higher quality) mainly affects the ratio of in-phase to out-of-phase amplitudes (A_R/A_I), a good conductor having a higher ratio (left side of Figure 4-41) and a poorer conductor having a lower ratio (right side of Figure 4-41).

(6) Of the large number of electrical methods, many of them are in the frequency domain electromagnetic (FDEM) category and are not often used in geotechnical and environmental problems. Most used for these problems are the so-called terrain conductivity methods, VLF (very low frequency EM method), and a case of instruments called metal detectors.

c. Interpretation procedures.

(1) Interpretation of electromagnetic surveys follows basic steps. Most of the common EM systems have nomograms associated with them. Nomograms are diagrams on which the measured parameters, e.g., in-phase and out-of-phase components, are plotted for varying model conductivity and one or more geometrical factors, e.g., depth to top, thickness, etc. The model responses available for most electromagnetic methods are those of the long, thin dike (to model thin tabular bodies), a homogeneous earth, and a horizontal layer for simulating conductive overburden.

(2) The first step is to attempt to determine from the shape of the anomaly a simple model geometry which can be thought to approximate the cause of the anomaly. The second step is to measure characteristics of the anomaly such as in-phase and out-of-phase amplitudes, and to plot these at the scale of the appropriate nomograms. From the nomogram and the shape of the anomaly, estimates generally can be made for: quality of the conductor, depth to top of the conductor, conductor thickness, dip, strike, and strike length.

4-8. Terrain Conductivity

a. Introduction. Terrain conductivity EM systems are frequency domain electromagnetic instruments which use two loops or coils. To perform a survey, one person generally carries a small transmitter coil, while a second person carries a second coil which receives the primary and secondary magnetic fields. Such devices can allow a

rapid determination of the average conductivity of the ground because they do not require electrical contact with the ground as is required with DC resistivity techniques. The disadvantage is that unless several (usually three) intercoil spacings for at least two coil geometries are measured at each location, minimal vertical sounding information is obtained. If the geology to the depth being explored is fairly homogeneous or slowly varying, then the lack of information about vertical variations may not be a problem, and horizontal profiling with one coil orientation and spacing is often useful. This technique is usually calibrated with a limited number of DC resistivity soundings. Horizontal profiling with the terrain conductivity meter is then used to effectively extend the resistivity information away from the DC sounding locations.

(1) McNeill (1990) gives an excellent review and tutorial of electromagnetic methods and much of his discussion on the terrain conductivity meter is excerpted here (see also Butler (1986)). He lists three significant differences between terrain conductivity meters and the traditional HLEM (horizontal loop electromagnetic) method usually used in mining applications. Perhaps the most important is that the operating frequency is low enough at each of the intercoil spacings that the electrical skin depth in the ground is always significantly greater than the intercoil spacing. Under this condition (known as "operating at low induction numbers") virtually all response from the ground is in the quadrature phase component of the received signal. With these constraints, the secondary magnetic field can be represented as

$$\frac{H_S}{H_P} = \frac{i\omega\mu_0\sigma s^2}{4} \tag{4-25}$$

where

H_S = secondary magnetic field at the receiver coil

H_P = primary magnetic field at the receiver coil

$\omega = 2\pi f$

f = frequency in Hz

μ_0 = permeability of free space

σ = ground conductivity in S/m (mho/m)

s = intercoil spacing in m

$i = (-1)^{1/2}$, denoting that the secondary field is 90 deg out of phase with the primary field

(a) Thus, for low and moderate conductivities, the quadrature phase component is linearly proportional to ground conductivity, so the instruments read conductivity directly (McNeill 1980). Given H_S/H_P, the apparent conductivity indicated by the instrument is defined as

$$\sigma_a = 4\frac{\left[\frac{H_S}{H_P}\right]}{\mu_0\omega s^2} \tag{4-26}$$

The low induction number condition also implies that the measured signals are of extremely low amplitude. Because of the low amplitude signals, terrain conductivity meters must have detection electronics which are an order of magnitude more sensitive than conventional HLEM systems.

(b) The second difference is that terrain conductivity instruments are designed so that the quadrature phase zero level stays constant with time, temperature, etc., to within about 1 millisiemen/meter (or mS/m). The stability of this zero level means that at moderate ground conductivity, these devices give an accurate measurement of bulk conductivity of the ground. These devices, like the conventional HLEM system, do not indicate conductivity accurately in high resistivity ground, because the zero error becomes significant at low values of conductivity.

(c) The third difference is that operation at low induction numbers means that changing the frequency proportionately changes the quadrature phase response. In principle and in general, either intercoil spacing or frequency can be varied to determine variation of conductivity with depth. However, in the EM-31, EM-34, and EM-38 systems, frequency is varied as the intercoil spacing is varied. Terrain conductivity meters are operated in both the horizontal and vertical dipole modes. These terms describe the orientation of the transmitter and receiver coils to each other and the ground, and each mode gives a significantly different response with depth as shown in Figure 4-42. Figure 4-43 shows the cumulative response curves for both vertical dipoles and horizontal dipoles. These curves show the relative contribution to the secondary magnetic field (and hence apparent conductivity) from all material below a given depth. As an example, this figure shows that for vertical dipoles, all material below a depth of two intercoil spacings yields a

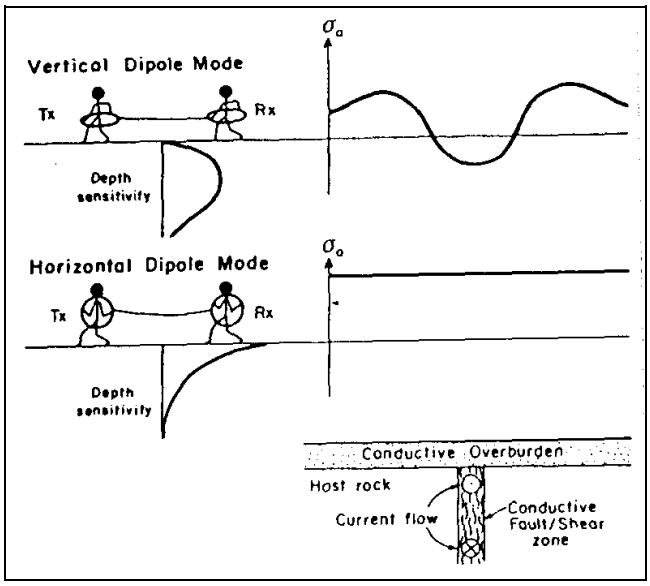

Figure 4-42. Terrain conductivity meter response over conductive dike (McNeill 1990; copyright permission granted by Society of Exploration Geophysicists)

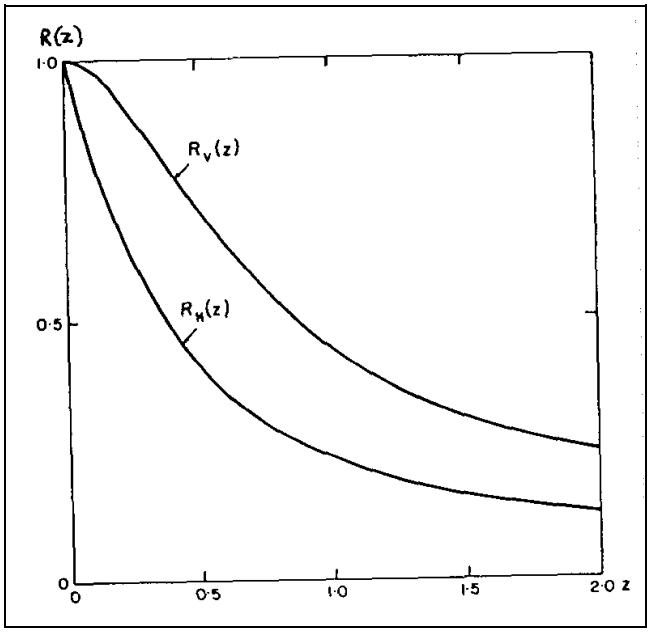

Figure 4-43. Cumulative response curves for both vertical coplanar and horizontal coplanar dipoles. *z* is actually depth/intercoil spacing (McNeill 1980; copyright permission granted by Geonics Limited)

relative contribution of approximately 0.25 (25 percent) to the response, i.e. the conductivity measurement. Thus, effective exploration depth in a layered earth geometry is approximately 0.25 to 0.75 times the intercoil spacing for the horizontal dipole mode and 0.5 to 1.5 for the vertical dipole mode. The commonly used systems use intercoil spacings of 1 m, 3.66 m, 10 m, 20 m, and 40 m.

(d) Terrain conductivity meters have shallower exploration depths than conventional HLEM, because maximum intercoil spacing is 40 m for the commonly used instruments. However, terrain conductivity meters are being widely used in geotechnical and environmental investigations. Of particular interest is the fact that when used in the vertical dipole mode the instruments are more sensitive to the presence of relatively conductive, steeply dipping structures, whereas in the horizontal dipole mode the instruments are quite insensitive to this type of structure and can give accurate measurement of ground conductivity in close proximity to them.

(2) Phase and other information is obtained in real time by linking the transmitter and receiver with a connecting cable. The intercoil spacing is determined by measuring the primary magnetic field with the receiver coil and adjusting the intercoil spacing so that it is the correct value for the appropriate distance. In the vertical dipole mode, the instruments are relatively sensitive to intercoil alignment, but much less so in the horizontal dipole mode. Terrain conductivity is displayed on the instrument in mS/m. (A conductivity of 1 mS/m corresponds to a resistivity of 1 kΩm or 1,000 Ωm.)

b. Interpretation. Because terrain conductivity meters read directly in apparent conductivity and most surveys using the instrument are done in the profile mode, interpretation is usually qualitative and of the "anomaly finding" nature. That is, the area of interest is surveyed with a series of profiles with a station spacing dictated by the required resolution and time/economics consideration. Typical station spacings are one-third to one-half the intercoil spacing. Any anomalous areas are investigated further with one or more of the following: other types of EM, resistivity sounding, other geophysical techniques, and drilling. Limited information about the variation of conductivity with depth can be obtained by measuring two or more coil orientations and/or intercoil separations and using one of several commercially available computer programs. The maximum number of geoelectric parameters, such as layer thicknesses and resistivities, which can be determined, is less than the number of independent observations. The most common instrument uses three standard intercoil distances (10, 20, and 40 m) and two intercoil orientations, which results in a maximum of six observations. Without other constraints, a two-layer model is the optimum.

(1) Example 1 - mapping industrial groundwater contamination.

(a) Non-organic (ionic) groundwater contamination usually results in an increase in the conductivity of the groundwater. For example, in a sandy soil the addition of 25 ppm of ionic material to groundwater increases ground conductivity by approximately 1 mS/m. The problem is to detect and map the extent of the contamination in the presence of conductivity variations caused by other parameters such as changing lithology. Organic contaminants are generally insulators and so tend to reduce the ground conductivity, although with much less effect than an equivalent percentage of ionic contaminant. Fortunately, in many cases where toxic organic substances are present, there are ionic materials as well, and the plume is mapped on the theory that the spatial distribution of both organic and ionic substances is essentially the same, a fact which must be verified by subsequent sampling from monitoring wells installed on the basis of the conductivity map.

(b) McNeill (1990) summarizes a case history by Ladwig (1982) which uses a terrain conductivity meter to map the extent of acid mine drainage in a rehabilitated surface coal mine in Appalachia. Measurements were taken with an EM ground conductivity meter in the horizontal dipole mode at both 10- and 20-m intercoil spacings (10-m data are shown in Figure 4-44). Ten survey lines, at a spacing of 25 m, resulted in 200 data points for each spacing; the survey took 2 days to complete. In general, conductivity values of the order of 6-10 mS/m

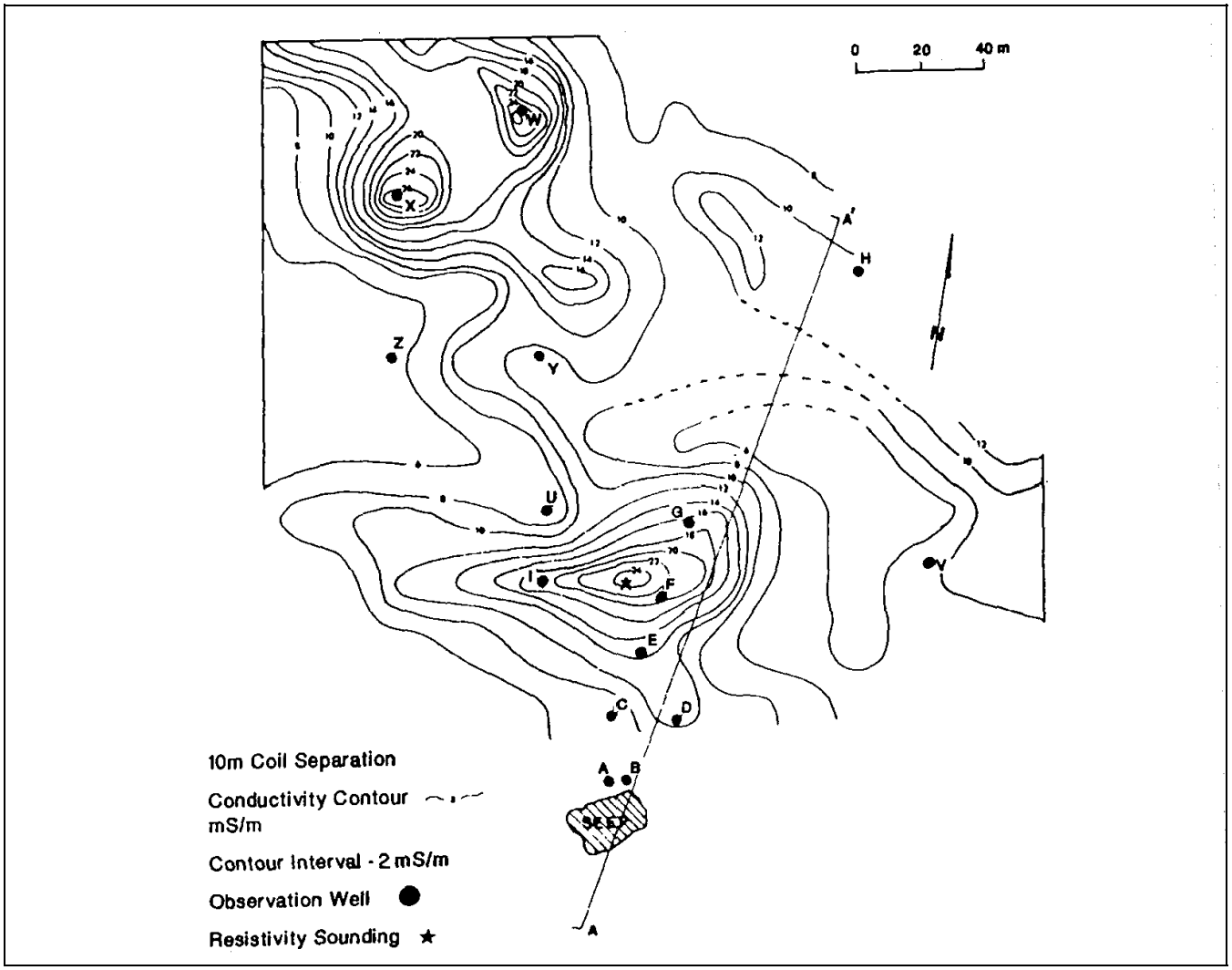

Figure 4-44. Contours of apparent resistivity for an acid mine dump site in Appalachia from terrain conductivity meter (Ladwig (1982) in McNeill (1990); copyright permission granted by Society of Exploration Geophysicists)

are consistent with a porous granular material reasonably well-drained or containing nonmineralized groundwater. Superimposed on this background are two steep peaks (one complex) where conductivities rise above 20 mS/m.

Wells F, G, and X were the only wells to encounter buried refuse (well W was not completed), and all three are at or near the center of the high conductivity zones. The water surface at well F is about 3 m below the surface, and at well X is 16.2 m below the surface. In fact, the only region where the water surface is within 10 m of the surface is at the southern end of the area; the small lobe near well D corresponds to the direction of groundwater flow to the seep (as the result of placement of a permeability barrier just to the west of the well). It thus appears that in the area of wells X and W, where depth to water surface is large, the shape and values of apparent conductivity highs are due to vertically draining areas of acidity. Further to the south the conductivity high is probably reflecting both increased acidity and proximity of the water surface.

(2) Examples 2 and 3 - mapping soil and groundwater salinity.

(a) EM techniques are well suited for mapping soil salinity to depths useful for the agriculturalist (the root zone, approximately 1 m) and many salinity surveys have been carried out with EM ground conductivity meters (McNeill 1990). In arid areas where the water surface is near the surface (within a meter or so), rapid transport of water to the surface as a result of capillary action and evaporation takes place, with the consequence that dissolved salts are left behind to hinder plant growth (McNeill 1986).

(b) An EM terrain conductivity meter with short intercoil spacing (a few meters or less) is necessary to measure shallow salinity. Fortunately the values of conductivity which result from agriculturally damaging salinity levels are relatively high and interfering effects from varying soil structure, clay content, etc. can usually be ignored. Equally important, because salt is hygroscopic, those areas which are highly salinized seem to retain enough soil moisture to keep the conductivity at measurable levels even when the soil itself is relatively dry.

(c) McNeill (1990) summarizes the results of a high-resolution survey of soil salinity carried out by Wood (1987) over dry farm land in Alberta, Canada (Figure 4-45). For this survey an EM terrain conductivity meter with an intercoil spacing of 3.7 m was mounted in the vertical dipole mode on a trailer which was in turn towed behind a small four-wheeled, all-terrain vehicle. The surveyed area is 1,600 m long by 750 m wide. The 16 survey lines were spaced 50 m apart resulting in a total survey of 25 line km, which was surveyed in about 7 hr at an average speed of 3.5 km/hour. Data were collected automatically every 5.5 m by triggering a digital data logger from a magnet mounted on one of the trailer wheels.

(d) Survey data are contoured directly in apparent conductivity at a contour interval of 20 mS/m. The complexity and serious extent of the salinity is quite obvious. The apparent conductivity ranges from a low of 58 mS/m, typical of unsalinized Prairie soils, up to 300 mS/m, a value indicating extreme salinity. Approximately 25 percent of the total area is over 160 mS/m, a value indicating a high level of salinity. The survey revealed and mapped extensive subsurface salinity, not apparent by surface expression, and identified the areas most immediately threatened.

(e) An example of a deeper penetrating survey to measure groundwater salinity was conducted by Barker (1990). The survey illustrates the cost-effective use of electromagnetic techniques in the delineation of the lateral extent of areas of coastal saltwater intrusion near Dungeness, England. As with most EM profiling surveys, a number of resistivity soundings were first made at the sites of several drill holes to help design the EM survey. In Figure 4-46, a typical sounding and interpretation shows a three-layer case in which the low resistivity third layer appears to correlate with the conductivity of water samples from the drill holes and the formation clay/sand lithology. To achieve adequate depth of investigation so that changes in water conductivity within the sands would be clearly identified, large coil spacings of 20 and 40 m were employed. The area is easily accessible and measurements can be made rapidly but to reduce errors of coil alignment over some undulating gravel ridges, a vertical coil configuration was employed. This configuration is also preferred as the assumption of low induction numbers for horizontal coils breaks down quickly in areas of high conductivity. The extent of saline groundwater is best seen on Figure 4-47, which shows the contoured ground conductivity in mS/m for the 40-m coil spacing. This map is smoother and less affected by near-surface features than measurements made with the 20-m coil spacing, and shows that the saline intrusion generally occurs along a coastal strip about 0.5 km wide. However, flooding of inland gravel pits by the sea during storms has allowed marine incursion in the west, leaving an isolated body of fresh water below Dungeness.

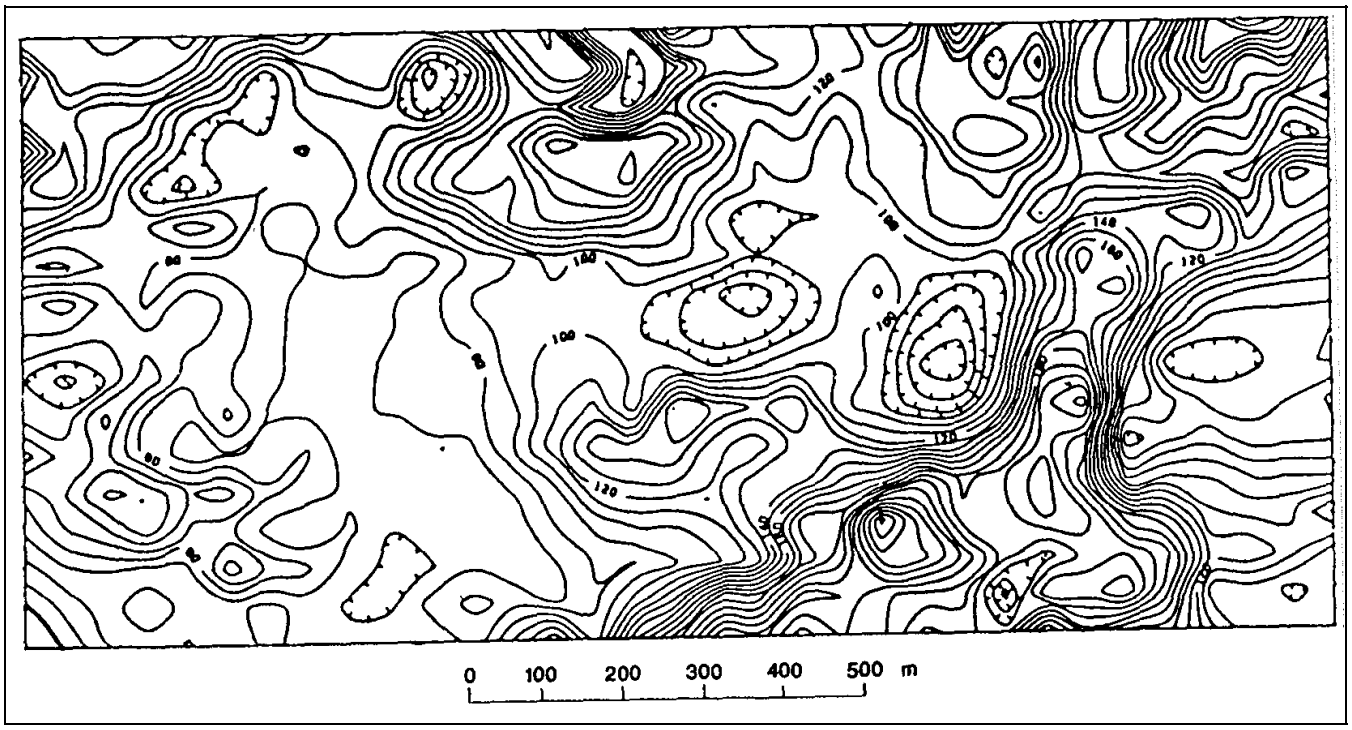

Figure 4-45. Contours of apparent conductivity measured with ground conductivity meter over dry farm land, Alberta, Canada (Wood (1987) in McNeill (1990); copyright permission granted by Society of Exploration Geophysicists)

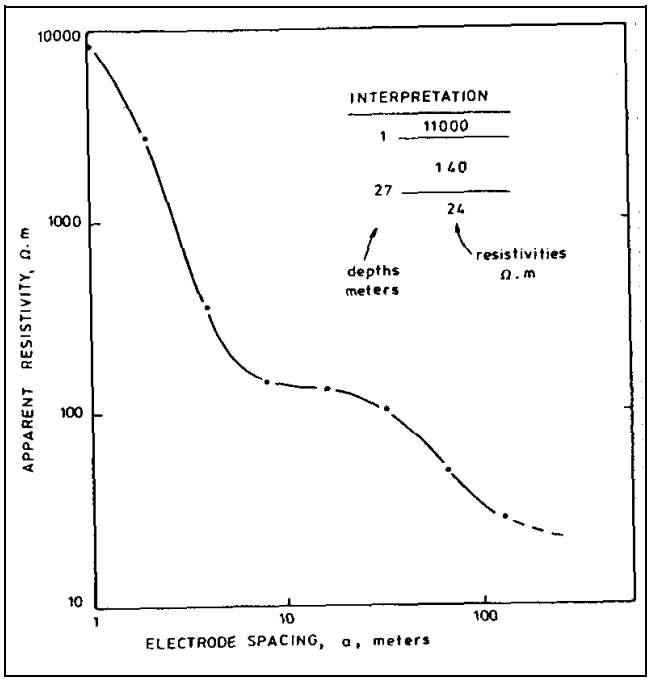

Figure 4-46. Typical resistivity sounding and interpretation, Dungeness, England (Barker 1990; copyright permission granted by Society of Exploration Geophysicists)

(3) Example 4 - subsurface structure. Dodds and Ivic (1990) describe a terrain conductivity meter survey to investigate the depth to basement in southeast Australia. During the first part of the survey, time domain EM and resistivity soundings were used to detect a basement high which impedes the flow of saline groundwater. In the second part of the survey, a terrain conductivity meter was used to map the extent of the basement high "as far and as economically as possible." The largest coil separation available with the instrument, 40 m, was used to get the deepest penetration with horizontal coil orientation. A very limited amount of surveying, using short traverses, successfully mapped out a high-resistivity feature (Figure 4-48). This zone is confirmed by the plotted drilling results.

4-9. Metal Detector Surveys

The term "metal detector" (MD) generally refers to some type of electromagnetic induction instrument, although traditional magnetometers are often used to find buried metal. The disadvantage of magnetometers is that they can be used only for locating ferrous metals. MD instruments in geotechnical and hazardous-waste site investigations have several uses:

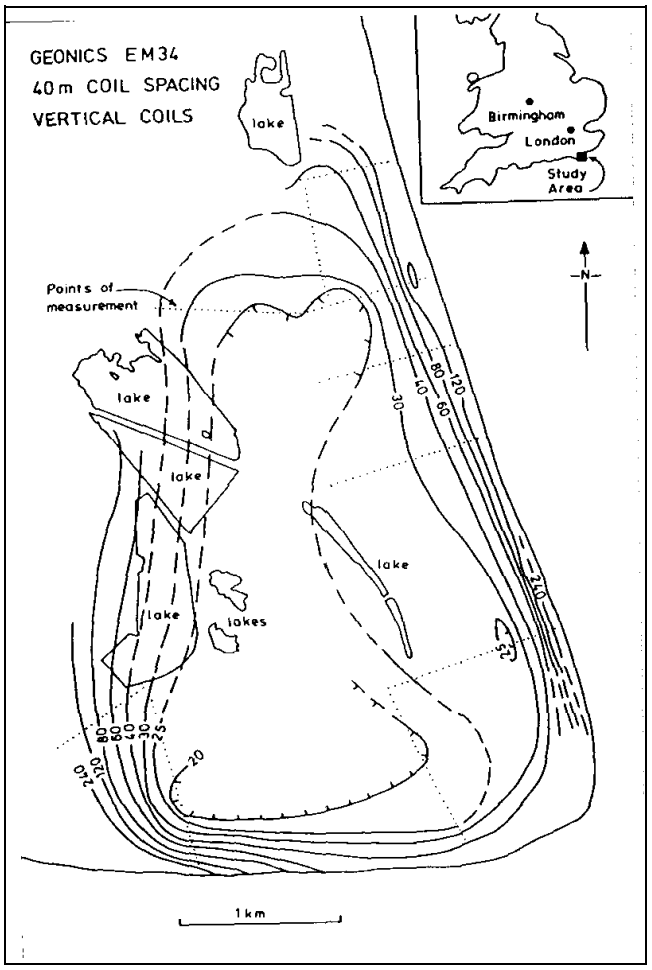

Figure 4-47. Contours of ground conductivity in mS/m, Dungeness, England (Barker 1990; copyright permission granted by Society of Exploration Geophysicists)

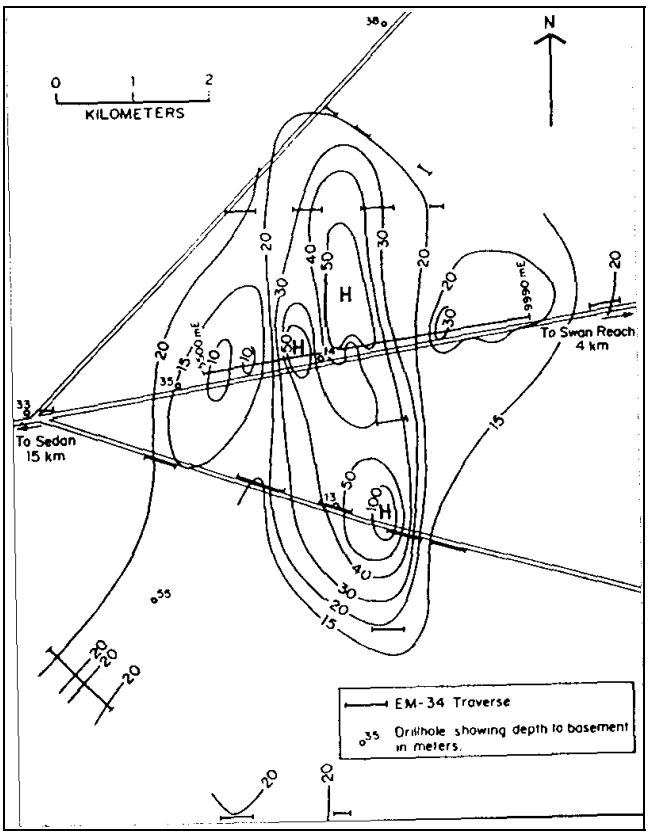

Figure 4-48. Apparent resistivity contours in Ωm from a terrain conductivity meter in southern Australia (Dodds and Ivic 1990; copyright permission granted by Society of Exploration Geophysicists)

Location of shallow metal drums, canisters, cables, and pipes.

Progress assessment during metal object removal and location of additional objects.

Avoidance of old buried metal objects during new construction, remediation, or well placement.

a. MD use.

(1) In the smaller terrain conductivity meters, the transmitter and receiver coils are rigidly connected, allowing the in-phase response to be measured in addition to the quadrature response (McNeill 1990). Some basic equations are given in Section 4-7, "Frequency-Domain EM Methods." This feature allows systems such as the EM-31 and EM-38 to function as MD's. Several coil arrangements are favored by different commercial manufacturers. The smallest units have coil diameters of as little as 0.2 m and use a vertical-axis, concentric coil arrangement. These instruments are the coin and jewelry "treasure finders" used on every tourist beach in the world; they have very limited depth of investigation for geotechnical targets (Figure 4-49 from Benson, Glaccum, and Noel (1983)). One of the newest and most sophisticated MD uses three vertical-axis, 1-m^2 coils: one transmitter coil, one main receiving coil coincident with the transmitter, and one "focussing" coil 0.4 m above the main coil. This instrument continuously records the data and has sophisticated computer software which can yield depth of the object and other properties. In a third, and very common, coil arrangement, the transmitter loop is horizontal and the receiver loop is perpendicular in the vertical plane (Figure 4-50 from Benson, Glaccum, and Noel (1983)).

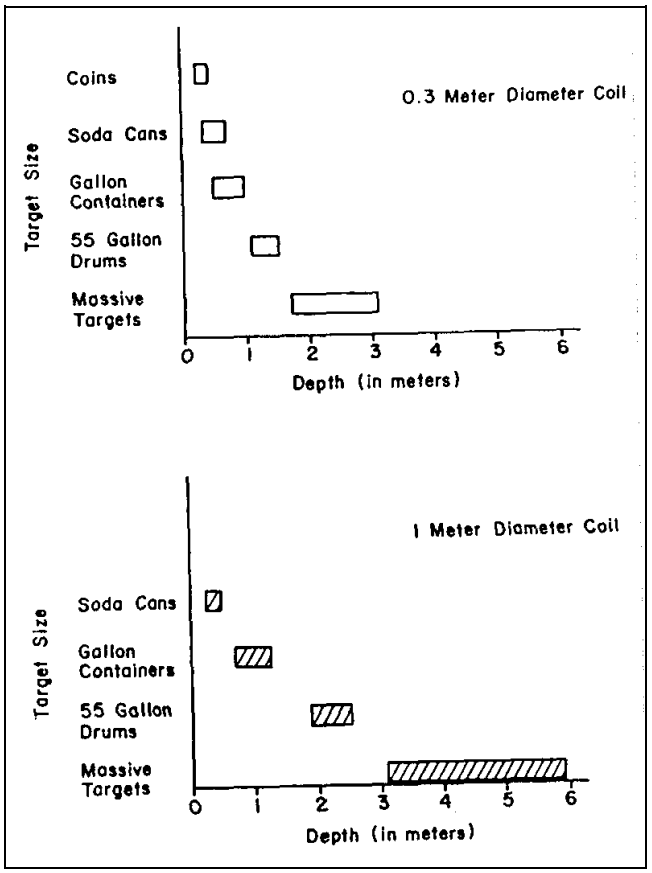

Figure 4-49. Approximate metal detector (MD) detection depths for various targets with two coil sizes (Benson, Glaccum, and Noel 1983)

(2) Another method of classifying MD instruments is by typical application: "hobby" and "treasure finding" equipment, sensitive to very shallow and smaller surface area targets; utility-location and military instruments, sensitive to deeper and larger objects, but usually without data recording and post-processing provisions; and, specialized instruments with large coils, possibly vehicle-mounted with continuous data recording and postprocessing.

(a) The two most important target properties which increase the secondary field (and thus optimize detection) are increased surface area within the target mass and decreased depth of burial. Overall target mass is relatively unimportant; response is proportional to surface area cubed (Hempen and Hatheway 1992). Signal response is proportional to depth; so, depths of detection rarely exceed 10 to 15 m even for sizable conductors. Often of great importance, and unlike magnetometers, MD produce a response from nonferrous objects such as aluminum, copper, brass, or conductive foil.

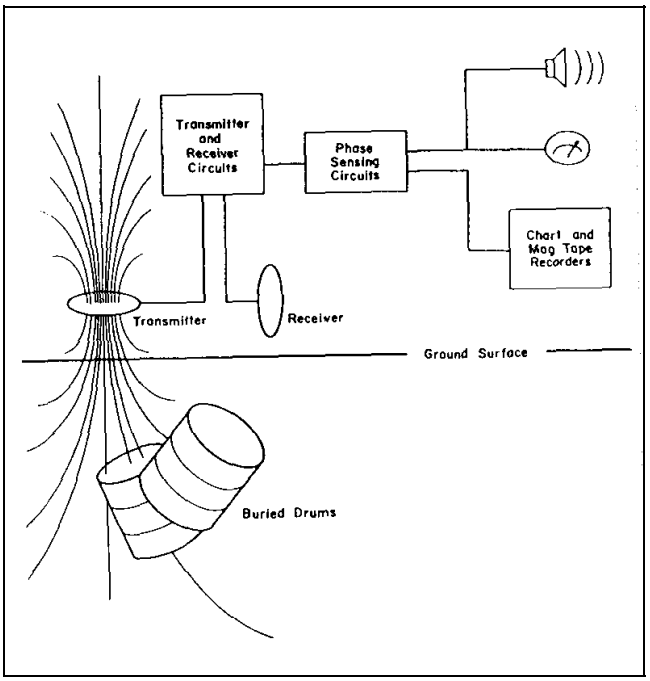

Figure 4-50. Block diagram of one MD coil arrangement and associated electronics (Benson, Glaccum, and Noel 1983)

(b) The main advantages of MD instruments are: both ferrous and nonferrous metals may be detected; the surface area of the target is more important that its mass; and surveys are rapid and detailed and inexpensive. The main disadvantages are: depth of investigation is very limited with most instruments; and metallic litter and urban noise can severely disrupt MD at some sites.

b. MD example. Figure 4-51 shows a test survey made with one of the new generation of sophisticated MD over a variety of buried metal objects and compared with a magnetic gradiometer (Geonics 1993). Both instruments appear to have "detected" all of the buried objects but the quality of spatial resolution is quite different. Spatial resolution is judged by how tightly the response of an instrument fits the target. The magnetometer resolves the single barrels very well. Spurious dipolar-lows become evident for the barrel clusters, and complex responses are recorded around the pipes and sheets. The MD responses fit all the targets very well, regardless of shape, orientation, or depth. This particular MD also shows the value of a second receiver coil to help distinguish between near surface and deeper targets.

Columbia Test-Site
EM61 vs. Gradiometer

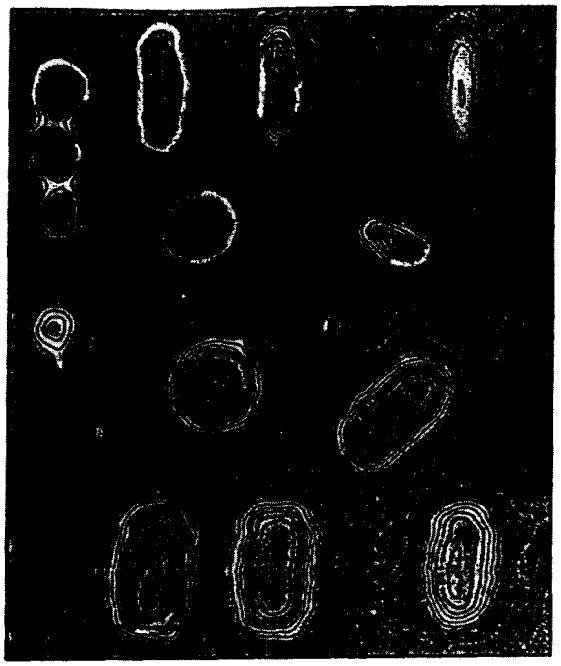

EM61 Amplitude (millivolts)

EM61 Metal Detector
Good depth of exploration
Excellent spatial resolution
Excellent Interpretability

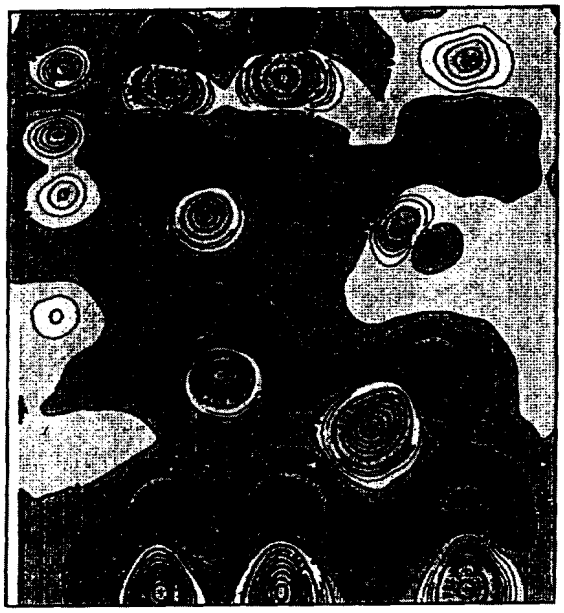

Gradiometer (Magnetics)

Gradiometer
Excellent depth of exploration
Poor spatial resolution
Poor interpretability

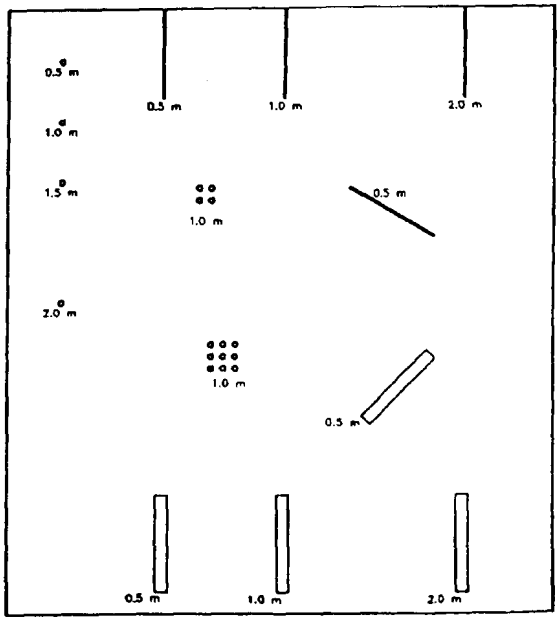

Columbia Test-Site Map

LEGEND:

○ Vertical barrel, 0.6m by 0.9m high
_____ Pipe, 0.1m by 8m
▭ Sheet metal, 1m by 8m

Plotted next to the hazards are their burial depths in meters.

Figure 4-51. Test survey using a metal detector and a magnetic gradiometer (Geonics (1993); copyright permission granted by Geonics Limited)

4-10. Ground-Penetrating Radar

a. Introduction. Ground-penetrating radar (GPR) uses a high-frequency (80 to 1,000 MHz) EM pulse transmitted from a radar antenna to probe the earth. The transmitted radar pulses are reflected from various interfaces within the ground and this return is detected by the radar receiver. Reflecting interfaces may be soil horizons, the groundwater surface, soil/rock interfaces, man-made objects, or any other interface possessing a contrast in dielectric properties. The dielectric properties of materials correlate with many of the mechanical and geologic parameters of materials.

(1) The radar signal is imparted to the ground by an antenna that is in close proximity to the ground. The reflected signals can be detected by the transmitting antenna or by a second, separate receiving antenna. The received signals are processed and displayed on a graphic recorder. As the antenna (or antenna pair) is moved along the surface, the graphic recorder displays results in a cross-section record or radar image of the earth. As GPR has short wavelengths in most earth materials, resolution of interfaces and discrete objects is very good. However, the attenuation of the signals in earth materials is high and depths of penetration seldom exceed 10 m. Water and clay soils increase the attenuation, decreasing penetration.

(2) The objective of GPR surveys is to map near-surface interfaces. For many surveys, the location of objects such as tanks or pipes in the subsurface is the objective. Dielectric properties of materials are not measured directly. The method is most useful for detecting changes in the geometry of subsurface interfaces.

(3) Geologic problems conducive to solution by GPR methods are numerous and include the following: bedrock configuration, location of pipes and tanks, location of the groundwater surface, borrow investigations, and others. Geologic and geophysical objectives determine the specific field parameters and techniques. Delineation of the objectives and the envelope of acceptable parameters are specified in advance. However, as the results cannot be foreseen from the office, considerable latitude is given to the field geophysicist to incorporate changes in methods and techniques.

(4) The following questions are important considerations in advance of a GPR survey.

(a) What is the target depth? Though target detection has been reported under unusually favorable circumstances at depths of 100 m or more, a careful feasibility evaluation is necessary if the investigation depths need to exceed 10 m.

(b) What is the target geometry? Size, orientation, and composition are important.

(c) What are the electrical properties of the target? As with all geophysical methods, a contrast in physical properties must be present. Dielectric constant and electrical conductivity are the important parameters. Conductivity is most likely to be known or easily estimated.

(d) What are the electrical properties of the host material? Both the electrical properties and homogeneity of the host must be evaluated. Attenuation of the signal is dependent on the electrical properties and on the number of minor interfaces which will scatter the signal.

(e) Are there any possible interfering effects? Radio frequency transmitters, extensive metal structures (including cars) and power poles are probable interfering effects for GPR.

(f) Electromagnetic wave propagation. The physics of electromagnetic wave propagation are beyond the scope of this manual. However, there are two physical parameters of materials which are important in wave propagation at GPR frequencies. One property is conductivity (σ), the inverse of electrical resistivity (ρ). The relationships of earth material properties to conductivity, measured in mS/m (1/1,000 Ωm), are given in Table 4-1 on resistivity.

(g) The other physical property of importance at GPR frequencies is the dielectric constant (ε), which is dimensionless. This property is related to how a material reacts to a steady-state electric field; that is, conditions where a potential difference exists but no charge is flowing. Such a condition exists between the plates of a charged capacitor. A vacuum has the lowest ε and the performance of other materials is related to that of a vacuum. Materials made up of polar molecules, such as water, have a high ε. Physically, a great deal of the energy in an EM field is consumed in interaction with the molecules of water or other polarizable materials. Thus waves propagating through such a material both go slower and are subject to more attenuation. To complicate matters, water, of course, plays a large role in determining the conductivity (resistivity) of earth materials.

b. Earth material properties. The roles of two earth materials, which cause important variations in the EM

response in a GPR survey, need to be appreciated. The ubiquitous component of earth materials is water; the other material is clay. At GPR frequencies the polar nature of the water molecule causes it to contribute disproportionately to the displacement currents which dominate the current flow at GPR frequencies. Thus, if significant amounts of water are present, the ε will be high and the velocity of propagation of the electromagnetic wave will be lowered. Clay materials with their trapped ions behave similarly. Additionally, many clay minerals also retain water.

(1) The physical parameters in Table 4-3 are typical for the characterization of earth materials. The range for each parameter is large; thus the application of these parameters for field use is not elementary.

Simplified equations for attenuation and velocity (at low loss) are:

$$V = (3x10^8)/\varepsilon^{1/2} \quad (4\text{-}27)$$

$$a = 1.69\sigma/\varepsilon^{1/2} \quad (4\text{-}28)$$

where

V = velocity in m/s

ε = dielectric constant (dimensionless)

a = attenuation in decibels/m (db/m)

σ = electrical conductivity in mS/m

A common evaluation parameter is dynamic range or performance figure for the specific GPR system. The performance figure represents the total attenuation loss during the two-way transit of the EM wave that allows reception; greater losses will not be recorded. As sample calculations, consider a conductive material (σ = 100 mS/m) with some water content (ε=20). The above equations indicate a velocity of 0.07 m per nanosecond (m/ns) and an attenuation of 38 db/m. A GPR system with 100 db of dynamic range used for this material will cause the signal to become undetectable in 2.6 m of travel. The transit time for 2.6 m of travel would be 37 to 38 ns. This case might correspond geologically to a clay material with some water saturation. Alternatively, consider a dry material (ε=5) with low conductivity (σ = 5 mS/m). The calculated velocity is 0.13 m/ns and the attenuation is 3.8 db/m, corresponding to a distance of 26-27 m for 100 db of attenuation and a travel time of 200 ns or more. This example might correspond to dry sedimentary rocks.

(2) These large variations in velocity and especially attenuation are the cause of success (target detection) and failure (insufficient penetration) for surveys in apparently similar geologic settings. As exhaustive catalogs of the properties of specific earth materials are not readily available, most GPR work is based on trial and error and empirical findings.

c. Modes of operation.

(1) The useful item of interest recorded by the GPR receiver is the train of reflected pulses. The seismic

Table 4-3
Electromagnetic Properties of Earth Materials

Material	ε	Conductivity (mS/m)	Velocity (m/ns)	Attenuation (db/m)
Air	1	0	.3	0
Distilled Water	80	.01	.033	.002
Fresh Water	80	.5	.033	.1
Sea Water	80	3,000	.01	1,000
Dry Sand	3-5	.01	.15	.01
Wet Sand	20-30	.1-1	.06	.03-.3
Limestone	4-8	.5-2	.12	.4-1
Shales	5-15	1-100	.09	1-100
Silts	5-30	1-100	.07	1-100
Clays	5-40	2-1,000	.06	1-300
Granite	4-6	.01-1	.13	.01-1
Dry Salt	5-6	.01-1	.13	.01-1
Ice	3-4	.01	.16	.01
Metals		∞		∞

reflection analogy is appropriate. The two reflection methods used in seismic reflection (common offset and common midpoint) are also used in GPR. Figure 4-52 illustrates these two modes. A transillumination mode is also illustrated in the figure which is useful in certain types of nondestructive testing. The typical mode of operation is the common-offset mode where the receiver and transmitter are maintained at a fixed distance and moved along a line to produce a profile. Figure 4-53 illustrates the procedure. Note that as in seismic reflection, the energy does not necessarily propagate only downwards and a reflection will be received from objects off to the side. An added complication with GPR is the fact that some of the energy is radiated into the air and, if reflected off nearby objects like buildings or support vehicles, will appear on the record as arrivals.

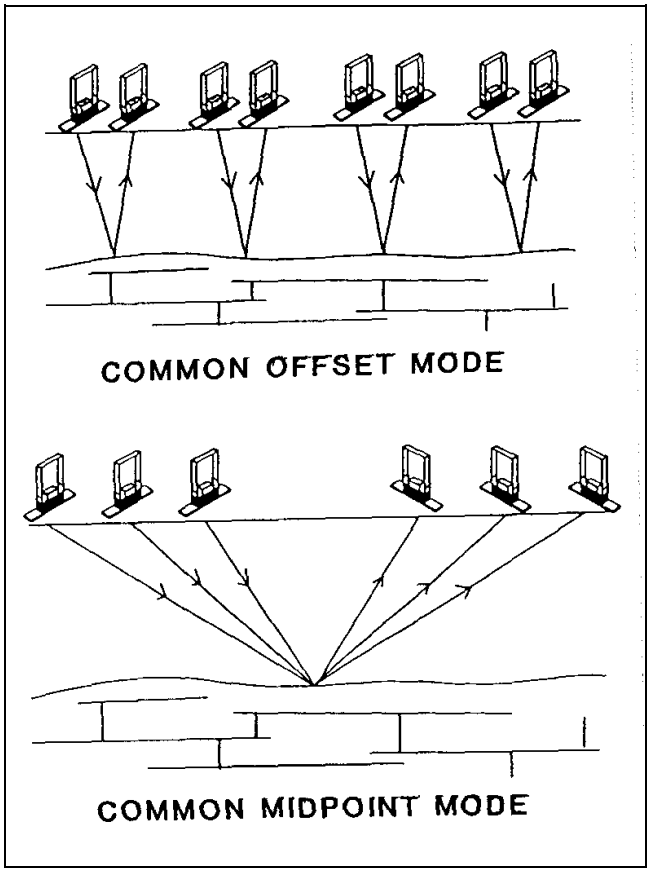

Figure 4-52. Common offset and common midpoint acquisition modes (Annan (1992))

(2) GPR records can be recorded digitally and reproduced as wiggle trace or variable area record sections. Figure 4-54 illustrates the presentation used when a graphic recorder is used to record analog data. Both

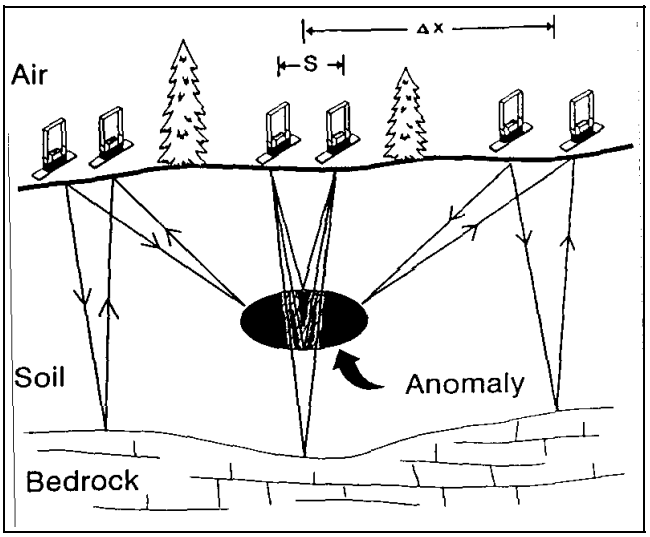

Figure 4-53. Schematic illustration of common-offset single-fold profiling

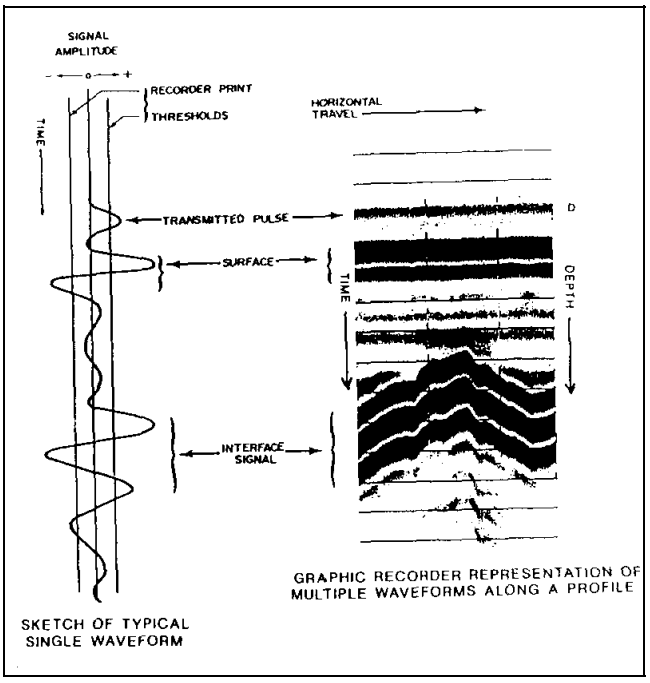

Figure 4-54. GPR received signal and graphic profile display (Benson, Glaccum, and Noel 1983)

negative and positive excursions in excess of the "threshold" appear as blackened portions of the record. This presentation is adequate for most tasks where target detection is the object and post-survey processing is not anticipated. Wide variations in the appearance of the record are possible, depending on the gain settings used.

d. Field work.

(1) A GPR crew consists nominally of two persons. One crew person moves the antenna or antenna pair along the profiles and the other operates the recorder and annotates the record so that the antenna position or midpoint can be recovered.

(2) The site-to-site variation in velocity, attenuation, and surface conditions is so large, that seldom can the results be predicted before field work begins. Additionally, the instrument operation is a matter of empirical trial and error in manipulating the appearance of the record. Thus, the following steps are recommended for most field work:

(a) Unpack and set up the instrument and verify internal operation.

(b) Verify external operation (one method is to point the antenna at a car or wall and slowly walk towards it. The reflection pattern should be evident on the record).

(c) Calibrate the internal timing by use of a calibrator.

(d) Calibrate the performance by surveying over a known target at a depth and configuration similar to the objective of the survey (considerable adjustment of the parameters may be necessary to enhance the appearance of the known target on the record).

(e) Begin surveying the area of unknown targets with careful attention to surface conditions, position recovery, and changes in record character.

Often a line will be done twice to be sure that all the features on the record are caused by the subsurface.

e. Interpretation methods. Because of the strong analogy between seismic reflection and GPR, the application of seismic processing methods to GPR data is a fertile field of current research. Such investigations are beyond the scope of this manual. The focus herein is on the most frequent type of GPR survey, location of specific targets.

(1) GPR surveys will not achieve the desired results without careful evaluation of site conditions for both geologic or stratigraphic tasks and target-specific interests. If the objectives of a survey are poorly drawn, often the results of the GPR survey will be excellent records which do not have any straightforward interpretation. It is possible to tune a GPR system such that exceptional subsurface detail is visible on the record. The geologic evaluation problem is that, except in special circumstances (like the foreset beds inside of sand dunes), there is no ready interpretation. The record reveals very detailed stratigraphy, but there is no way to verify which piece of the record corresponds to which thin interbedding of alluvium or small moisture variation. GPR surveys are much more successful when a calibration target is available. GPR can be useful in stratigraphic studies; however, a calibrated response (determined perhaps from backhoe trenching) is required for geologic work.

(2) Figure 4-55 indicates that localized objects will produce a hyperbola on the record. The hyperbolic shape is due to reflection returns of the EM pulse before and after the antenna system is vertically above the target. The shortest two-way travel distance is when the antenna (or center of the antennae pair) is on the ground surface directly above the object. All other arrivals are at greater distances along a different hypotenuse with each varying horizontal antenna location.

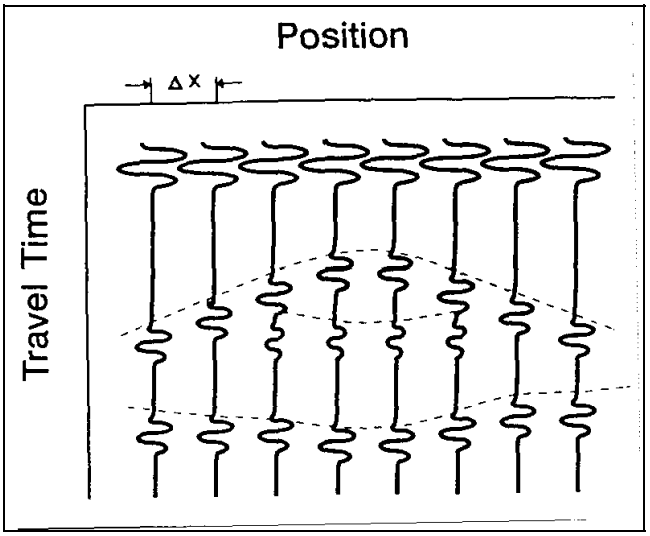

Figure 4-55. Format of a GPR reflection section with radar events shown for features depicted in Figure 4-53

(3) Figure 4-56 is the schematic of a set of targets surveyed by GPR. The record section of Figure 4-57 indicates the excellent detection of the targets.

f. GPR case histories. GPR has been widely used and reports on its effectiveness are available both in government and professional documents. Some useful references are:

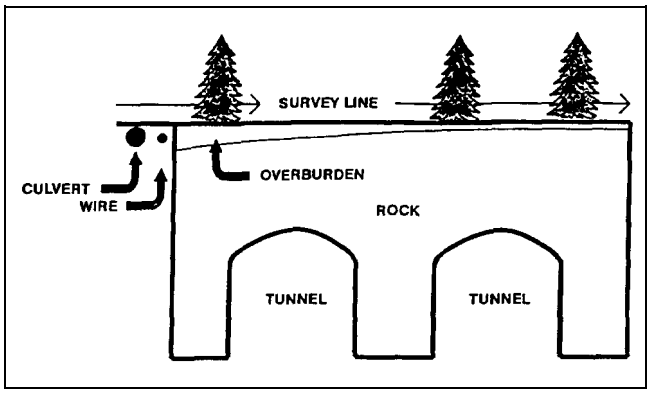

Figure 4-56. Schematic of a set of targets surveyed by GPR

(1) Butler (1992), which is the proceedings of a GPR workshop and includes a tutorial and a collection of case histories.

(2) Butler, Simms, and Cook (1994), which provides an archaeological site evaluation.

(3) Sharp, Yule, and Butler (1990), which reports the GPR assessment of an HTRW site.

4-11. Very Low-Frequency EM Procedures

a. General methodology.

(1) The VLF (very low-frequency) method uses powerful remote radio transmitters set up in different parts of the world for military communications (Klein and Lajoie 1980). In radio communications terminology, VLF means very low-frequency, about 15 to 25 kHz. Relative to frequencies generally used in geophysical exploration, these are actually very high frequencies. The radiated field from a remote VLF transmitter, propagating over a uniform or horizontally layered earth and measured on the earth's surface, consists of a vertical electric field component and a horizontal magnetic field component each perpendicular to the direction of propagation.

(2) These radio transmitters are very powerful and induce electric currents in conductive bodies thousands of kilometers away. Under normal conditions, the fields produced are relatively uniform in the far field at a large distance (hundreds of kilometers) from the transmitters. The induced currents produce secondary magnetic fields which can be detected at the surface through deviation of the normal radiated field.

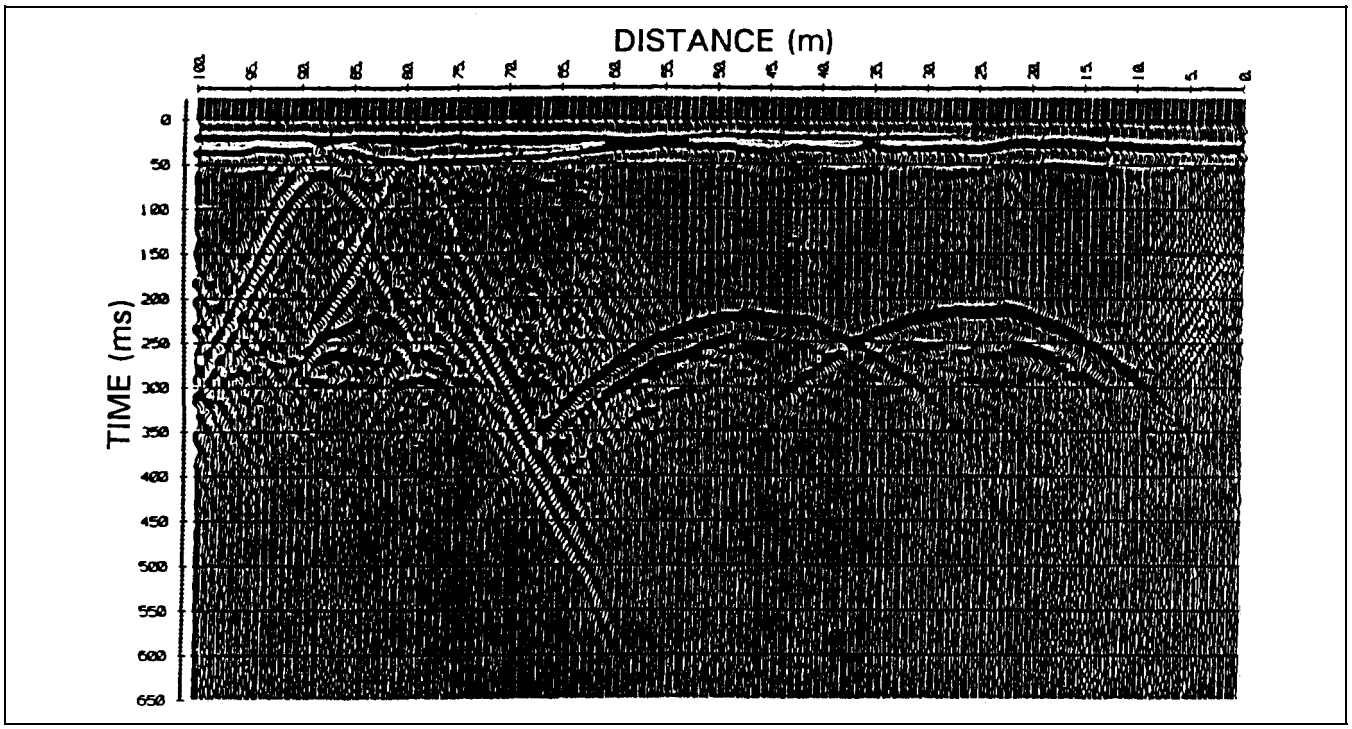

Figure 4-57. Actual GPR record over a culvert, pipe, and two tunnels showing the hyperbolic shape of the reflected/diffracted energy (Annan (1992))

(3) The VLF method uses relatively simple instruments and can be a useful reconnaissance tool. Potential targets include tabular conductors in a resistive host rock like faults in limestone or igneous terrain. The depth of exploration is limited to about 60 to 70 percent of the skin depth of the surrounding rock or soil. Therefore, the high frequency of the VLF transmitters means that in more conductive environments the exploration depth is quite shallow; for example, the depth of exploration might be 10-12 m in 25-Ωm material. Additionally, the presence of conductive overburden seriously suppresses response from basement conductors while relatively small variations in overburden conductivity or thickness can themselves generate significant VLF anomalies. For this reason, VLF is more effective in areas where the host rock is resistive and the overburden is thin.

b. VLF interpretation.

(1) VLF response is a maximum when the target strikes in the direction of the transmitter, falling off roughly as the cosine of the strike angle for other directions. However, there are a number of transmitters worldwide and seldom is the selection of an appropriate transmitter a problem. Because of the rudimentary nature of VLF measurements, simple interpretational techniques suffice for most practical purposes. The conductor is located horizontally at the inflection point marking the crossover from positive tilt to negative tilt and the maximum in field strength. A rule-of-thumb depth estimate can be made from the distance between the positive and negative peaks in the tilt angle profile.

(2) One cannot make reliable estimates of conductor quality, however. Finally, the major disadvantage of the VLF method is that the high frequency results in a multitude of anomalies from unwanted sources such as swamp edges, creeks and topographic highs. A VLF receiver measures the field tilt and hence the tilt profile shown in Figure 4-58 (Klein and Lajoie 1980). Figure 4-58 also shows schematically how the secondary field from the conductor is added to the primary field vector so that the resultant field is tilted up on one side of the conductor and down on the other side. Some receivers measure other parameters such as the relative amplitude of the total field or any component and the phase between any two components. Figure 4-59 (Klein and Lajoie 1980) shows a comparison of the main types of measurements made with different VLF receivers. A variant of VLF measures the electric field with a pair of electrodes simultaneously with the tilt measurement.

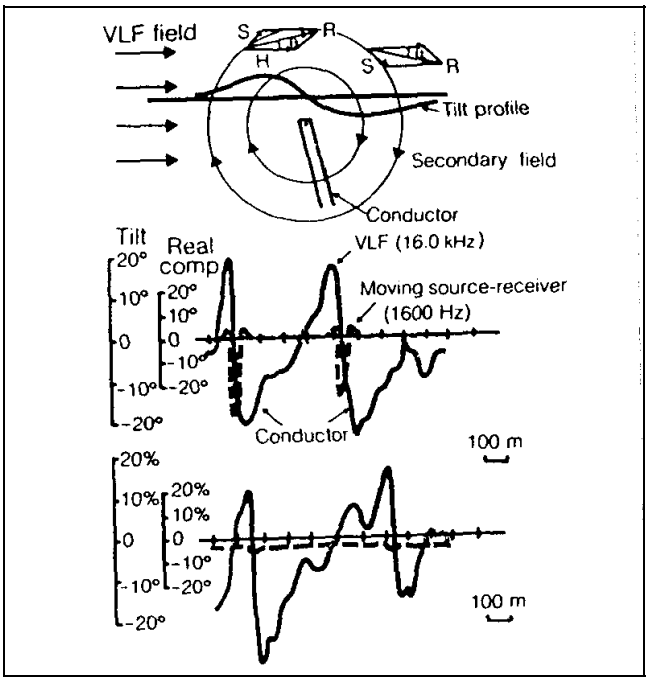

Figure 4-58. Tilt of the VLF field vector over a conductor (Klein and Lajoie 1980; copyright permission granted by Northwest Mining Association and Klein)

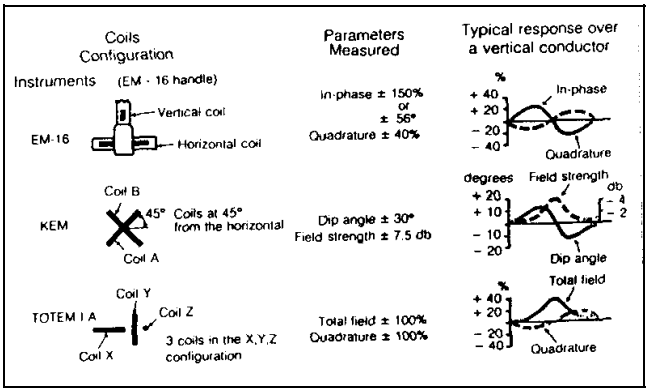

Figure 4-59. Comparison of VLF instruments (Klein and Lajoie 1980; copyright permission granted by Northwest Mining Association and Klein)

c. VLF examples.

(1) Groundwater study. Figure 4-60 presents VLF results taken over granite terrain in Burkina Faso, Africa (Wright (1988), after Palacky, Ritsema, and De Jong (1981)). The objective of the survey was to locate depressions in the granite bedrock which could serve as catchments for groundwater. Depressions in the very

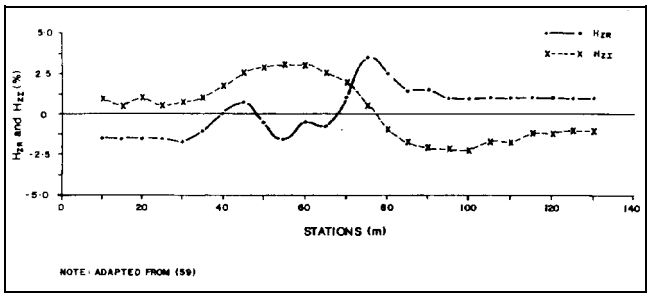

Figure 4-60. VLF profile, Burkina Faso, Africa (Wright 1988; copyright permission granted by Scintrex)

resistive bedrock beneath poorly conductive overburden (100 to 300 Ωm at this site) likely produce VLF responses as a result of galvanic current flow. That is, the large current sheet flowing in the overburden, as a result of the primary electric field, is channelled along these bedrock depressions and appears as a line of anomalous current. The conductor axis is centered near station 70 to 75. A water well was drilled at station 70 and encountered bedrock beneath approximately 20 m of overburden and flowed at a rate of 1.0 m^3/hour.

(2) Detection of buried cables. Figure 4-61 presents VLF measurements along a profile crossing a buried telephone line (Wright 1988). A classic crossover is observed which places the line beneath station -2.5. However, this curve is a good example of a poorly sampled response, because the exact peaks on the profile are probably not determined. One possible model is presented on Figure 4-61 for a line current at a depth of 1.25 m and station -2.5. The fit is only fair, which could be the result of poor station control, inapplicability of the line current model, or distortion of the measured profile by adjacent responses.

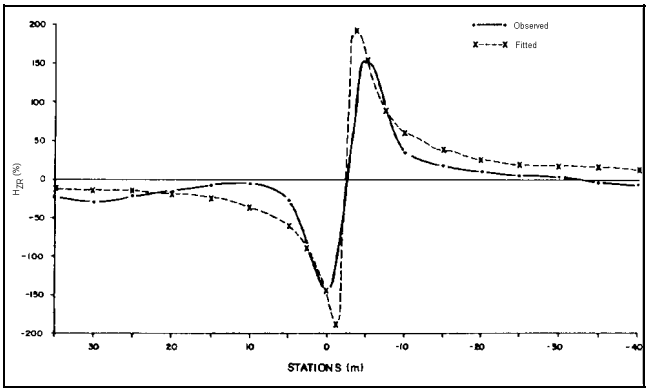

Figure 4-61. VLF profile over buried telephone line (Wright 1988; copyright permission granted by Scintrex)